Signaling networks regulated by the kinase p38α in cancer cell homeostasis

Yuzhen Dan

TESI DOCTORAL UPF / 2021

Thesis supervisor: Dr. Angel Rodríguez Nebreda

Institut de Recerca Biomèdica de Barcelona (IRB Barcelona)

DEPARTAMENT DE CIÈNCIES EXPERIMENTALS I DE LA SALUT - UNIVERSITAT POMPEU FABRA

To my beloved family

and Changxin

道生一，一生二，二生三，三生万物。

万物负阴而抱阳，冲气以为和。

The Tao produced One; One produced Two; Two produced Three; Three produced All things.

All things leave behind them the Obscurity (out of which they have come), and go forward to embrace the Brightness (into which they have emerged), while they are harmonised by the Breath of Vacancy.

Laozi

ACKNOWLEDGEMENTS

Time flies. Remembering the time when I arrived at Barcelona. I cannot imagine the moment when I was a little girl, from a rural mountain village in China. I never forsee me here today, even in my wildest dream.

The work would have not been finished without the support of a number of people.

First, I would like to extend my sincere gratitude to Prof. Angel Nebreda, not only for offering me the opportunity to carry out my PhD in his group, but also for all the enlightening discussions over the years. As the saying goes, “Give a man a fish, and you feed him for a day; teach a man to fish, and you feed him for a lifetime”. I am so grateful to have had you as my mentor and I really appreciated it. This will help me lifelong both at professional and personal levels.

I would also like to sincerely acknowledge the thesis advisory committee, Patrick Aloy, Travis Stracker and Francesc Posas for their helpful advises during these years. Especially, thanks Patrick for being always willing to help.

I’m lucky to be a member of the Nebreda’s lab, besides it is the best place to work, everyone is so kind that looks like a family.

First, I would like to express my genuine gratitude to Nevenka Radic. Thanks for helping me out with both my personal and academic life. You were always there when I felt frustrated about experiments. Thank you for being a patient listener and always encourage me when

I was confused. Many thanks to Clara, your passion for life and art really helped me to overcome my timidness and to start expressing myself comfortably. Lore, I really appreciated the numerous discussions with you, I am deeply impressed by your clear mind and soul-touched laughter. I also owe a large debt of gratitude to Bego, for lots of inspired discussions and suggestions throughout the years, not setting on before thinking more. I am grateful to Monica, for helping and teaching me experimental skills at the beginning, and you are so nice and patient every time I turned to you. Thank you Eli, for always being there and support with your smile. Laura, thanks for all your trust and joy. Marga, thanks for all the interesting sharing. Nerea and Jordi, thanks for your daily energy and enthusiasm.

Thanks Adria for kindly helping and guiding me with data analysis, which really expanded my computational skills and horizon.

I also would like to thank the people at the IRB facilities. Thanks to Marina, Gianluca and Marta for helping me with whatever was needed. Thanks also to the microscopy and FACS facilities. Also, thanks to the secretaries from IRB and UPF. Thanks to everyone who helped me with everything I needed for my work.

I want to thank my friends Zhang Kun, Wenjing, and Chen Yuan, you never mind the time difference to chat with and support me whenever I need you.

Thank you Changxin for your support and for always being there. I am so happy I can be myself when I am with you. I appreciate your care and love for me.

And last but hardly least in my gratitude, to my devoted parents, Chengwu and Xiaoqin, who raised me with unconditional love and endowed me with character and courage to pursue my life. I would have never been here without the sacrifices you made. My exceptional sister, Yu'e, a gifted programmer, I am very proud of you. Thank you for standing with me, encouraging me and supporting me to achieve my goals as always.

To the fascinating planet earth, and the wonderful world.

ABSTRACT

p38α (encoded by *MAPK14*) is a major regulator of cellular responses to almost all types of environmental and intracellular stresses. Upon activation, p38α phosphorylates various substrates both in the cytoplasm and nucleus, allowing this pathway to regulate a wide variety of cellular processes, including cell proliferation, differentiation, or survival. Given the plethora of functions that can be controlled by p38α, we performed proteomic and phosphoproteomic analysis to study the signaling networks regulated by p38α during cancer cell homeostasis. Our study identifies 35 proteins and 114 phosphosites that are modulated by p38α, and highlights the importance of other kinase pathways, such as MK2 and mTOR, for p38α-regulated functions. Moreover, the functional analysis of the (phospho-)proteome revealed the implication of p38α in the regulation of cell adhesion, DNA replication and RNA processing. We further show that p38α negatively regulates cell-cell adhesion, which is likely mediated by the transcriptional modulation of ArgBP2. Collectively, our results illustrate the complexity of the p38α regulated signaling networks, provide valuable information on p38α-dependent phosphorylation events in cancer cells, and document a mechanism by which p38α regulates cell-cell adhesion during cancer cell homeostasis.

RESUMEN

p38α (codificada por el gen MAPK14) es una proteína reguladora crucial en las respuestas celulares a casi todos los tipos de estrés tanto provenientes del ambiente extracelular como del interior de la célula. Una vez activada, p38α fosforila varios sustratos en el citoplasma y en el núcleo, lo que permite que esta vía regule una amplia variedad de procesos celulares, que incluyen la proliferación, la diferenciación o la supervivencia celular. Dado la gran cantidad de funciones que pueden ser controladas por p38α, en este trabajo realizamos análisis proteómicos y fosfoproteómicos para estudiar las redes de señalización reguladas por p38α en las células tumorales en homeostasis. Nuestro estudio ha identificado 35 proteínas y 114 sitios de fosforilación que son modulados por p38α, así como la importancia de otras vías de señalización por quinasas, como MK2 y mTOR, en las funciones reguladas por p38α. Además, el análisis funcional del (fosfo)proteoma ha revelado que p38α participa en la regulación de la adhesión celular, la replicación del ADN y el procesamiento del ARN. También mostramos que p38α regula negativamente la adhesión célula-célula, lo que probablemente está mediado por la modulación transcripcional de ArgBP2. En conjunto, nuestros resultados ilustran la complejidad de las redes de señalización reguladas por p38α, proporcionan información valiosa sobre las fosforilaciones dependientes de p38α en células tumorales y documentan un mecanismo por el que p38α regula la adhesión célula-célula durante la homeostasis de las células tumorales.

PREFACE

The signaling pathway based on p38α plays prominent roles in the process of integration of information, which allows cells to interpret environmental stimuli and elaborate the appropriate responses. Upon activation, p38α can phosphorylate many substrates both in the cytoplasm and nucleus, which allows this pathway to regulate a wide variety of cellular processes, including cell proliferation and survival. The set of p38α substrates that are phosphorylated in response to each stimulus is likely to contribute to the particular cellular response. Several protein kinases are activated by direct p38α phosphorylation and further amplify the number and type of proteins that can be phosphorylated upon activation of the signaling pathway.

In this Thesis, proteome and phosphoproteome analyses were performed in cancer cells in which p38α signalling was inhibited using two different reagents to identify with high confidence signaling networks regulated by p38α in cell homeostasis. In total, 25 proteins were found to be positively regulated and 10 proteins negatively regulated by p38α. At the phosphoprotein level, 26 phosphosites (on 21 proteins) were positively regulated and 88 phosphosites (on 62 proteins) negatively regulated by p38α. Functional analysis suggested that these (phospho-)proteins were mainly involved in the regulation of cell adhesion, RNA processing, DNA replication and the cell cycle.

Sequence signature analysis of the phosphosites downregulated upon p38α inactivation revealed that about 52% corresponded to RxxS

motifs and 30% to SP/TP motifs, which can be targeted by p38α and its downstream substrate MK2, respectively. Curiously, 77% of the upregulated phosphosites were also SP/TP motifs, which could be targeted by MAPKs or CDKs. In addition, we found that MK2 and mTOR activities were significantly decreased when p38α signaling was inhibited, and the activity of several other proteins kinases was also predicted to be altered upon p38α inhibition.

Moreover, the role of p38α in cell adhesion was evaluated using different assays. We concluded that p38α can negatively regulate cell-cell adhesion and identified the adapter protein ArgBP2 (encoded by *SORBS2*) as a target that is negatively regulated by p38α at the transcription level. ArgBP2 assembles signaling complexes in stress fibers and is a component of the actomyosin ring at the apical junctional complex in epithelial cells. We provide evidence that ArgBP2 is involved in the regulation of cell-cell adhesion by p38α.

Taken together, our results illustrate the complexity of the p38α-regulated signaling networks in cancer cell homeostasis and provide new insights into the mechanisms modulated by p38α in cell-cell adhesion.

CONTENTS

ABBREVIATIONS

4-OHT	4-hydroxitamoxifen

A

AGC	PKA, PKB, and PKC family
AKAP	A-kinase–anchoring protein
APC/C	Anaphase-promoting complex/cyclosome
aPK	Atypical protein kinase
APS	Ammonium persulfate
Arg	Arginine
ASK1	Apoptosis signal-regulating kinase 1
Asp	Aspartate
ATF	Activating transcription factor
ATM	Serine-protein kinase ATM
ATP	Adenosine triphosphate
ATR	Ataxia telangiectasia and rad3-related protein
AUF1	AU-rich element RNA-binding protein 1

B

BAF60c	BRG1-associated factor 60
Bax	Bcl-2 Associated X protein
Baz1b	Tyrosine-protein kinase BAZ1B
BimEL	Bcl-2-like protein 11
BRN2	POU domain transcription factor
BSA	Bovine Serum Albumin
BTB	Blood-testis barrier

C

C3G	Rap Guanine Nucleotide Exchange Factor 1
CAK	CDK-activating kinase
CAMK	Ca2+/calmodulin-dependent protein kinase
cAMP	Cyclic adenosine monophosphate
CAM	Cell adhesion molecule
Cdc25	Cell division cycle 25
Cdc42	Cell division cycle 42

$CdCl_2$	Cadmium chloride
CdGAP	GTPase-activating protein
CDK	Cyclin-dependent kinase
CEBP	CCAAT/enhancer-binding protein
c-Fos	AP-1 transcription factor subunit
CHK1	Cell cycle checkpoint kinase 1
CIN	Chromosomal instability
CK1	Casein kinase 1
CMGC	CDKs, MAPKs, GSK, and CDK-like kinases family
CREB	cAMP responsive element binding protein
CrkL	Crk-like protein
CV	Coefficient of variation
Cys	Cysteine

D

Ddx52	DEAD (Asp-Glu-Ala-Asp) box polypeptide 52
DLK1	Dual-leucine-zipper-bearing kinase 1
DLX5	Distal-less homeo box 5
DMEM	Dulbecco's modified Eagle´s medium
DMSO	Dimethyl sulfoxide
DNA-PKcs	DNA-dependent protein kinase catalytic subunit
DSP/DUSP	Dual-specificity phosphatase
DTT	Dithiothreitol

E

ECM	Extracellular matrix
EEA1	Early endosome antigen 1
EGF	Epidermal growth factor
EGFR	Epidermal growth factor receptor
eIF4E	Eukaryotic initiation factor 4E
Eif4ebp1	Eukaryotic translation initiation factor 4E binding protein 1
ELK1	ETS domain-containing protein Elk-1
EMT	Epithelial-to-mesenchymal transition
Ep300	E1A binding protein p300
ePK	Conventional protein kinase
ERK1/2	Extracellular signal-regulated kinases 1/2

ES	Embryonic stem
EZH2	Histone-lysine N-methyltransferase EZH2

F

FAK	Focal adhesion kinase 1
Fdw	Forward
FERM	Ezrin Radixin Moesin
FGFR1	Fibroblast growth factor receptor 1
Flna	Filamin A

G

GDI-2	GDP dissociation inhibitor 2
Glu	Glutamate
GPCR	G protein-coupled receptor
GSEA	Gene Set Enrichment Analysis
GSK	Glycogen synthases kinase

H

H2AX	H2A histone family member X
HBP1	HMG-Box Transcription Factor 1
HEPES	4-(2-hydroxyethyl)-1-piperazineethanesulfonic acid
HePTP	Hematopoietic protein tyrosine phosphatase
His	Histidine
Hnrnpa1	Heterogeneous nuclear ribonucleoprotein A1
Hsp27	Heat-shock protein 27
Hspbp1	Heat shock protein-binding protein 1
HuR	Human antigen R

I

ICAM-1	Intercellular cell adhesion molecule-1
IFN-γ	Interferon gamma
IL-1	Interleukin-1

J

JNK	C-Jun N-terminal kinase

K

KIM	Kinase interaction motif
Krt14	Keratin 14
KSEA	Kinase-Substrate Enrichment Analysis
KSR1	ERK scaffolding protein 1

L

Leu	Leucine
LPS	Lipopolysaccharides
LSP1	lymphocyte-specific protein 1
LY	LY222882
Lys	Lysine

M

MAP2K	MAPK kinase
MAP3K	MAPK kinase kinase
MAPK	Mitogen-activated protein kinase
MEF2	myocyte-specific enhancer factor 2
MEKK	MAPK/ERK kinase
MK2	MAPKAPK2
MK2i	MK-2 Inhibitor III
MKP	MAP kinase phosphatase
MLK	Mixed-lineage kinase 3
MNK1/2	MAPK Interacting Ser/Thr Kinase 1 and 2
MRF4	Muscle-specific regulatory factor 4
MSK	Mitogen- and stress-activated protein kinase
MyoD	Myogenic differentiation

N

Nav1.6	Sodium voltage-gated channel alpha subunit 8
Nelfe	Negative elongation factor complex member E
NFATc4	Nuclear factor of activated T cells 4
NHE1	Sodium/proton exchanger 1
NLK	Nemo-like kinase

O

OGT	O-GlcNAc transferase

P

p130Cas	Breast cancer anti-estrogen resistance protein 1
p38α	Mitogen- activated protein kinase 14
p57kip2	Cyclin-Dependent Kinase Inhibitor 1C
p65-NFkB	Nuclear factor NF-Kappa-B p105 subunit
PBS	Phosphate buffer solution
PDE4	phosphodiesterase
PDHK	Pyruvate dehydrogenase kinase
PH	PH797804
PIKK	Phosphatidylinositol 3-kinase-related kinase
PKA	Protein Kinase A
PKB	Protein kinase B; also known as AKT
PKC	Protein kinase C
PLA2	Phospholipase A2
Pla2g4a	Phospholipase A2 group IVA
Plk1	Polo-like kinase 1
PMSF	Phenylmethylsulfonyl fluoride
PP2A	Protein phosphatase 2A
PP2B	Protein phosphatase 2B
PP2C	Protein phosphatase 2C
PPARγ2	Peroxisome proliferator-activated receptor γ2
PPI	Protein-protein interaction
PPM	Mg2+- or Mn2+-dependent phosphatase
PPP	Phosphoprotein phosphatase
PPP3CA	Protein phosphatase 3 catalytic subunit alpha
Pro	Proline
PROTAC	Proteolysis targeting chimera
pSer	Phosphoserine
pThr	Phosphothreonine
PTM	Post-translational modification
PTP	Protein Tyrosine phosphatase
PTPN21	Tyrosine-protein phosphatase non-receptor type 21
PTPRJ	Protein tyrosine phosphatase receptor type J
PTP-SL	Receptor-type tyrosine-protein phosphatase R
pTyr	Phosphotyrosine
PyMT	Polyoma middle T

Q

qRT-PCR	Quantitative real time-Polymerase chain reaction

R

Ranbp2	RAN binding protein 2
RB	Retinoblastoma protein
Rbm17	RNA binding motif protein 17
Rbm22	RNA binding motif protein 22
Rbm7	RNA binding motif protein 7
Rbsn	Rabenosyn-5
Rev	Reverse
RGC	Regulator of cell cycle
RNF2	Ring finger protein 2
ROS	Reactive oxygen species
Rpl29	60S ribosomal protein L29
Rps3	40S ribosomal protein S3
Rps8	40S ribosomal protein S8
rRNA	Ribosome RNA
Runx1/2	Runt related transcription factor 1 and 2

S

Ser	Serine
sgRNA	Small guide RNA
SH	SRC-homology
SILAC	Stable isotope labeling by amino acids in cell culture
SIP1	Calcyclin-binding protein/Siah-1 interacting protein
SLiM	short linear motif
SoHo	Sorbin Homology
Sp1	Specificity Protein 1
Spag9	Sperm Associated Antigen 9
SRC	Non-receptor tyrosine kinase
SRCAP	Snf2 related CREBBP activator protein
Srpk1	Serine/Arginine-Rich Splicing Factor Kinase 1
STAT	Signal transducer and activator of transcription
STE	Sterile
STE20	Serine/threonine-protein kinase STE20

STEP	Striatal-enriched protein tyrosine phosphatase
SWI/SNF	SWItch/Sucrose Non-Fermentable) subunit

T

TAB1	TAK1-binding protein 1
TACE	Tumor necrosis factor alpha converting enzyme
TAK1	Transforming growth factor β-activated kinase 1
TAO1/2	Thousand-and-one amino acid 1 and 2
Tcf20	Transcription factor 20
TCR	T-cell receptor
TEAD4	Transcriptional enhancer factor domain family member 4
TEMED	Tetramethylethylenediamine
TGFβ	Transforming growth factor β
Thr	Threonine
TJ	Tight junction
TK	Tyrosine kinase
TKL	Tyrosine kinase–like
TNFα	Tumoral necrosis factor alpha
TPL2	Tumor progression loci 2
TTP	Tristetraprolin
Tyr	Tyrosine

V

VCAM-1	Vascular cell adhesion molecule-1

Z

ZAK1	Leucine-zipper and sterile-αmotif kinase 1
ZAP70	Zeta-chain-associated protein kinase 70
Zfp36l1/2	ZFP36 ring finger protein 1ike 1/2
ZO-1	Tight junction protein 1

INTRODUCTION

1. Post-translational modifications in cell signaling

Cells need to constantly sense changes in the cellular environment to respond accordingly, so they have developed sophisticated mechanisms to receive, process and transmit the signals that orchestrate the appropriate responses. For example, ligand binding to the extracellular domain of a receptor initiates a signal transduction network that affects multiple processes, from metabolism to motility, proliferation, survival and differentiation(Graves and Krebs, 1999).

Post-translational modifications (PTMs) play fundamental roles in the cellular response to environmental alterations, by allowing cells to diversify their protein functions and dynamically coordinate signaling networks. PTMs are covalent modifications that alter the protein properties by proteolytic cleavage or by addition of groups such as acetyl, phosphoryl, glycosyl and methyl, to one or more amino acids (Ramazi et al., 2020). To date, more than 400 different PTM types are listed in the Uniprot database (Khoury GA et al., 2011). These modifications can affect almost all kinds of protein behaviors and characteristics, including enzyme activity, protein life span, protein-protein interactions, cell-cell and cell-matrix interactions, molecular trafficking, receptor activation, protein solubility, folding and localization(Ramazi and Zahiri, 2021).

1.1 Phosphorylation

Protein phosphorylation is perhaps the most prevalent and acute type of reversible PTM in eukaryotes. Indeed, it is an efficient way to control cell response to internal and external cues. It is rapid, taking as little as a few seconds, does not require new proteins to be

synthesized or degraded, and can be easily reverted. Protein phosphorylation plays a crucial role in controlling various cellular processes, impinging on enzyme catalytic activity, protein-protein and protein-DNA/RNA interactions, protein localization and stability (Cohen, 2002; Hunter, 2012). The history of protein phosphorylation began with the discovery of phosphate in the protein vitellin in 1906 (Levene P A and Beatty W A, 1906). However, the first enzymatic phosphorylation of a protein was reported 20 years later in rat liver mitochondrial (Burnett G and Kennedy E P, 1954). In 1968, Fischer and Krebs discovered the first protein kinase, Protein Kinase A (PKA), and they won the 1992 Nobel Prize for their discovery of this important and reversible process as a major biological regulatory mechanism (Fischer E H and Krebs E G, 1955).

The phosphorylation status of a protein is regulated by protein kinases and phosphatases. In particular, protein kinases transfer a phosphate group (PO_4) from adenosine triphosphate (ATP) to the polar group of some amino acids. Consequently, the substrate protein may undergo a conformational change affecting its enzymatic activity or its ability to interact with other molecules (Ardito et al., 2017). Conversely, phosphatases remove the phosphate group in a process called dephosphorylation (**Figure 1**). Kinases and phosphatases work in balance and independently to regulate protein function. Eukaryotic protein phosphorylation mainly occurs on Ser, Thr or Tyr residues. In particular, about 84.6% of the phosphorylation appears on Ser, 11.8% on Thr and only 1.8% on Tyr (Olsen J V et al., 2006). However, phosphorylation has also been reported on His, Pro, Asp, Glu, Lys, Arg and Cys residues (Huang et al., 2019).

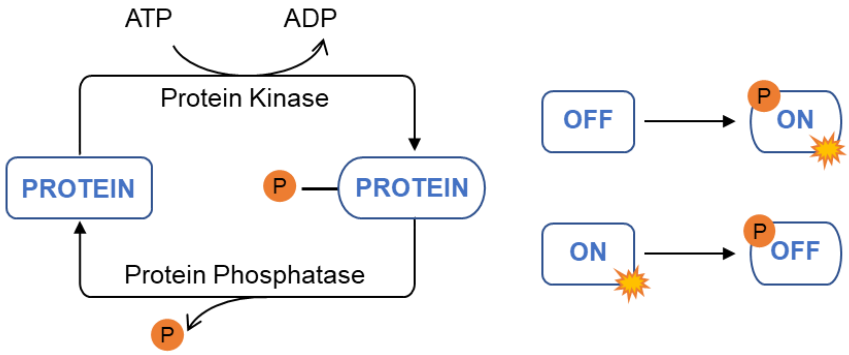

Figure 1. Scheme of phosphorylation and dephosphorylation. Phosphorylation is mediated by kinases and phosphatases. As a key reversible post-translational modification, phosphorylation causes protein conformational changes, which may activate or inactivate the protein function. Adapted from (Ardito et al., 2017).

To date, over 200,000 known human phosphosites are listed in the Cell Signaling Technology PhosphoSitePlus (www.phosphosite.org) and the Kinexus PhosphoNET (www.phos-phonet.ca) websites (Ardito et al., 2017). It is estimated that 30% of all cellular proteins are phosphorylated in at least one residue. Assuming that there are ~10,000 different proteins in a typical eukaryotic cell, with an average length of ~400 amino acids (~17% of which are Ser (8.5%), Thr (5.7%) or Tyr (3.0%), there are ~700,000 potential phosphorylation sites for any given protein kinase (Ubersax and Ferrell, 2007).

1.2. Protein kinases

In eukaryotes, the protein kinase gene family comprises about 2% of the genome. To date, 522 human protein kinases have been identified, which can transiently phosphorylate specific amino acids on ~30% of all human proteins (Manning G et al., 2002). Of these protein

kinases**,** 372 are known or predicted to phosphorylate Ser and Thr, 90 phosphorylate Tyr, and the remaining 56 are transmembrane receptor tyrosine kinases.

The human kinome is broadly classified into two superfamilies, "conventional" (ePKs) and "atypical" protein kinases (aPKs) (**Figure 2**). ePKs are the largest group and have been subclassified into 8 groups (AGC, CAMK, CK1, CMGC, RGC, STE, TK, and TKL families) based on the sequence similarity between the catalytic domains, the presence of auxiliary domains, and considering any known regulatory models (Manning G et al., 2002).

In contrast, aPKs are a small set of protein kinases that do not share apparent sequence similarity with ePKs, and comprise the following four groups: Alpha, PIKK, PDHK and RIO. Protein phosphorylation act as molecular switches in essentially every aspect of cellular activity, and mutations or dysregulation of protein kinases are often associated with many human diseases (Greenman et al., 2007; Lahiry et al., 2010). Therefore, protein kinases are considered valuable targets for precision medicine (Klaeger et al., 2017; Zhang J et al., 2009).

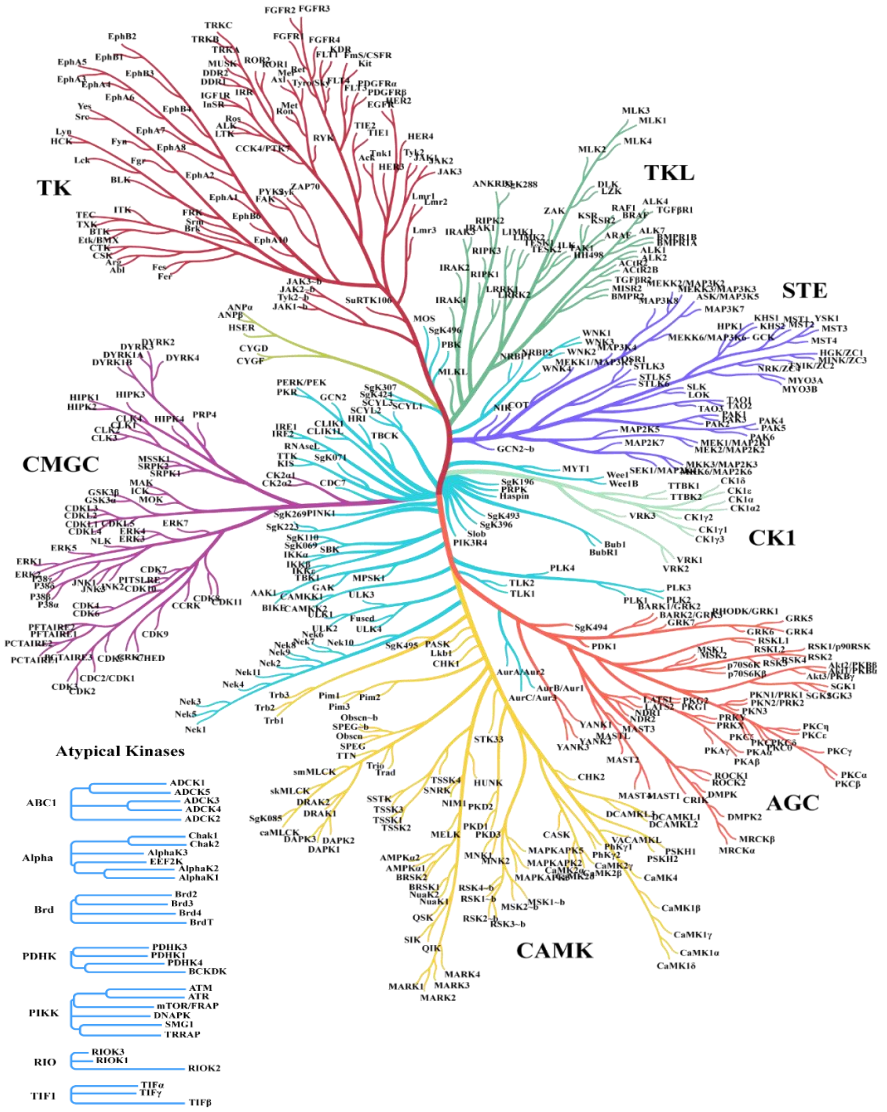

Figure 2. Protein kinase families. TK, tyrosine kinase. TKL, tyrosine kinase–like. STE, sterile. CK1, casein kinase 1. AGC is a family that includes PKA (protein kinase A), PKB (protein kinase B; also known as AKT), and PKC (protein kinase C). CAMK, Ca2+/calmodulin-dependent protein kinase. CMGC is a family that includes CDKs (cyclin-dependent kinases), MAPKs (mitogen-activated protein kinases), GSK (glycogen synthase kinases), and CDK-like kinases. Kinome tree was created using Coral (http://phanstiel-lab.med.unc.edu/CORAL/).

1.3. Protein kinase structure

The majority of human protein kinases share a common fold consisting of a small N-terminal lobe, formed by a five-stranded β-sheet with an α-helix called the C-helix, and a bigger C-terminal lobe comprising six α-helices (**Figure 3**). The two lobes are connected by a flexible hinge region forming the ATP-binding site. The active site is located in the cleft between the two lobes, comprising several crucial structural elements for enzymatic activity. The activation loop is typically 20 to 30 residues in length, beginning with a conserved DFG motif (usually Asp-Phe-Gly) and extending up to an APE motif (usually Ala-Pro-Glu). In active kinase structures, this loop forms a cleft that binds the substrate, and the bound substrate peptide forms specific interactions with the conserved HRD motif (usually His-Arg-Asp) located in the catalytic loop of the protein.

Other structural changes that occur in the active conformation are: (1) the Asp of the DFG motif is oriented in a way that allows it to bind to a magnesium ion that interacts directly with an oxygen atom of the β phosphate of ATP; (2) the C-helix is in an inward disposition, which positions a conserved Glu in the helix to form a salt bridge with a Lys residue in the β3 strand, and the Lys side chain forms hydrogen bonds with oxygen atoms of the α and β phosphates of ATP. In addition, the N-lobe has a GxGxxG motif in a loop that stabilizes the phosphates of the bound ATP molecule during catalysis. The catalytically active state of a protein kinase requires a unique assembly of these elements that create an environment conducive to the phosphotransferase reaction (Modi and Dunbrack,

2019). The flexibility of these structural elements contributes to the regulation of the kinase activity.

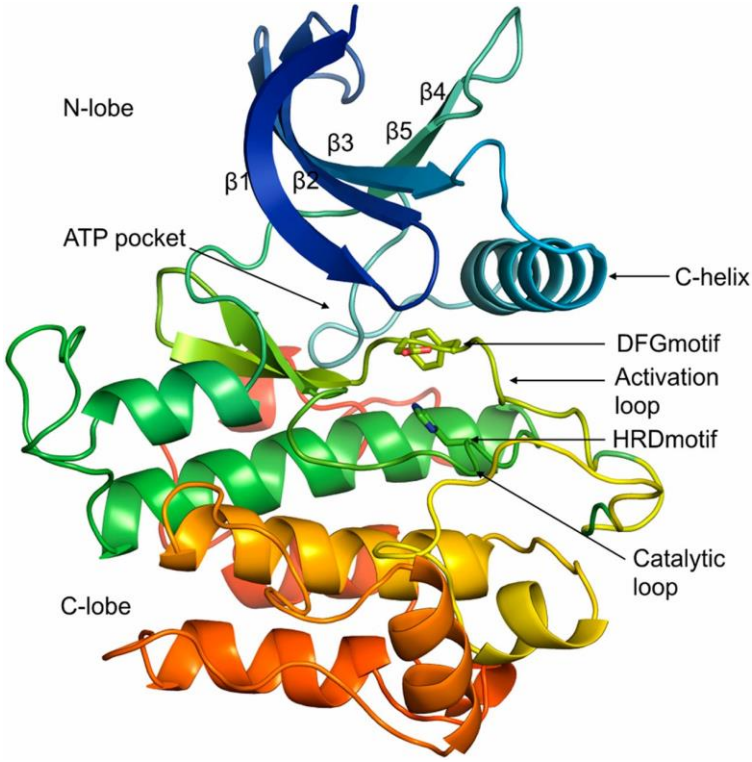

Figure 3. Crystal structure of a typical protein kinase. Human protein kinases are composed of an N-terminal lobe (N-lobe), containing five β-sheet strands and a C-helix, and a C-terminal lobe (C-lobe) containing six α-helices. ATP binding site and conserved elements around it are labelled. Adapted from (Modi and Dunbrack, 2019).

1.4. Protein kinase specificity

Protein kinases differ from one another based on their modes of regulation and their substrate repertoires to maintain the specificity observed in signaling pathways. A typical kinase must distinguish its targets in a background of ~700,000 potentially phosphorylatable

sites. Multiple factors modulate the specificity of the kinase, such as the structure of the kinase catalytic site, subcellular localization and the formation of complexes with regulatory scaffolds and adaptor proteins (**Figure 4**). The most notable difference between kinases regarding their specificity is the identity of the phosphoacceptor Ser, Thr and Tyr, which are determined by conserved features of the kinase active site. For instance, Tyr kinases have a deeper catalytic cleft than Ser/Thr kinases: a Tyr residue can span the distance between the peptide backbone and γ-phosphate of ATP, while the smaller side groups of Ser and Thr residues cannot (Hubbard S R, 1997; Ubersax and Ferrell, 2007). Moreover, as a general rule, Ser/Thr protein kinases tend to prefer Ser over Thr.

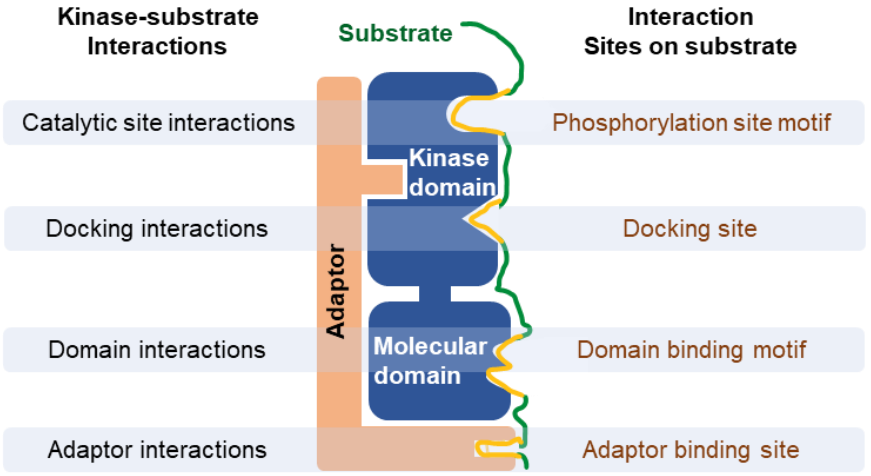

Figure 4. Overview of the main types of protein kinase-substrate interactions. Kinases selectively target specific substrates through a combination of multiple interactions, including the structure of the catalytic site, local and distal interactions between the kinase and substrate, and the formation of complexes with scaffolding and adaptor proteins. Adapted from (Miller and Turk, 2018).

Consensus sequences

The interface between the protein kinase active site and the residues flanking the target phosphoacceptor often contributes substantially to kinase–substrate recognition, usually described as a short linear sequence motif (Pearson and Kemp, 1991; Pinna and Ruzzene, 1996). Therefore, identification of the linear sequence motif has been, in many cases, an essential hint for finding the physiological kinase. For example, Protein kinase A (PKA) substrate motif is Arg-Arg-X-Ser/Thr-Φ (where X is any amino acid and Φ represents a hydrophobic residue), indicating that Arg at -3 and -2 position and a hydrophobic residue at +1 to the target Ser/Thr is preferred by the PKA active site (Songyang et al., 1994; Taylor et al., 2005; Zheng et al., 1993). Examples of other kinase consensus sequence motifs are provided in **Table 1** (Miller and Turk, 2018). However, some protein kinases share the same linear sequence motif, for instance, Ser/Thr-Pro sites for mitogen-activated protein kinases (MAPKs) and cyclin-dependent kinases (CDKs), and other protein kinases do not seem to have a clear consensus sequence motif in their substrates.

Although docking motifs are found in various kinases, they usually occur in different parts of the kinases. Unlike Ser/Thr kinases, of which the docking domains are often part of the kinase domain, Tyr kinases docking motifs tend to separate from the kinase domain. Non-receptor Tyr kinases have well-defined domains, like SRC-homology-2 (SH2), SH3, integrin binding, pleckstrin homology, or Janus tyrosine kinase (JAK) homology domains (Hubbard and Till, 2000; Ubersax and Ferrell, 2007). In recent years, docking motifs that increase kinase-substrate interactions have been identified in many

kinases, suggesting that this may be a widespread mechanism of specificity.

The docking domains in MAPKs are among the best studied (See 3.1). MAPKs share a common phosphorylation sequence motif (Ser/Thr-Pro), but the different subfamilies (ERK1/2, p38s and JNKs) usually target different sets of substrates. Two distinct regions of the MAPK catalytic domains are known to increase substrate specificity: the D domain (also known as the D box or DEJL domain or Kinase interaction motif (KIM-motif) (Kallunki et al., 1994) and the DEF domain (also known as the FXF motif) (Jacobs et al., 1998).

D domains are typically 50-100 residues away from the MAPK phosphosite, consisting of a cluster of basic residues positioned amino-terminal to a Leu/Iso-X-Leu/Iso(Φ-X-Φ) motif followed by a triplet of hydrophobic amino acids that precedes a series of Pro residues (Barsyte-Lovejoy et al., 2002; Caldwell et al., 2006; Ho et al., 2003). D domains are ubiquitous in MAPK substrates. For example, activated transcription factor-2 (ATF2) carries a JNK docking site, the transcription factor ELK1 has an ERK docking site, and myocyte enhancer factor (MEF)-2A and MEF2C carry docking sites for p38 MAPK (Gupta S et al., 1995; Tanoue et al., 2000; Yang et al., 1998, 1999). Although some of the D-domains can be recognized by more than one subfamily of MAPKs, the importance of the D-domains was validated by mutation of specific acidic residues in the MAPK that were predicted to interact with the Lys or Arg residues of the substrate docking sequences (Tanoue and Nishida, 2003; Yang et al., 1998).

Table 1. Consensus sequences of protein kinase phosphorylation sites. Kinase preferences are indicated in the first column. The residue 0 is the phosphoacceptor: Ser, Thr or Tyr. Amino acids are indicated by the single letter codes. x=any amino acid, Φ=hydrophobic, pS=phosphorylated Ser, pY= phosphorylated Tyr. Adapted from Miller and Turk, 2018.

	Kinase	Consensus sequence																		
		-5		-4		-3		-2		-1		0		+1		+2		+3		+4
Basophilic	PKA					R	–	R/K	–	x	–	S	–	Φ						
	PAK					R/K	–	R	–	x	–	S	–	Φ						
	PKC			R/K	–	R/K	–	R/K	–	G/R	–	S/T	–	Φ	–	R/K	–	R/K		
	PIM/S6K	R	–	x	–	R	–	x	–	x	–	S/T								
	AKT/RSK	R	–	x	–	R	–	x	–	x	–	S/T	–	Φ						
	CAMK/PKD	Φ	–	x	–	R	–	Q	–	x	–	S	–	Φ						
	AMPK/MARK	Φ	–	x	–	R	–	x	–	x	–	S	–	x	–	x	–	x	–	I/L
	Haspin							A/V	–	R	–	- T	–	K						
Pro-directed	MAPK							P/Φ	–	x	–	S/T	–	P						
	CDK											S/T	–	P	–	x	–	K/R		
	DYRK					R	–	x	–	x	–	S/T	–	P						
Acidophilic	CK1	D/E	-	D/E	–	D/E	–	x	–	x	–	S/T	–	Φ						
						pS/pT	–	x	–	x	–	S/T	–	Φ						
	CK2											S/T	–	D/E	–	x	–	D/E		
												S/T	–	D/E	–	x	–	pS		
	GSK3b											S	–	x	–	x	–	x	–	pS
	PLK							D/E	–	x	–	S/T	–	Φ						
	FAM20C											S	–	x	–	E/pS				
Other	ULK					L/M	–	x	–	x	–	S/T	–	Φ	–	Φ				
	NEK					L/F	–	x	–	x	–	S/T	–	Φ						
	LKB1							L/I	–	x	–	T								
	ATM/ATR/DNAPK											S/T	–	Q						
Tyrosine	EGFR					E/D	–	E/D	–	E/D	–	Y	–	pY/F	–	x	–			
	SRC					E	–	E	–	I/V	–	Y	–	E/G	–	x	–	Φ		
	ZAP70									D/E	–	Y	–	E/Φ	–	x	–	Φ		
	ABL									I	–	Y	–	A	–	x	–	P		

DEF domains are generally Ω-X-Ω sequence, where Ω represents an aromatic residue and is mainly located between 6 and 20 amino acids C-terminal to the phosphoacceptor (Lee et al., 2004; Sheridan et al., 2008). It was first found in the *Caenorhabditis elegans* ETS transcription factor LIN-1 and the scaffold protein KSR-1, which contain the Phe-X-Phe-Pro sequence, where X is any amino acid, and one of the Phe residues can also be a Tyr residue (Jacobs et al., 1998; Murphy et al., 2002; Roux and Blenis, 2004). DEF domains engage a small hydrophobic pocket proximal to the catalytic cleft of ERK1/2 and p38 MAPKs (Lee et al., 2004; Sheridan et al., 2008). Distinct DEF-site sequence preferences among p38 family members have been rationalized based primarily on the size of this pocket. DEF domains have been identified in several MAPK substrates, most of which are transcription factors including Elk1, c-Fos, c-Myc, and JunD (Jacobs et al., 1999; Murphy et al., 2002, 2004; Vinciguerra et al., 2004). Other proteins with various functions were also reported to contain DEF domains, like the ERK scaffolding protein KSR1 (Jacobs et al., 1999), the proapoptotic Bcl-2 family protein BimEL (Ley et al., 2005), the GTPase-activating protein CdGAP (Tcherkezian et al., 2005), and the focal adhesion protein vinexin (Mitsushima et al., 2004). Interestingly, the DEF domains have been found in ERK2 and p38α/p38γ, but not in JNKs and p38β (Sheridan et al., 2008).

DEF and D domains can sometimes be found on the same protein, such as Elk-1 and KSR1, where these domains may act synergistically to strengthen MAPK interaction (Roux and Blenis, 2004).

Scaffolds

Besides the direct interactions between protein kinases and their substrates, adaptors or scaffolds can sometimes act as organizing platforms to recruit the kinase and the substrate to the same complex within specific subcellular locations (Bhattacharyya et al., 2006). Scaffolds are similar to targeting subunits, except that targeting subunits tend to associate stably with the kinase, whereas the interaction between a kinase and a scaffold might be more dynamic (van Drogen et al., 2001). Scaffolds allow protein kinases to attain distinct substrate specificity depending on the scaffolding complex composition, bringing kinases and substrates together in space and precisely tuning the quantitative characteristics of the pathway.

There are several examples of PKA and MAPK signals that are dependent on scaffolding proteins to maintain kinase specificity. For example, the A-kinase–anchoring proteins (AKAPs) have distinct subcellular targeting sequences or mechanisms and can anchor inactive PKA to different locations in the cell promoting substrate kinase interactions upon increased cAMP concentrations, which results in PKA activation (Wong and Scott, 2004). In addition to controlling the localization of inactive PKA, AKAPs can also recruit other signaling proteins, such as the phosphatase PP2B (Coghlan VM et al., 1995), the kinase PKC (Klauck T M et al., 1996) and the phosphodiesterase PDE4, which collapses local cAMP concentrations to inactivate PKA and maintain a gradient of PKA activation (Dodge et al., 2001). Another example is the scaffold protein JNK interacting protein-1 (JIP1), which recruits JNK and its upstream MAP2K and MAP3K (Whitmarsh et al., 1998), and can

also recruit the phosphatase MKP7 to induce JNK dephosphorylation (Willoughby et al., 2003).

In summary, protein kinases use multiple mechanisms to maintain their specificity and phosphorylate the proper substrates in their associated signaling networks. However, kinase substrate predictions based on linear kinase recognition motifs is tricky, especially considering that multiple substrate-binding modes are possible, and that indirect kinase-substrate interactions may also be important in some contexts. It is also unclear which mechanisms are essential for each kinase as well as the factors that determine the degree of interaction required for substrate phosphorylation.

1.5. Protein phosphatases

The phosphorylation state of a protein is not only regulated by changes in protein kinase activity, but also depends on the activity of protein phosphatases, which may be as important as protein kinases (Cuadrado and Nebreda, 2010). There are approximately 264 known human protein phosphatases, accounting for 1.17% of the human proteome (Chen et al., 2017). These phosphatases are structurally and functionally diverse and classified into four families according to their sequences, catalytic mechanism, inhibitor sensitivity, and substrate preference: the phosphoprotein phosphatase (PPP) family, the protein phosphatase $Mg2^{+}$- or $Mn2^{+}$-dependent (PPM) family represented by PP2C, the protein Tyr phosphatase (PTP) superfamily, and the aspartate-based protein phosphatase family represented by FCP/SCP (TFIIF-associating component of RNA

polymerase II CTD phosphatase/small CTD phosphatase) (**Table 2**) (Andersen et al., 2001; Shi, 2009; Tonks, 2006).

Table 2. Classification of protein phosphatases. The number of genes that encode the phosphatases in each family or class is in parentheses. Adapted from Meeusen & Janssens, 2018.

Class	Subclasses		Examples
Protein Serine/Threonine phosphatases (PSP)	Phosphoprotein phosphatases (PPP) (13)		PP1
			PP2A
			PP2B
			PP4
			PP5
			PP6
			PP7
	Metal dependent protein phosphatases (PPM) (18)		PP2C
			Pyruvate dehydrogenase phosphatases
	Aspartate-based protein phosphatases (7)		FCP1
			SCP
Protein Tyrosin phosphatases (PTP)	Class I	Classical protein tyrosin phosphatases(PTP)	Transmembrane PTPs (20)
			Non-receptor PTP (17)
		Dual Specificity phosphatases (DSP) or VH1-like PTPs	MKPs (11)
			PTENs (5)
			Atypical DSPs (20)
			Myotubularins (15)
			PRLs (3)
			Slingshots(3)
			CDC14s (4)
	Class II	CDC25	CDC25A
			CDC25B
			CDC25C
	Class III	Low molecular weight protein tyrosine	ACP1
			SSU72

Protein phosphatases catalyze the removal of phosphate groups from their substrates by hydrolysis of phosphoric acid monoesters into a phosphate ion, therefore reversing the action of protein kinases. Unlike protein kinases, which have a structurally conserved catalytic

domain (Manning G et al., 2002), phosphatase activity is associated with many different protein folds and catalytic mechanisms due to their evolution in separate families, which are structurally and mechanistically distinct (Tonks, 2006). In each superfamily, the linkage of regulatory and targeting domains and/or subunits to protein catalytic domains achieve considerable structural diversity. Regulatory subunits and domains are used to localize protein phosphatases to specific subcellular locations and to regulate their specificity and functions through allosteric modification (Barford et al., 1998).

1.6. Substrate recognition and specificity of protein phosphatases

Although significant progress has been made in understanding how protein kinases recognize their substrates through protein-protein interactions, scaffolding proteins, and linear sequence motifs surrounding the phosphoacceptor sites, protein phosphatases are considered more promiscuous. Sacco et al. (Sacco et al., 2012) summarized three main strategies that phosphatases use to target their substrates, which are Module-based, SLiM-mediated, and Regulatory subunit-assisted, as described below and in **Figure 5**. The three mechanisms contribute to phosphatase substrate recognition, though their relative importance in different phosphatase families remains to be determined.

Module-based specificity employs targeting domains that are covalently linked to the catalytic domains. For instance, PTPN11 requires its SH2 domain to be recruited to specific targets such as a

surface-receptor signaling complex either through direct recruitment or through scaffolding adaptor proteins. PTPN11 binds its substrates via SH2-mediated recognition of phosphorylated tyrosines on the C-terminus of the substrates (Feng, 1999; Neel et al., 2003; Östman et al., 2006). Another example is the 4.1 Ezrin Radixin Moesin (FERM) domain, a lipid-binding domain that connects actin filaments with membranes. PTPN21 uses a FERM domain to recruit SRC kinase and after once the FERM-mediated complex is formed, SRC is activated via dephosphorylation of its C terminal inhibitory phosphotyrosine. PTPN21 mutants lacking either catalytic activity or the FERM domain are unable to activate SRC (Carlucci et al., 2008).

Some phosphatases use SLiM-mediated specificity to recognize their substrates. SLiMs are often located in intrinsically disordered regions and their sequence composition determines protein-protein interaction and binding affinity. For instance, the Pro-rich motif in PTPN12 can interact with the SH3 domain of p130Cas to facilitate its dephosphorylation (Angers-Loustau et al., 1999; Garton et al., 1997). Similarly, some dual specificity phosphatases (DSPs or MKPs) can target MAPKs by direct interaction of the SLiMs in their non-catalytic amino-terminal domain with a region in the MAPK. For example, the interaction between the MKP-3 phosphatase and ERK1/2, which stimulates the catalytic activity of the MKP-3, involves a 14-residue motif called KIM that is also present in the Tyr c both of which regulate ERK1/2 phosphorylation but not JNKs or p38s (Pulido R et al., 1998). Sacco et al. demonstrated that the transmembrane receptor protein tyrosine phosphatase density-enhancing phosphatase-1 (DEP-1/PTPRJ) also targets ERK1/2

through the juxta-membrane KIM motif (Ding et al., 2010; Sacco et al., 2009).

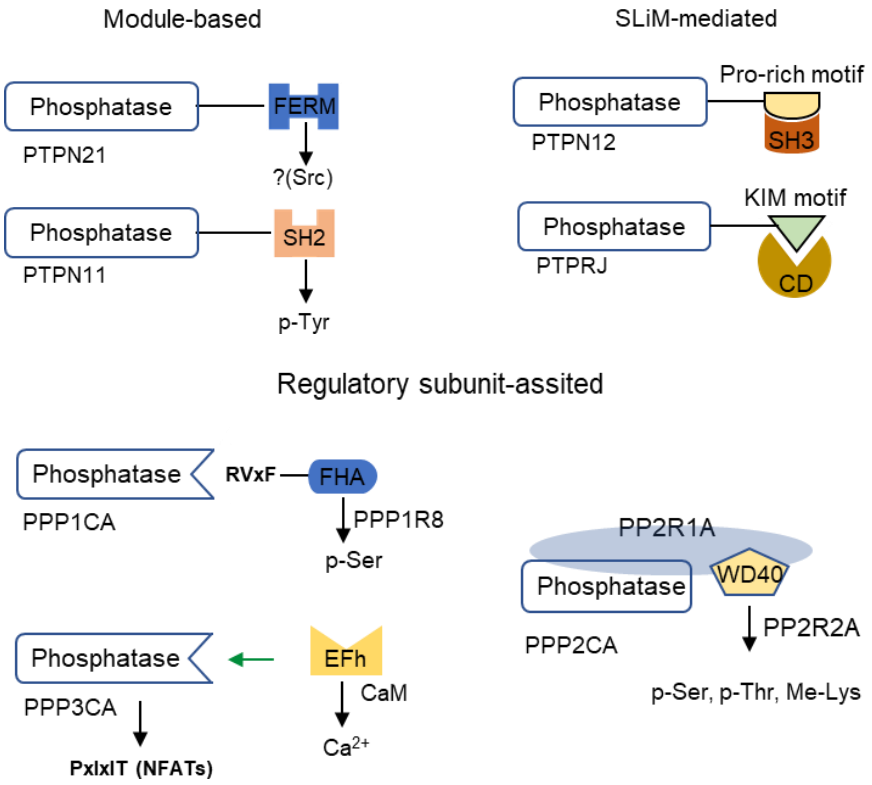

Figure 5. Overview of the main types of phosphatase-substrate recognition. Module-based: the catalytic domain is covalently linked to an accessory domain that targets the substrate; SLiM-mediated: the phosphatase contains one (or more) short linear motif (SLiM), which is recognized by a binding domain in the substrate; Regulatory subunit-assisted: the phosphatases bind non-covalently to regulatory subunits or scaffold proteins and act in concert to target substrate dephosphorylation. Adapted from (Sacco, et al., 2012).

Phosphatases catalytic subunit can also associate with multiple regulatory subunits and other proteins, which provide the ability to form different holoenzymes, each with potentially distinct substrate specificity (Shi, 2009). In this case, the catalytic and targeting

domains are located in different proteins and work together to target substrate dephosphorylation. This is exemplified by PP2A, which has a unique tripartite organization. The scaffold and the catalytic subunits are each encoded by two genes, and the regulatory subunits of PP2A comprise four families. Combining these three subunits allows a large number of heterotrimeric PP2A holoenzymes, each of which could have different substrates and functions. For example, The δ isoform of regulatory B′ subunit allows the dephosphorylation of the phosphatase Cdc25 triggering cell-cycle progression (Margolis et al., 2006). Other interacting proteins may help PP2A to target specific cellular locations. This is the case of shugoshin that recruits PP2A where it dephosphorylated cohesin, thereby preventing premature sister chromatid separation (Xu et al., 2009). Another example is PPP3CA/calcineurin whose activation requires that both its regulatory protein B subunit and calmodulin bind to calcium ions and displace the self-inhibitory fragment of the phosphatase domain from the catalytic cleft (Perrino et al., 1995).

2. p38α as a master regulator of cell signaling

2.1. The mitogen-activated protein kinase family

MAPKs are evolutionary conserved Ser/Thr protein kinases belonging to the CMGC kinase group that also includes glycogen synthases kinase (GSK), CDKs and CDK-like kinases. CDKs are the closest relatives to MAPKs (Manning G et al., 2002). MAPKs play a key role in transduction extracellular signals to various cellular responses, including gene expression, cell cycle control, metabolism, motility, survival, apoptosis and differentiation.

In mammals, 14 distinct MAPKs are classified as conventional or atypical based on their sequence and activation mechanism (**Figure 6**). Conventional MAPK families comprise four subfamilies: the extracellular signal-regulated kinases 1/2 (ERK1/2) (Cobb MH et al., 1991), c-Jun N-terminal kinases 1/2/3 (JNK1/2/3) (Dérijard et al., 1994; Kyriakis et al., 1994), p38α, β, γ, and δ (Freshney et al., 1994; Han et al., 1995; Lee et al., 1994; Rouse et al., 1994) and ERK5 (Lee et al., 1995; Zhou et al., 1995). Atypical MAPKs include ERK3/4, ERK7, and Nemo-like kinase (NLK).

Conventional MAPK pathways consist of three components: a MAPK, a MAPK kinase (MAP2K), and a MAP2K kinase (MAP3K). The MAP3Ks are often activated through phosphorylation and/or as a result of their interaction with a small GTP-binding protein of the Ras/Rho family. MAP3K activation leads to the phosphorylation and activation of a MAP2K, which then stimulates MAPK activity through dual phosphorylation on Thr and Tyr residues within a conserved Thr-X-Tyr motif located in the activation loop of the kinase domain, whose phosphorylation is essential for enzymatic activity. Each pathway regulates several distinct and sometimes overlapping cellular functions.

In general, the ERK1/2 cascade is strongly activated in response to mitogenic signals elicited by growth factors and phorbol esters, and play a central role in cell growth and survival (Krishna M and Narang H, 2008), whereas JNK and p38 cascades are activated mainly by intracellular and environmental stresses, including proinflammatory cytokines, oxidative stress and DNA damage (Kyriakis and Avruch, 2012; Owens and Keyse, 2007; Pearson et al., 2001). The ERK5

cascade seems to respond equally to specific stresses and mitogenic signals. Once activated, MAPKs phosphorylate target substrates on Ser or Thr residues, usually followed by a Pro (Ser/Thr-Pro).

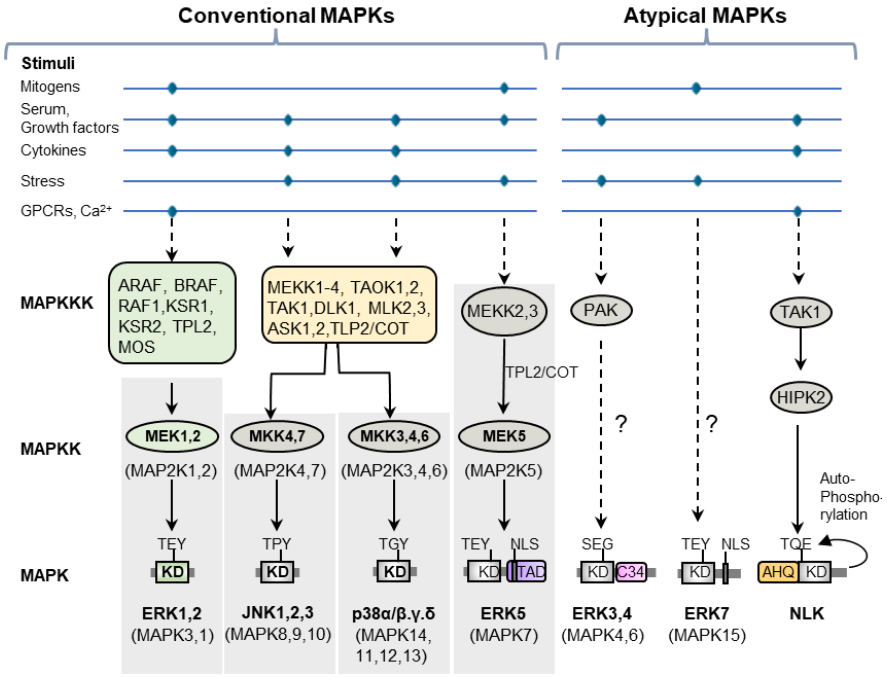

Figure 6. The MAPK signaling cascades. MAPKs are classified as conventional or atypical according to their sequence and activation mode. Conventional MAPKs have a TXY motif in their activation loop and a single kinase domain (KD) with short N- and C-terminal regions. Atypical MAPKs have a phospho-activating motif that diverges from the TXY consensus sequence, except for ERK7 and they have long N- or C-terminal sequences containing additional domains that may serve regulatory purposes. Conventional MAPKs are part of three-tiered kinase cascades that include upstream MAP2Ks and MAP3Ks, which receive signals from membrane-bound receptors. Each pathway differs from the others in its sensitivity to external stimuli. Adapted from Lavoie et al., 2020.

Atypical MAPKs have long N- terminal or C- terminal sequences that may serve regulatory purposes and, except for ERK7, their phospho-

activating motif diverges from the Thr-X-Tyr consensus sequence (Lavoie et al., 2020). MAPK phosphorylation events can be inactivated by MAPK phosphatases (MKPs or DUSPs) that dephosphorylate both phospho-Thr and phospho-Tyr residues on MAPKs (Liu et al., 2007; Pimienta and Pascual, 2007; Zhang and Dong, 2007).

2.2. The p38 MAPK family

There are four genes encoding mammalian p38 MAPKs: *MAPK14* for p38α, *MAPK11* for p38β, *MAPK12* for p38γ, and *MAPK13* for p38δ. The best characterized family member is p38α that is expressed in most cell types and is the homolog of Hog1 in *Saccharomyces cerevisiae*. p38α was discovered independently in four studies: as a tyrosine phosphoprotein of 38 kDa that was detected in cells following lipopolysaccharide (LPS) stimulation; as a protein kinase named RK that phosphorylates MAPKAPK2 (MAP kinase-activated protein kinase 2) and was activated in response to sodium arsenite, heat shock, or osmotic stress; as a protein kinase named p40 that was activated in response to interleukin-1(IL-1); and as CSBP2, the target of pyridinyl imidazole compounds such as SB203580 with anti-inflammatory properties (Canovas B and Nebreda AR, 2021). p38 MAPKs share more than 60% amino acid sequence identity, with p38β sharing more amino acid sequence identity with p38α (~75%), while p38γ and p38δ share ~60% identity with p38α. p38γ and p38δ, are 75% identical, share high sequence homology with CDKs and are sensitive to some CDK inhibitors (Tomás-Loba et al., 2019). Moreover, several alternatively spliced variants of p38α have been

described, such as CSBP1(Lee et al., 1994), Exip (Sudo et al., 2002), and Mxi2 (Sanz et al., 2000), but their roles in and contribution to cell pathophysiology are unclear.

Despite the high sequence homology, p38α, p38β, p38γ, and p38δ differ in their tissue expression pattern, upstream activators and target preferences, as well as their sensitivity to chemical inhibitors (Coulthard et al., 2009). p38α and p38β are expressed ubiquitously in all the tissues, with p38α usually at higher levels than p38β except in some brain regions. In contrast, p38γ is highly expressed in skeletal muscle, and p38δ is mainly found in the salivary, pituitary, and adrenal glands (Ono and Han, 2000). Notably, p38α knockout mice die at the embryonic stage due to placental morphological defects (Adams et al., 2000; Mudgett et al., 2000), while p38β, p38δ, or p38γ knockout mice are viable and do not have development defect (Beardmore et al., 2005; Sabio et al., 2005).

2.3. Mechanism of p38 MAPK activation

The p38 MAPK pathway is activated by most stress stimuli, including LPS, UV light, heat shock, osmotic shock, inflammatory cytokines, glucose starvation, and oncogene activation. It is also activated by growth factor receptors in some circumstances as well as by the T-cell receptor (Han et al., 2020). Of note, the activation of p38 MAPKs is context-dependent since cell type or disease-specific genetic alterations may affect the wiring of signal networks.

The canonical activation pathway

The canonical activation of p38 MAPKs involves a three-tiered kinase cascade. In response to appropriate stimuli, p38 MAPK is

activated through dual phosphorylation of Thr180 and Tyr 182 on the Thr-Glu-Tyr motif located in the activation loop by a MAP2K, which in turn is phosphorylated by MAP3K. This phosphorylation induces a conformational change in the protein, enabling ATP and substrate binding (Cuenda and Rousseau, 2007). Three MAP2Ks can phosphorylate p38 MAPKs: MKK6, MKK3 and MKK4. MKK6 is capable of activating all four p38 MAPKs, whereas MKK3 activates p38α, p38γ and p38δ, but not p38β (Alonso et al., 2000; Cuadrado and Nebreda, 2010). MKK4 has also been reported to phosphorylate p38α and p38δ in specific cell types (Dérijard et al., 1995). Of note, MKK6 and MKK3 share 80% sequence identity(Stein et al., 1996) and are highly selective for p38 MAPKs (Cuenda and Rousseau, 2007; Enslen et al., 1998), while MKK4 is a typical activator for JNKs. The selective activation of p38 MAPKs by each MAP2K depends on both the stimulus and the cell type.

In mammals, up to10 MAP3Ks have been identified to trigger p38 MAPK activation: ASK1 (apoptosis signal-regulating kinase 1), DLK1 (dual-leucine-zipper-bearing kinase 1), TAK1 (transforming growth factor β-activated kinase 1), TAO1 and 2 (thousand-and-one amino acid 1 and 2), TPL2 (tumor progression loci 2), MLK3 (mixed-lineage kinase 3), MEKK3 and 4 (MAPK/ERK kinase 3 and 4), and ZAK1 (leucine-zipper and sterile-αmotif kinase 1) (Cuadrado and Nebreda, 2010). Some of them can also trigger activation of other MAPKs, mostly JNKs. Upstream of the cascade, the regulation of MAP3Ks is complicated, including phosphorylation by STE20 family kinases, binding of small GTP-binding proteins of the Rho family such as Rac or Cdc42, or ubiquitination-based mechanisms.

The diversity and regulatory mechanism of p38 MAPK upstream components allow the pathway to integrate a broad range of stimuli and provide versatility to the response (Canovas B and Nebreda AR, 2021).

Non-canonical activation mechanisms

Although MAP2K-catalyzed phosphorylation is considered the primary mechanism for p38 MAPK activation, two alternative non-canonical mechanisms can also activate p38α through autophosphorylation. One is the direct binding of TAK1-binding protein 1 (TAB1), which induces autophosphorylation of p38α on the activation loop, but not of other p38 MAPKs (Ge et al., 2002). TAB1-dependent p38α activation has been implicated in ischemic myocardial injury, T cell senescence, skin inflammation, triiodothyronine-mediated browning of white adipose tissue and endothelial inflammation triggered by G protein-coupled receptor (GPCR) agonists (Canovas B and Nebreda AR, 2021). More recently, other proteins have been reported to bind to and induce p38α autophosphorylation (de Nicola et al., 2013). The other non-canonical activation mechanism is mediated by the Src-family Tyr kinase ZAP70 (zeta-chain-associated protein kinase 70), which is exclusive to T-cells and involves T-cell receptor (TCR) activation. ZAP70 phosphorylates p38α or p38β on Tyr323, triggering their autophosphorylation on Thr180. This mono-Thr180 phosphorylated p38 has been reported to have partial kinase activity and to target specific substrates (Mittelstadt et al., 2009).

2.4. Inactivation of the p38 MAPK pathway

p38 MAPKs are often transiently activated under physiological conditions, and their hyperactivation is usually deleterious for the cells. Therefore, inactivation/termination of the pathway is crucial for cell homeostasis. Inactivation of p38 MAPKs and signal termination is mainly achieved through dephosphorylation of both Thr and Tyr residues in the kinase activation loop by phosphatases.

The most studied phosphatases responsible for p38 MAPK dephosphorylation are dual-specificity phosphatases (DUSPs) also known as MAP kinase phosphatases (MKPs), which belong to the protein-Tyr phosphatase superfamily and can dephosphorylate both phospho-Thr and phospho-Tyr residues. MKP1, MKP4, MKP5 and MKP7, can efficiently dephosphorylate p38α and p38β in addition to JNKs (Cuadrado and Nebreda, 2010), whereas p38γ and p38δ are resistant to all known MKP family members. In addition to MKPs, p38 MAPKs can be also targeted by the Ser/Thr protein phosphatases Wip1/Ppm1d (Yu et al., 2006) and PP2Cα (Takekawa et al., 1998), and by the protein tyrosine phosphatases HePTP (Hematopoietic protein tyrosine phosphatase) (Zhang et al., 2008), and SIP1 (calcyclin-binding protein/Siah-1 interacting protein) (Topolska-Woś et al., 2017). Targeting by these phosphatases results in monophosphorylated forms of the p38 MAPKs. However, the specificity among phosphatases and their roles in controlling the p38 MAPK pathway are still not well understood.

2.5. Downstream substrates of p38α

Upon phosphorylation-mediated activation, p38α can phosphorylate many substrates on Ser or Thr residues, which are usually followed by a Pro residue. To date, more than 115 substrates have been identified, which are located throughout the cells and regulate a wide variety of cellular processes, including transcription and chromatin remodeling, mRNA stability and translation, protein degradation and localization, cell cycle progression, endocytosis, metabolism and cytoskeleton dynamics (**Figure 7**) (Han et al., 2020; Trempolec et al., 2013).

Protein kinases

An important group of p38α substrates are protein kinases, which in turn phosphorylate additional proteins, expanding the versatility of the pathway to regulate diverse processes. The first identified p38α substrate was MAPKAPK2 also known as MK2, together with its related family members MK3 and MK5, which can phosphorylate many substrates. For instance, phosphorylation of Heat-shock protein 27 (Hsp27) by MK2 controls cell mobility and actin cytoskeleton remodeling (Menon et al. 2009). Other MK substrates are LSP1 (lymphocyte-specific protein 1), ATF1 (activating transcription factor 1), and the RNA-binding proteins AUF1 **(**AU-rich element RNA-binding protein 1), TTP (tristetraprolin) and HuR (human antigen R) that modulate transcript stability of many genes like TNFα, Cyclin D1, Plk3, c-Fos and c-Myc (Soni et al., 2019).

p38α can also phosphorylate MSK1 and 2 (mitogen- and stress-activated protein kinase 1 and 2) (Deak et al., 1998), which in turn

control transcription by mediating CREB, NFkB or STAT activation and chromatin remodeling via histone phosphorylation (Arthur, 2008; Soloaga et al., 2003). Other kinases phosphorylated by p38α are MNK1 and 2 (MAPK Interacting Ser/Thr Kinase 1 and 2), which regulate protein synthesis by phosphorylating the eukaryotic initiation factor 4E (eIF4E), and glycogen synthase kinase 3 β (GSK3β), which can be inactivated by Ser389 phosphorylation leading to β-catenin accumulation (Bikkavilli R K et al., 2008).

Interestingly, some proteins that are phosphorylated by p38α downstream kinases can also be phosphorylated by p38α itself, such as the MK2 substrates Cdc25B, Hsp27 and HuR, or the MSK1/2 substrate histone H3. This double targeting of downstream substrates might function as a fail-safe mechanism to limit inappropriate effector activation.

DNA/RNA-binding proteins

A larger number of p38α substrates are DNA- or RNA-binding proteins involved in the regulation of gene expression. There is good evidence that p38α can directly phosphorylate several transcription factors, usually leading to enhanced transcription activity. These transcription factors usually are stimulus- and cell-type-dependent and play important roles in many processes. For example, TEAD4 (transcriptional enhancer factor domain family member 4), RB (retinoblastoma protein), p53, and BRN2 (POU domain transcription factor) can be phosphorylated by p38α in response to stresses, such as DNA damage and autophagy. STAT1 and 4 (Signal transducer and activator of transcription 1 and 4), p65-NFkB and CREB are related

to the immune response; ATF1/2/6, the CEBP (CCAAT/enhancer-binding protein) family members CEBPα/β/ε, DLX5 (distal-less homeo box 5), the MEF2 (myocyte-specific enhancer factor 2) family members MEF2A/C/D, p63, Runx1/2, and Osterix are involved in in cell differentiation.

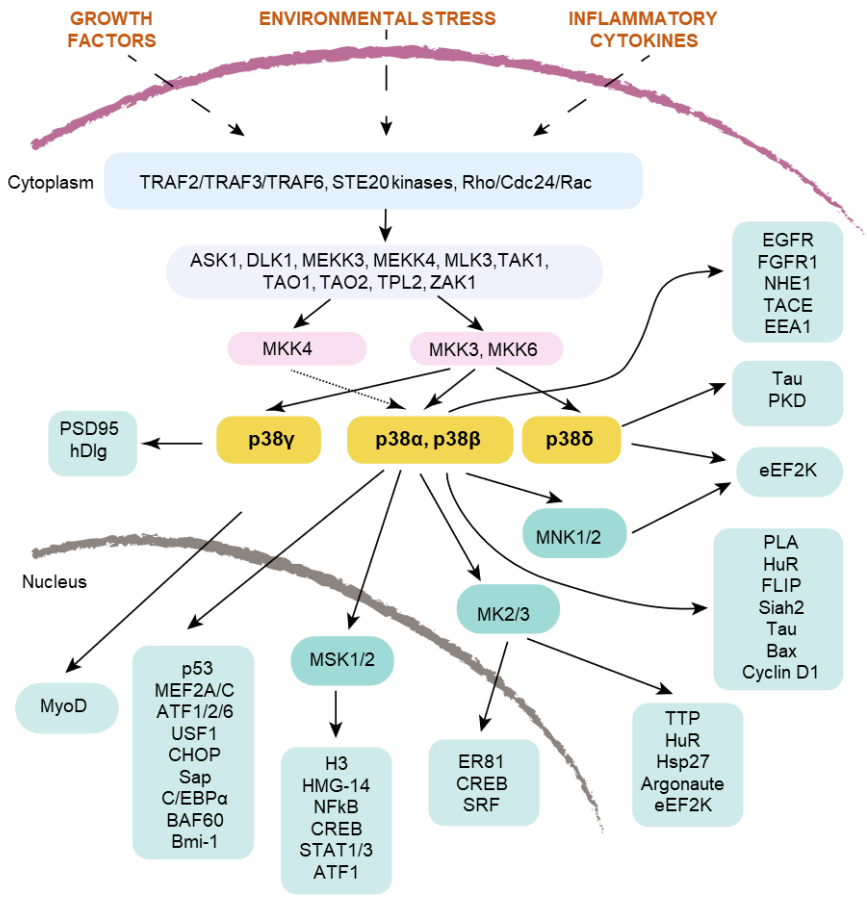

Figure 7. The p38 MAPK pathway. Mitogens and cellular stresses activate p38 MAPKs, which in turn phosphorylate many downstream targets, including protein kinases, cytosolic substrates, transcription factors and chromatin remodellers. Adapted from (Cuadrado & Nebreda, 2010).

However, p38α also represses transcription in some cases. For instance, phosphorylation of MRF4 (muscle-specific regulatory factor 4) on Ser31 and Ser42 by p38α represses its transcription activity resulting in downregulation of specific muscle genes at the terminal stages of muscle differentiation (Suelves et al., 2004). Likewise, p38α phosphorylates NFATc4 (nuclear factor of activated T cells 4) on Ser168 and Ser170, repressing PPARγ2 (peroxisome proliferator-activated receptor γ2) gene expression and adipocyte differentiation(Yang et al., 2002). In addition, p38α can also repress gene transcription by phosphorylating transcriptional repressors like HBP1 (HMG-Box Transcription Factor 1), which blocks the expression of various genes regulating cell cycle progression (Xiu et al., 2003).

Other DNA/RNA-binding proteins that are phosphorylated by p38α are chromatin remodeling regulators. Thus, phosphorylation of the SWI/SNF (SWItch/Sucrose Non-Fermentable) subunit BAF60c (BRG1-associated factor 60) on Thr229 by p38α is required for muscle differentiation by facilitating binding of the transcription factor MyoD to target genes and marking the chromatin for signal-dependent recruitment of the SWI/SNF core, which activates transcription of the MyoD-target muscle genes (Forcales et al., 2012). Other substrates include the transcriptional repressors EZH2 and RNF2, the chromatin remodeling SRCAP complex component p18Hamlet/Zn-Hit1, histone H2A family member H2AX. In addition, the RNA-binding proteins F2 and F3 (coagulation factor II and III) and RBM17 (RNA binding motif protein 17) regulate mRNA

processing, and HuR and KSRP regulate mRNA stability (Al-Ayoubi et al., 2012; Briata et al., 2005; Tiedje et al., 2012).

Other substrates

p38α can also phosphorylate several cytoplasmic proteins that are involved in different cellular processes, including cell cycle regulators (Cdc25A/B, Cyclin D1/3, p57kip2), cell death regulators (Bax, BimEL, Caspase-3/9) and MAPK pathway regulators (JIP4, Tip60, TAB1/3, FRS2). Other p38α substrates include membrane proteins (EGFR, FGFR1, Nav1.6, NHE1, PLA2, TACE), cytoskeleton proteins (Keratin 8, Lamin B1, Paxillin, Stathmin, Tau and Tensin) and endocytosis regulators (EEA1, GDI-2, Rabenosyn-5), which are involved in cytoskeleton organization, intracellular membrane trafficking and protein degradation (Han et al., 2020; Trempolec et al., 2013).

Altogether, the variety of known targets phosphorylated by p38α provide cells with the required information to orchestrate an adequate response to specific signals. However, the way in which p38α selectively regulates the targets in different disease settings and determines the signal strength and duration still needs further study.

3. Role of p38α in cell adhesion

Cell adhesion is the process by which cells contact each other or their extracellular matrix (ECM) components through specialized protein complexes. Homeostasis in healthy tissues strongly depends on cell-cell and cell-ECM contacts. Nevertheless, tumor cells often show a decrease in cell-cell and/or cell-matrix adhesion. In consequence, changes in cell adhesion may lead to tumorigenesis and metastasis.

In developing solid tumors, stable adhesion between epithelial cells is usually lost, allowing malignant cells to acquire the migratory properties required for invasion and metastasis. However, the invasion ability of metastatic tumor cells depends on effective cell adhesion during circulation, colonization of distant organs, and interaction with the ECM at the metastasis site.

Cell-cell adhesion can be regulated through adherens junctions, tight junctions and desmosomes, while cell-ECM adhesion is mainly regulated through focal adhesions (**Figure 8**). Proteins involved in these interactions are called cell adhesion molecules (CAMs) and are mainly classified into four groups: cadherins, integrins, selectins, and immunoglobulins. Among them, cadherins and immunoglobulins are homophilic CAMs, and they bind to the same type of CAM directly on another cell, while integrins and selectins are heterophilic CAMs that bind to different types of CAMs. These CAMs often contain an intracellular domain, a transmembrane domain, and an extracellular domain (Makrilia et al., 2009; Moh and Shen, 2009). The intracellular domain directly interacts with the cytoskeleton or through a scaffold protein and is responsible for signal transduction, while the extracellular domain interacts with other CAMs or ECM components. Therefore, although the primary role of CAMs is to maintain cell-cell contact and attachment to the ECM, they can also act as signaling effectors integrating extracellular signals with cell-intrinsic signaling to control many intracellular responses, cytoskeletal organization and gene expression (Janiszewska et al., 2020; Mui et al., 2016).

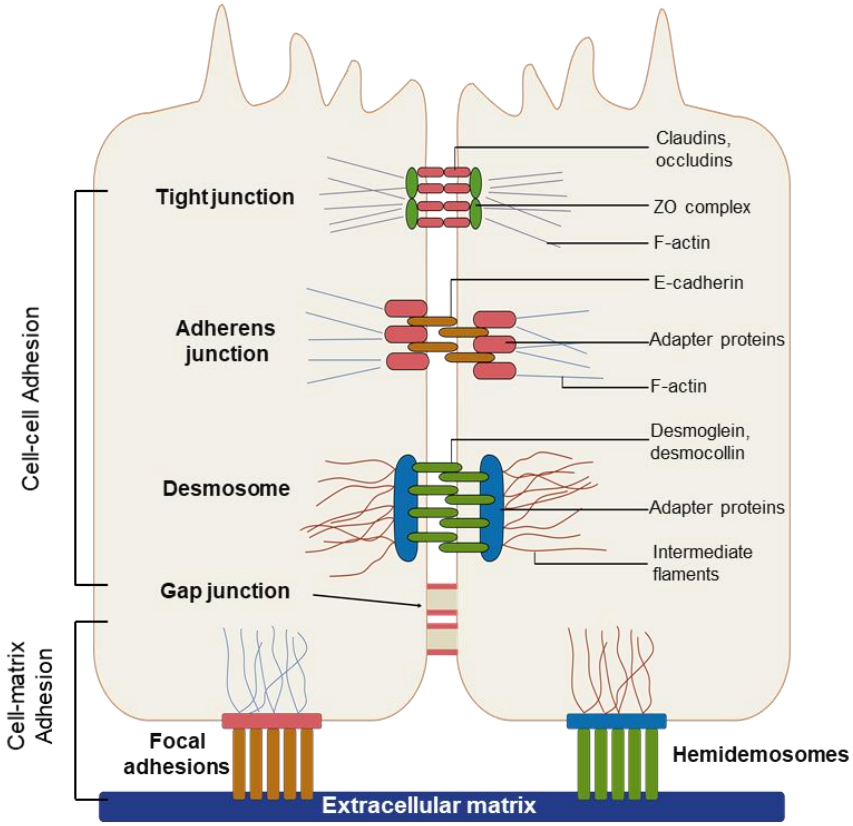

Figure 8. Scheme of different types of cell adhesion, including cell-cell adhesion and cell-matrix adhesion. Tight junctions build a seal between adjacent cells and are connected to actin filaments. Adherens junctions are plaques of classical cadherins linked to the actin cytoskeleton. Desmosomes are formed by desmosomal cadherins, linked to intermediate filaments. Gap junctions connect the cytoplasm of two adjacent cells and are linked to microfilaments. Focal adhesions (linked to actin) and hemidesmosomes (linked to intermediate filaments) are cell-matrix junctions that are formed by integrins. Adapted from (Schnell et al., 2001).

Cell adhesion is essential for cell migration, and several studies have implicated p38α in the regulation of cell migration. For example, p38α can promote the metastasis of breast cancer, ovarian cancer and melanoma by targeting various proteins involved in the regulation of

epithelial-mesenchymal transition, cell migration and extravasation (Canovas B and Nebreda AR, 2021). However, the specific role of p38α in cell adhesion is still poorly understood.

3.1. p38α in adhesion to the ECM

Several studies suggested that p38α may control cell adhesion to the ECM through the regulation of CAM expression, especially intercellular cell adhesion molecule-1 (ICAM-1), vascular cell adhesion molecule-1 (VCAM-1), E-selectin and paxillin. For example, in response to IL-1β, p38α represses the expression of E-selectin at the transcriptional and the post-transcriptional level via miR-146a and miR-31, respectively, impairing adhesion of colon cancer cells to the endothelium (Zhong et al., 2018). In human pulmonary microvascular endothelial cells (HPMVECs) stimulated with LPS/IFN-γ, JNK activation mediates ICAM-1 expression, thereby promoting leukocyte adherence and transmigration, while p38α inhibition significantly reduces ICAM-1 expression by blocking JNK activation (Suzuki et al., 2018). However, reduced ICAM-1 expression by p38α inhibition is not necessary for impaired adhesion. For instance, p38α inhibition by SCIO-469 can suppress multiple myeloma cell proliferation and adhesion in the bone marrow microenvironment in an ICAM-1- and VCAM-1-independent mechanism (Nguyen et al., 2006). Other studies also found that p38α regulates the adhesion of chronic myeloid leukemia cells to fibronectin through paxillin. In this case, p38α interacts with the Rap Guanine Nucleotide Exchange Factor 1 (C3G), adaptor protein CrkL, FAK and paxillin and regulates the expression of paxillin, CrkL and

α5 integrin, as well as the phosphorylation of paxillin, to modulate the formation of different protein complexes at focal adhesions (Maia et al., 2013).

TGFβ (transforming growth factor β) can regulate cell adhesion in a variety of cells, and it was suggested that p38α could mediate TGFβ-induced adhesion in metastatic prostate cancer cells through phosphorylation of the Smad transcription factors (Hayes et al., 2003).

Interestingly, p38α has been also reported to regulate cell adhesion negatively. Guo and Yang (Guo and Yang, 2006) found that embryonic stem (ES) cells isolated from p38α knockout mouse embryos show significantly increased cell adhesion to ECM proteins, gelatin, collagen, fibrinogen, and fibronectin, which correlated with elevated phosphorylation of FAK and paxillin. These findings suggest that p38α may integrate distinct mechanisms to regulate cell adhesion in somatic and stem cells.

3.2. p38α in cell-cell adhesion

It was reported that p38α could impair cell-cell adhesion mainly by modulating tight junction-related proteins such as occludin and ZO-1. In response to stimuli that disrupt cell-cell adhesion, p38α is activated, and ZO-1 is downregulated, which can be rescued by p38α inhibition. For instance, Clopidogrel-induced gastric epithelial cell tight junction destruction is accompanied by p38α activation and can be rescued by p38 dephosphorylation mediated by MKP-5 overexpression (Wu et al., 2020). Hyperoxia exposure enhances p38α activation by ROS and disrupts the tight junctions in the alveolar

epithelial cells MLE-12 by suppressing the expression of claudin-18. By contrast, p38α downregulation restored the expression of claudin-18 and the barrier function with higher transepithelial electrical resistance and lower transwell monolayer permeability (Shen et al., 2021). p38α activation also contributes to calcium oxalate monohydrate crystal-induced tight junction disruption by downregulating ZO-1 and occludin expression in distal renal tubular epithelial cells (Feldman et al., 2007).

It has also been reported that $CdCl_2$ induces disruption of the blood-testis barrier (BTB) through reducing occludin and ZO-1 expression from the BTB site in the seminiferous epithelium upon treatment with TGFβ3. This effect occurs concomitant with p38α activation, and p38α inhibition recovers occludin and ZO-1 expression (Lui et al., 2003). Intriguingly, $CdCl_2$-induced occludin and ZO-1 loss from the BTB is also associated with loss of the cadherin/catenin and the nectin/afadin protein complexes at the site of cell-cell actin-based adherens junctions suggesting that the TGFβ3/p38α axis participates in both tight junction and adheren junction dynamics in the testis, by mediating the effects of TGFβ3 on the tight junction and adheren junction-integral membrane proteins and adaptors.

p38α contributes to IL1β or sorbitol-induced inhibition of gap junction communication in Astrocytes through phosphorylation of connexin 43 (Zvalova et al., 2004). Also, p38α is activated during hepatocyte regeneration after liver injury in rats, accompanied by down-regulation of connexin 32 and up-regulation of claudin-1. In this model, administration of the p38 inhibitor SB203580 inhibited the downregulation of connexin 32 and enhanced the up-regulation

of claudin-1, maintaining the gap and tight junction structures, which are important for preventing hepatic damage (Yamamoto et al., 2005).

Paradoxically, there is also evidence that p38α positively controls cell adhesion in some cases. Thus, p38α inhibition was reported to compromise tight junction integrity during blastocyst formation by increasing tight junction permeability and shifting ZO-1 localization to tight foci at cell-cell contacts with punctate staining and losing F-actin colocalization, which is typically distributed along the apical-basal membrane in a smooth, continuous pattern and co-localized with the cytoskeleton (Bell and Watson, 2013). Likewise, p38 inhibition led to the disorganization and downregulation of cytokeratin filaments and ZO-1, whereas vimentin expression was increased during epithelial-to-mesenchymal transition (EMT), which is characterized by the disruption of intercellular junctions and acquisition of migratory and invasive phenotypes (Strippoli et al., 2010).

These observations indicate p38α is important in cell adhesion by regulating CAMs expression. However, little is known about the mechanisms involved in this modulation. Therefore, further studies are needed to understand the role of p38α in cell adhesion.

OBJECTIVES

The main goal of this study was to increase our understanding of the mechanisms and signaling networks regulated by p38α during cancer cell homeostasis, which may help identify specific targets for particular functions.

Specific objectives

Identify new p38α targets in cancer cells.

Explore new roles of p38α in maintaining cancer cell homeostasis.

Define signaling networks regulated by p38α.

RESULTS

1. Experimental strategy to study the p38α MAPK modulated proteome and phosphoproteome

To increase our understanding of how the p38 MAPK pathway regulates breast cancer cell homeostasis, we conducted quantitative proteomic and phosphoproteomic analysis to identify protein expression and site-specific phosphorylation changes controlled by p38 MAPK.

To this end, we used the mammary epithelial cancer cell line BBL358 (Cánovas et al., 2018). These cells were derived from the mammary tumor of a mouse expressing the transgene encoding the polyoma middle T (PyMT) antigen (Guy et al., 1992) together with ubiquitin-CreERT2 (UbCre) and floxed alleles of the gene encoding p38α (*Mapk14*), which allows the deletion of p38α upon 4-hydroxitamoxifen (4-OHT) administration (referred to as p38α KO from now on). In order to better understand the p38α-regulated mechanisms, we decided to compare the effect of p38α KO with the inhibition of p38α using PH797804 (PH), a highly specific ATP-competitive inhibitor (Selness et al., 2011).

To validate the system, we analyzed p38α expression and the phosphorylation of downstream pathway components by Western blotting. p38α was efficiently lost following 4-OHT treatment, and the downstream pathway was shut off as shown by the decreased p-MK2 and p-Hsp27 levels (**Figure 9**). Likewise, PH treatment inhibited p38α signaling as shown by the reduction of p-MK2 and p-Hsp27.

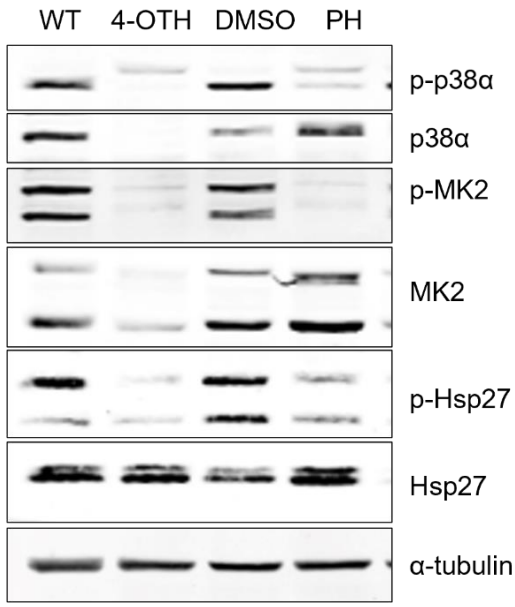

Figure 9. Incubation with 4-OHT and PH efficiently downregulates p38α signaling in BBL358 cells. For p38α KO induction, cells were treated with 4-OTH for 48 h and left to recover for another 48 h before collection. For p38α inhibition, cells were incubated with PH for 24 h and then collected for Western blotting.

To quantify changes in the p38α-regulated proteome and phosphoproteome, we used stable isotope labeling by amino acids in cell culture (SILAC) (Ong et al., 2002). Briefly, three groups of BBL358 cancer cells were metabolically labeled with stable isotope-containing heavy-, medium- and light- amino acids in culture. After culturing several passages to ensure the complete incorporation of labeled isotopes, the non-labeled (Light-) population was treated with 4-OHT to induce p38α deletion. The medium-labeled population was treated with PH to inhibit p38α kinase activity, and the heavy-labeled population was left untreated as WT. Cell lysates were prepared from the three groups of cells, combined in equal ratios (1:1:1) and

digested with trypsin. An aliquot of the lysate was used to analyze the proteome, and the remainder was run through titanium oxide columns to enrich phospho-peptides in order to analyze the phosphoproteome. Samples were analyzed by nano-liquid chromatography-electrospray ionization tandem mass spectrometry (nanoLC-ESI-MS/MS) in four biological replicates, of which three were re-analyzed as technical replicates (**Figure 10**).

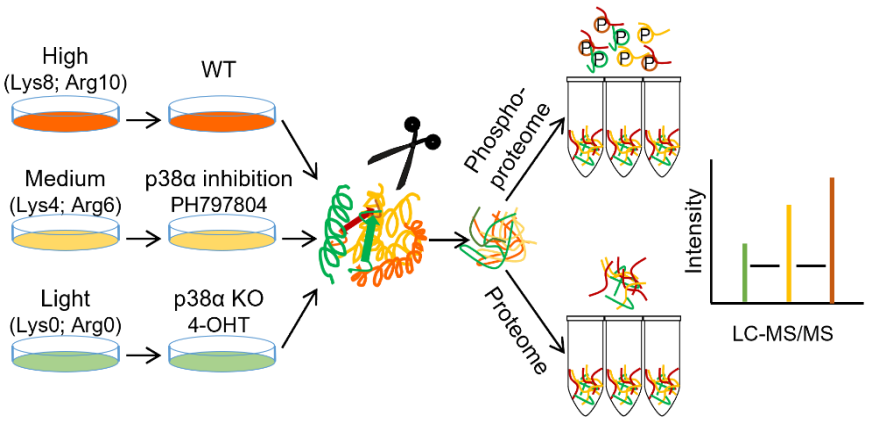

Figure 10. Strategy used to study the p38α modulated proteome and phosphoproteome by SILAC. Cells were metabolically labeled with stable isotope-containing heavy-, medium- and light-amino acids in the culture media. Light-labeled cells were treated with 4-OHT to induce p38α deletion. Medium-labeled cells were treated with the p38α inhibitor PH797804, and heavy-labeled cells were used as untreated controls. Whole-cell lysates were digested with trypsin, and an aliquot was directly analyzed to identify the proteomic changes. The rest of the lysate was run through titanium oxide columns to enrich for phosphorylated peptides.

To facilitate subsequent analysis, log2 fold changes and p-values of KO versus WT (KO/WT) and PH versus WT (PH/WT) were calculated. The data were filtered to retain only proteins that out of

the seven replicates analyzed show valid quantification values in at least four replicates for the proteomic dataset and at least three replicates for the phosphoproteomic dataset.

2. Global proteomic changes modulated by p38α

2.1. Quantification of p38α modulated global proteomics changes

In total, 3,920 proteins were identified in the proteome analysis, of which 2,560 were successfully quantified (**Figure 11A**), and at least two unique peptides were identified for 2,455 proteins (**Figure 11B**). To examine the effect of p38α KO and PH inhibition on global protein expression, we generated density plots depicting the distribution of log2-transformed fold changes (log2FC) (**Figure 11C**) and p-values (**Figure 11D**) of all quantified proteins for KO/WT and PH/WT comparisons.

We observed that in general, KO/WT has more log2FC close to 0 and fewer p-values close to 0 compared with PH/WT, indicating that p38α inhibition induced more changes than p38α KO. Surprisingly, the coefficient of variation (CV), which shows the dispersion among samples, for the intensity values was similar in all samples, and most values were lower than 2% (**Figure 11E**).

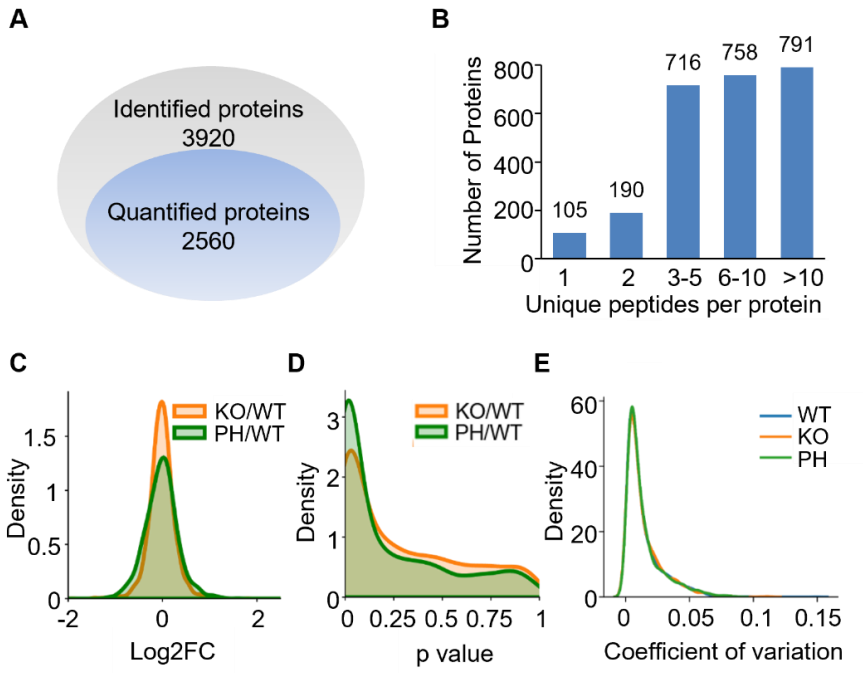

Figure 11. Overview of the p38α regulated global proteome. (A) Maxquant software identified proteins and the quantified proteins. The analysis was performed by removing the batch effect and performing a linear model. (B) Bar chart showing the distribution of the identified proteins based on the number of unique peptides. (C) Density plot showing the distribution of the log2FC change of proteins in p38α KO/WT and PH/WT. (D) Density plot showing the distribution of the p-values of proteins in p38α KO/WT and PH/WT. (E) Density plot showing the coefficient of variation (CV) distribution of normalized intensity per protein in the three samples.

Next, we calculated the correlation of the log2FC values between KO/WT and PH/WT analysis. With all quantified proteins, the correlation value was 0.419 (**Figure 12A**). We then limited this analysis to quantified proteins with p-values less than 0.05, which improved the correlation to 0.707 (**Figure 12B**), indicating that many protein changes were consistent upon p38α deletion and inhibition.

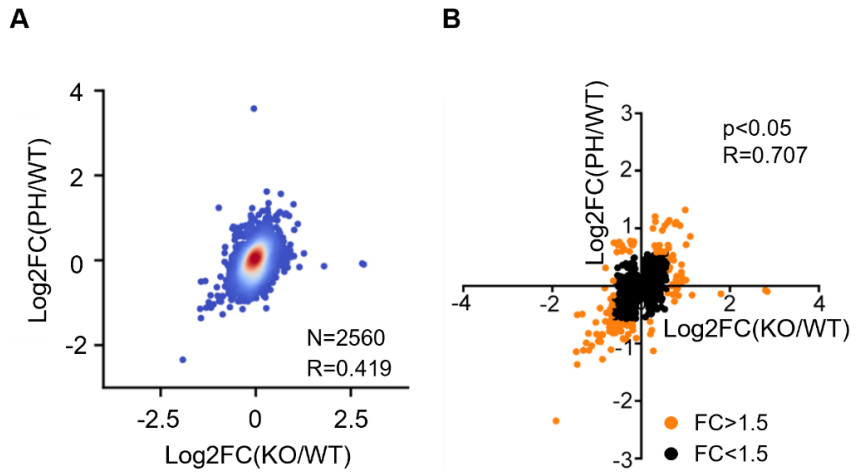

Figure 12. Correlation of proteomic changes between p38α KO/WT and PH/WT. (A) Correlation plot between p38α KO/WT and PH/WT log2FC of all quantified proteins. The color-coding indicates the density. Correlation is indicated by Pearson coefficient correlation (R). (B) Correlation plot between p38α KO/WT and PH/WT log2FC of quantified proteins with a p-value of less than 0.05. Orange-colored proteins had fold change higher than 1.5 or lower than -1.5 (log2(1.5)=0.58. Pearson coefficient correlation is indicated.

2.2. Identification of p38α dependent proteomic changes

To gain an insight into the biological meaning of the p38α regulated proteomic changes, we filtered both KO/WT and PH/WT datasets with a p-value less than 0.05 and a fold change higher than 1.5 or lower than -1.5 (**Figure 13A** & **B**). From all 2,560 quantified proteins, we identified that 43 proteins were positively and 37 negatively regulated in p38α KO cells compared with WT (**Figure 13A).** Upon PH inhibition, 130 proteins were positively and 99 proteins negatively regulated by p38α (Figure 12B). Among them, 25 proteins (16.9%) were down-regulated (**Figure 13C** & **Supplementary Table 1**), and 10 proteins (7.9%) upregulated in both p38α KO cells and PH treated cells compared with WT cells

(**Figure 13D** & **Supplementary Table 2**). Noteworthy, we found that the p38α protein level was downregulated in p38α KO cells, while no clear change was found in PH-treated cells, which was consistent with our observations by western blotting (**Figure 1**).

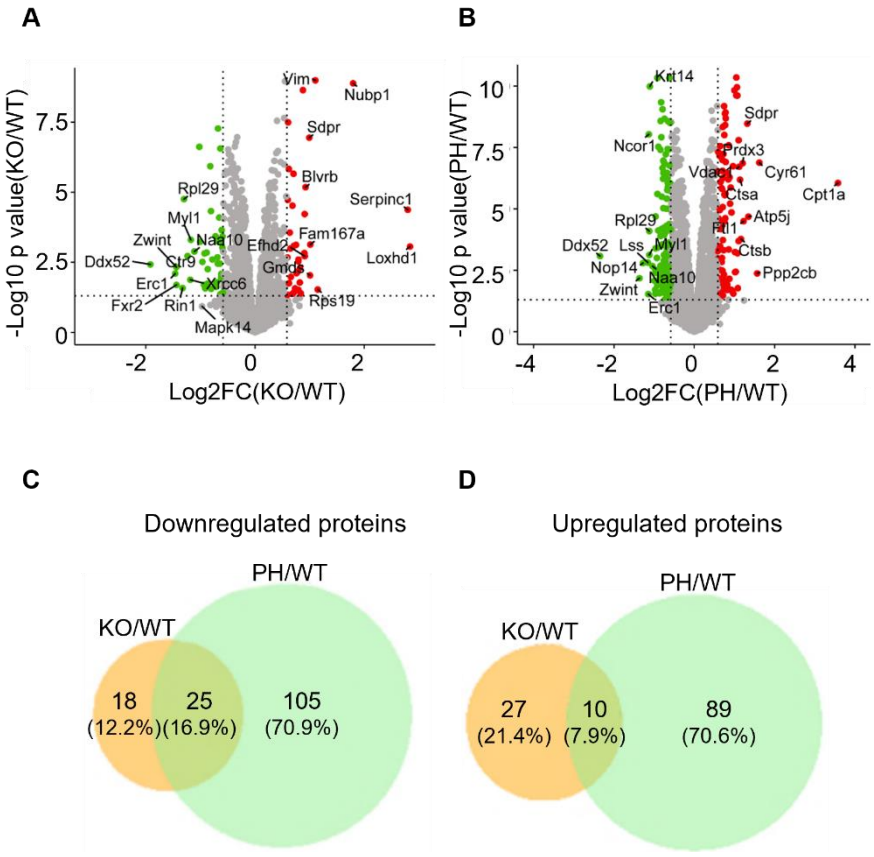

Figure 13. Changes in the proteome of p38α KO cells and p38α inhibidor-treated cells. (A) Volcano plots of log2FC of protein ratios in KO/WT. (B) Volcano plots of log2FC of protein ratios in PH/WT. Green indicates downregulated proteins with FC<-1.5, and red up-regulated proteins with FC>1.5 (C) Venn diagram showing the numbers of down-regulated proteins (p-value<0.05 and FC<-1.5 in KO/WT and PH/WT. (D) Venn diagram showing the numbers of up-regulated proteins (p-value<0.05 and FC>1.5) in KO/WT and PH/WT. Intersections in (C) and (D) indicate proteins significantly down- or up-regulated in both KO/WT and PH/WT (p-value<0.05 and FC >1.5 or <-1.5). Top 10 changed proteins are labeled.

2.3. Biological functions regulated by the p38α dependent proteome

To understand the biological functions potentially regulated by the p38α dependent proteome, we performed Gene Set Enrichment Analysis (GSEA v4.1.0). We found 36 enriched biological processes that were positively modulated by p38α and passed the filter criteria (FDR<0.05) for both KO/WT and PH/WT analysis. The enrichment results suggested that p38α positively regulated proteins related to DNA replication, DNA repair and translation, including ribosome and RNA processing (**Figure 14A).**

On the other hand, for p38α negatively modulated proteome, no enriched GO functions passed the FDR<0.05 filtering criteria in KO/WT analysis, and we decided to set the cutoff with FDR<0.25, which is appropriate according to GSEA guidelines. The results suggested the most enriched functions of p38α negatively modulated proteome were involved in extracellular structure, plasma membrane and cortical cytoskeleton organization, which may potentially affect cell adhesion ability. Another enriched function was related to ion transport, including cation, anion, and organic acid transport (**Figure 14B**).

A

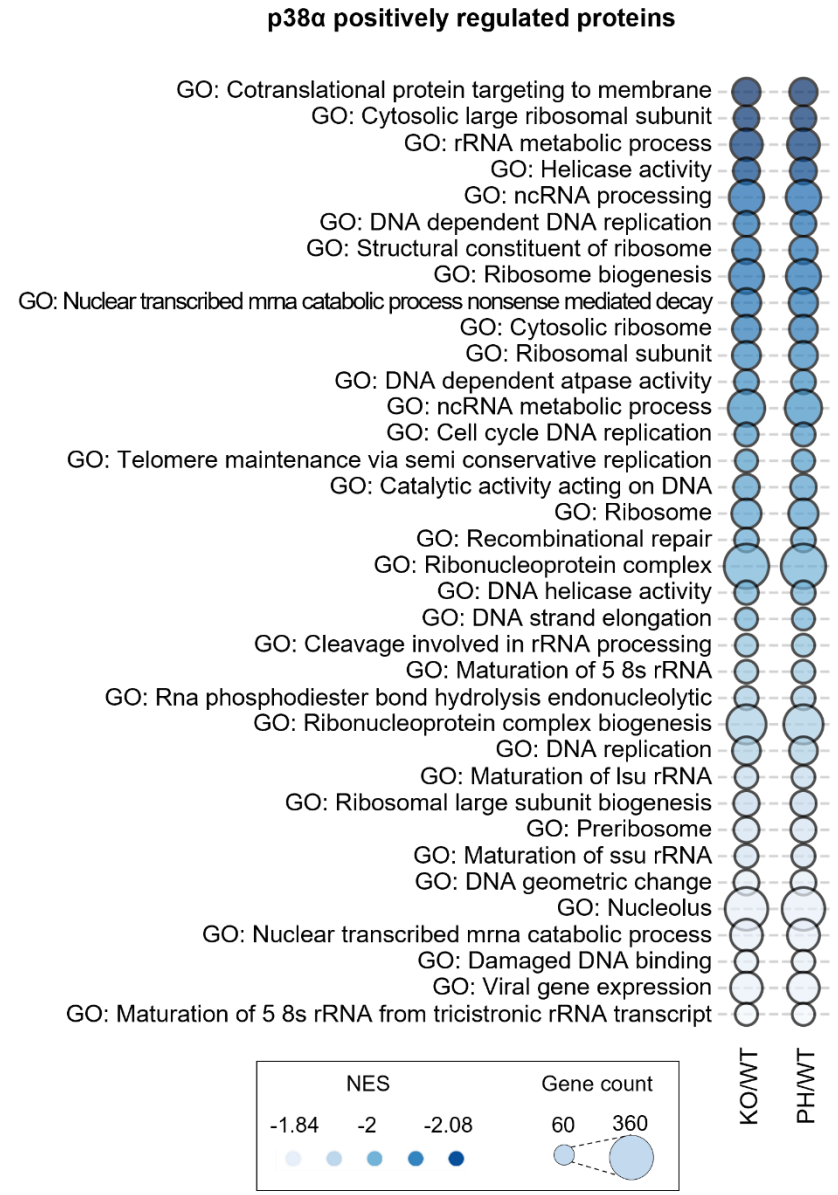

Continued on next page

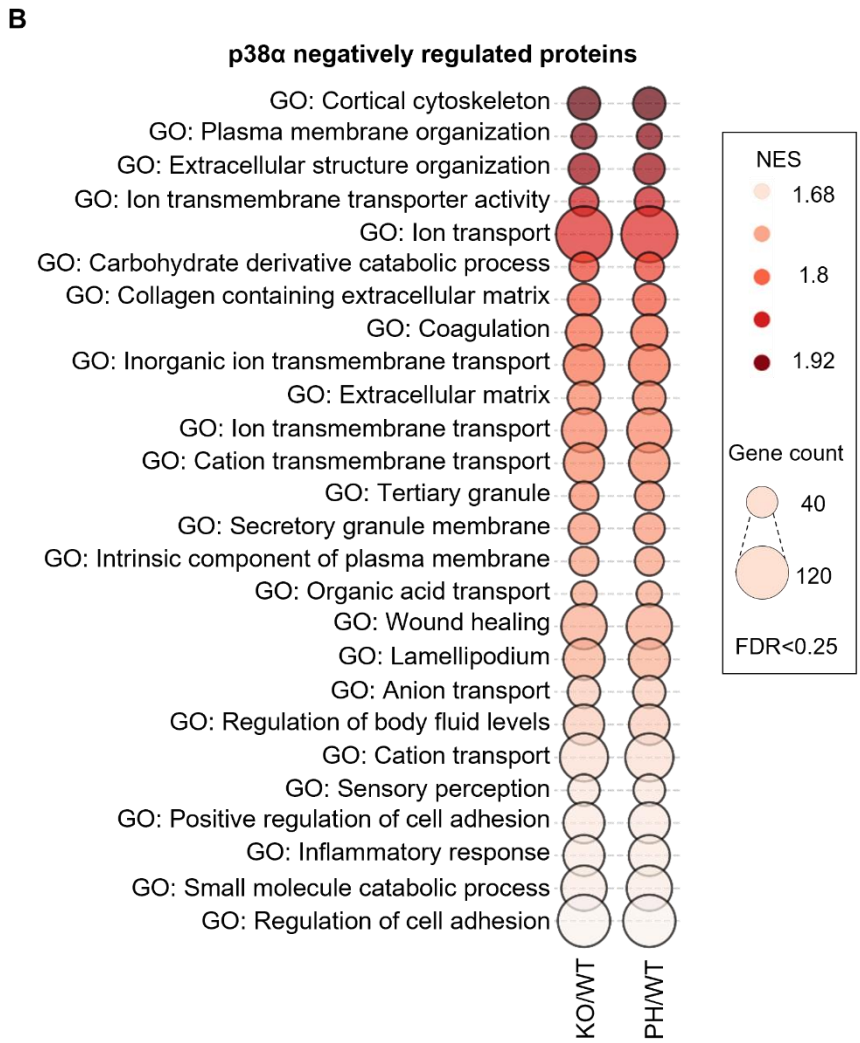

Figure 14. Biological processes represented in the p38α dependent proteome according to GSEA. (A) Biological processes represented in the proteins positively regulated by p38α (FDR<0.05). (B) Biological processes represented in the proteins negatively regulated by p38α (FDR<0.25). NES stands for normalized enrichment score. A negative value indicates that the member of this gene set tends to show up at the bottom of the ranked proteome (highest to lowest) regulated by p38α and that a positive value indicates the opposite. Gene count indicates the number of genes involved in the corresponding biological process according to the input datasets. FDR was determined using the Benjamini–Hochberg procedure.

3. Global phosphoproteomic changes modulated by p38α

3.1. Analysis of p38α regulated global phosphoproteomic changes

We identified 6,726 unique phosphosites on 1,726 proteins in total. After performing a linear model and removing the batch effect, a total of 2,935 phosphosites belonging to 1,202 phosphoproteins were quantified. As multisite phosphorylation in the same protein may influence the extent and duration of response, we analyzed the distribution of phosphosites per phosphoprotein. We found that more than half of the phosphoproteins (617) carried a single phosphosite, whereas 20%, 10% and 7% of the phosphoproteins contain two, three and four phosphorylated residues, respectively (**Figure 15A**).

We next examined the relative frequency of phosphoserine (pSer), phosphothreonine (pThr) and phosphotyrosine (pTyr) among the 2,935 quantified phosphosites. In agreement with previous studies (Huttlin et al., 2010), we mainly observed Ser phosphorylation (88%), followed by Thr (11%) and Tyr (1%) (**Figure 15B**).

To check the localization probability of the phosphosites, we adapted a published classification (Olsen J V et al., 2006). Localization probability is a PTM score that indicates the accuracy of the phosphosite identification within a peptide. For instance, if a phosphosite has a localization probability of 0.75, the added probability of all the other potential phosphosites is 0.25 in this peptide. In our dataset, 91.7% (2,690) phosphosites were identified

with a localization probability higher than 0.75, suggesting that the majority of the quantified phosphosites could be localized to specific positions on the phosphopeptide with high confidence (**Figure 15C**).

To examine the effect of p38α KO and inhibition on global phosphorylation changes, we generated density plots for KO/WT and PH/WT to show log2FC and p-value distribution for all the quantified phosphosites. The fold change density plot suggested KO/WT log2FC values were closer to 0, while PH/WT log2FC values were slightly shifted to the left in distribution (**Figure 15D**), suggesting that PH treatment may have a more substantial inhibitory effect on phosphorylation levels than the p38α deletion.

Meanwhile, the p-value density plot distribution of KO/WT and PH/WT showed a similar distribution pattern as we observed in p38α modulated global proteome, PH/WT had more statistically significant p-values (close to 0) than KO/WT (**Figure 15E**).

Next, we calculated intensity CV for all the quantified phosphosites among sample replicates; the result suggested most of the quantified phosphosites had a very low dispersion (< 1.7%) for all KO, PH and WT conditions (**Figure 15F**). In summary, this analysis indicates that our dataset is of good quality and that PH treatment causes more substantial phosphorylation changes than the p38α KO, both in the number of phosphosites and in the extent of phosphorylation.

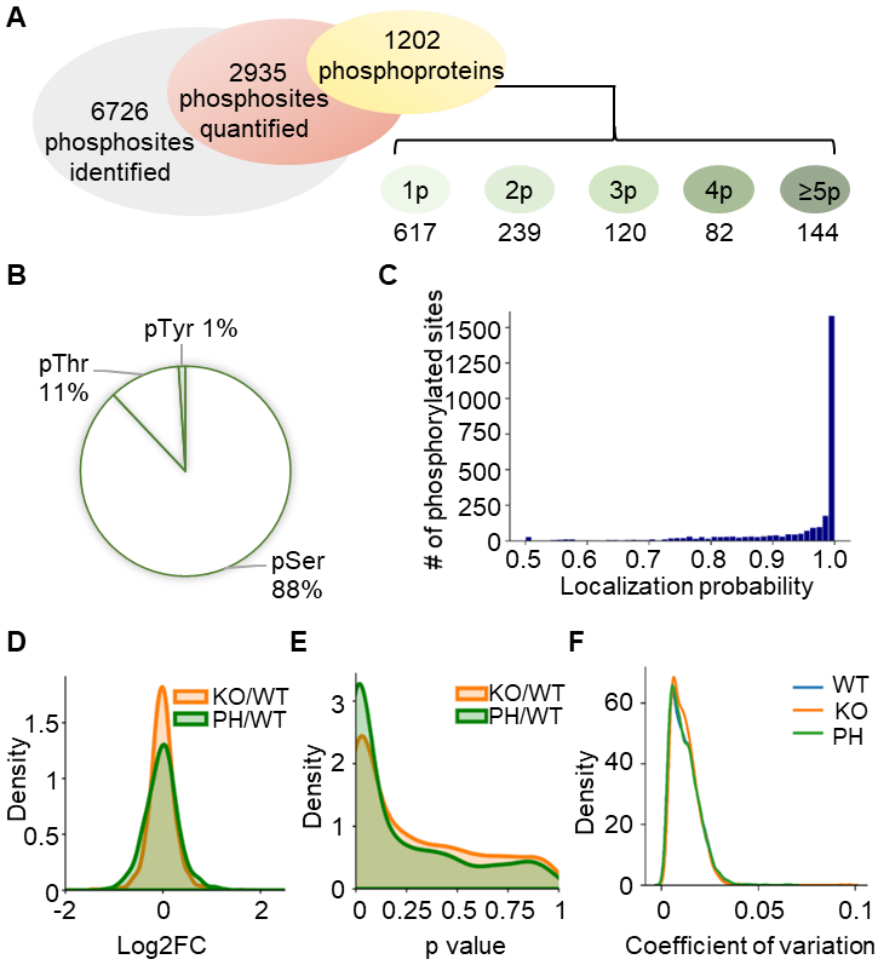

Figure 15. Overview of the p38α regulated global phospho-proteome. (A) Phosphosites identified using the Maxquant software, indicating their quantification, the number of phosphoproteins, and the distribution of phosphosites per protein. (B) Percentages of phosphorylated Serine, Threonine and Tyrosine for all the quantified phosphosites. (C) Distribution of the localization probability of determined phosphosites in peptide sequences and the percentage of phosphosites with highest confidence (localization probability ≥ 0.75). (D) Density plot showing the distribution of the log2-transformed fold change of phosphosites in KO/WT and PH/WT. (E) Density plot showing the distribution of the p-values of phosphosites in p38αKO/WT and PH/WT. (F) Density plot showing the coefficient of variation (CV) distribution of normalized intensity for each phosphosite in all samples.

3.2. Conservation and functional importance of the quantified phosphosites

To determine the functional importance of each phosphosite in the p38α regulated phosphoproteome, we took advantage of a recent study (Ochoa et al., 2019), which conducted a meta-analysis of 112 phosphoproteomic datasets from 104 different human cell types or tissues and extracted 59 features annotating phosphosite functions, further integrating these features to a single score that prioritizes phosphosites relevant for cell fitness. First, as functionally important modification sites are more likely to be evolutionarily conserved and our dataset was derived from a mouse model, we aligned the mouse sites to their human orthologs.

To do so, we downloaded the Phosphorylation site dataset from the PhosphositePlus database, which includes 239,562 human phosphosites and 104,920 mouse phosphosites. Nevertheless, we only identified 59,587 orthologous phosphosites (15%) between the two species from the database. Then, we aligned our phosphosites dataset to their conserved sites in human. Surprisingly, 2,613 (89%) phosphosites on 1,131 (94%) proteins matched human orthologs, while the remaining 11% p-sites were either replaced by non-phosphorylatable amino acids or missing in the human sequences (**Figure 16A**). The evolutionary conservation suggests that most of the phosphosites in our dataset are likely to be functionally important.

Next, we mapped the functional scores for all the conserved phosphosites in our dataset and the functional score distribution of phosphosites, which have reported or unreported functions, and

showed it in a density plot (**Figure 16B**). The analysis showed that most phosphosites (2,273, 89%) in our dataset were mapped to a function score, suggesting these phosphosites could be functionally important, although many of them do not have reported functions yet.

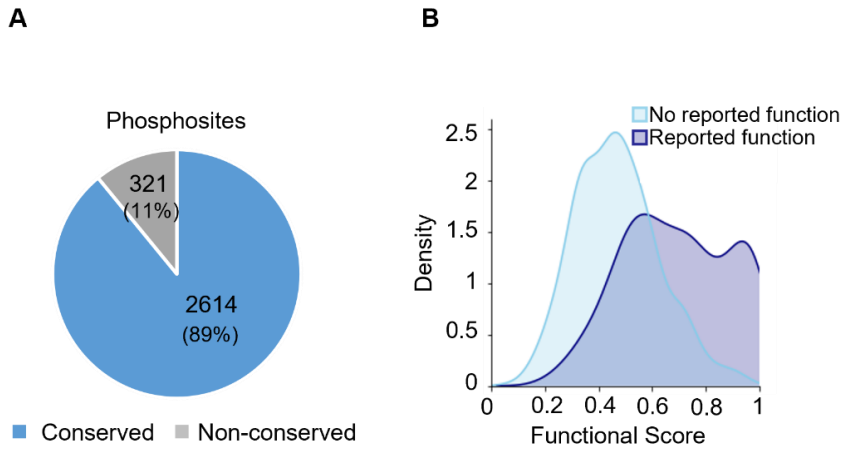

Figure 16. Conservation and functional importance of the p38α regulated phospho-proteome. (A) Bar chart showing the results of mapping human orthologous for the p38α regulated mouse phospho-sites using the PhosphositePlus dataset. (B) Density plot showing functional scores (Ochoa D, et al., 2019) for all mapped phosphosites indicating their distribution between reported and unreported functions.

3.3. p38α dependent phosphorylation events

Identification of p38α dependent phosphorylation events

In order to know the correlation between the phosphoproteomic changes in p38α KO and p38α inhibited conditions, we firstly plotted log2FC (KO/WT) and log2FC (PH/WT) for all the 2,935 quantified phosphosites. We found an overall Pearson correlation of R-value 0.576 (**Figure 17A**). When we limited this analysis to phosphosites quantified with a p-value less than 0.05, the correlation further

improved to an R-value of 0.758, suggesting a strong correlation between phosphosite changes induced by p38α KO and PH inhibition (**Figure 17B**).

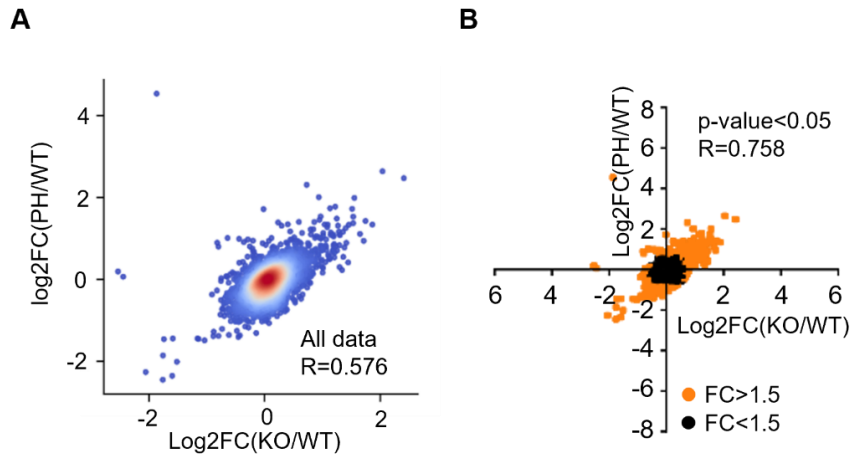

Figure 17. Correlation of the phospho-proteome changes between p38α KO/WT and PH/WT. (A) Correlation between the log2 transformed foldchanges (FC) of all quantified phosphosites in KO/WT and PH/WT. Color-coding indicates the density. Pearson coefficient correlation (R) is indicated. (B) Correlation plot of log2 transformed foldchanges of the quantified phosphosites with a p value<0.05. Orange-colored proteins had foldchange higher than 1.5 or lower than <-1.5. Pearson coefficient correlation is indicated.

To further classify the phosphosites as either positively or negatively regulated by p38α, we used the same cutoff for p38α regulated proteome analysis with a p-value less than 0.05 and the fold change for KO/WT and PH/WT higher than 1.5 or lower than -1.5. After filtering, we obtained 53 phosphosites on 45 proteins that were downregulated (**Figure 18A** & **C**) and 198 phosphosites on 144 proteins that were upregulated (**Figure 18A** & **D**) in KO compared with WT samples. For for PH treated samples, 257 phosphosites on

146 proteins were downregulated (**Figure 18B** & **C**) and 155 phosphosites on 108 proteins were upregulated (**Figure 18B** & **D**) compared with WT samples. Interestingly, similar to the protein expression data, there were about 5-fold more downregulated phosphosites in PH/WT than in KO/WT (**Figure 18C**).

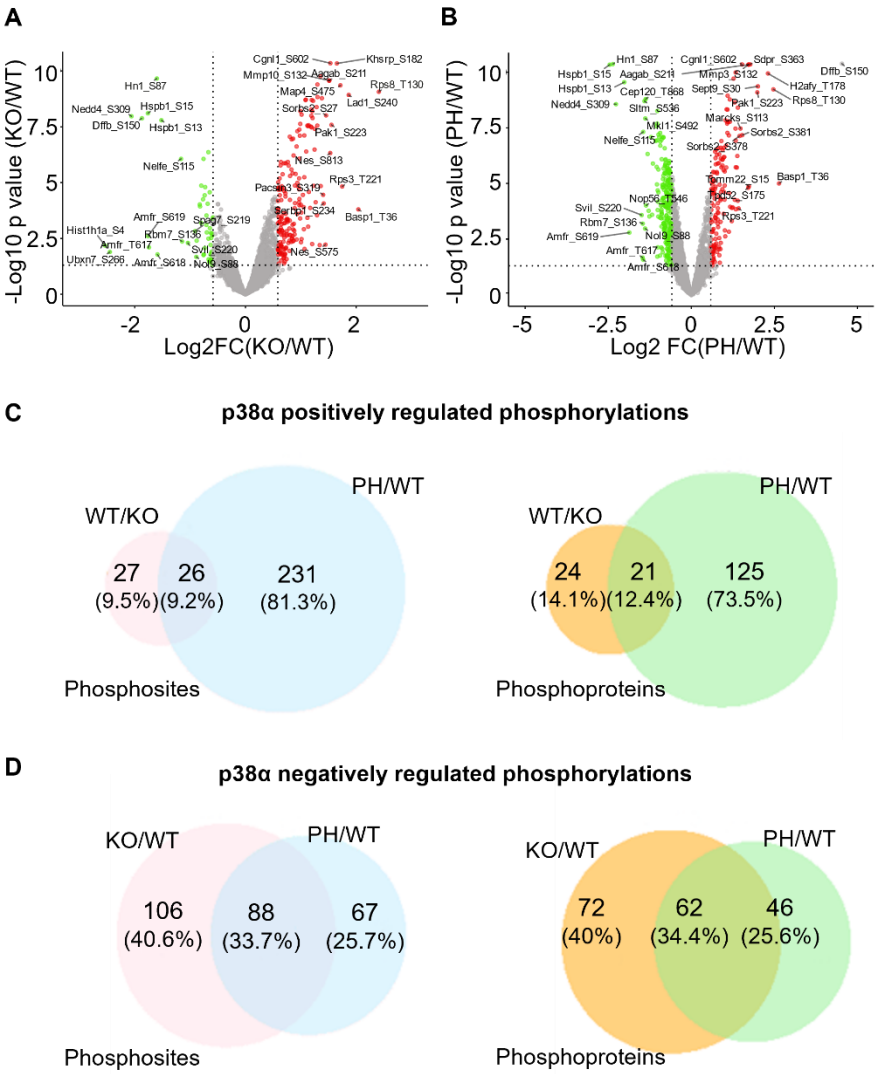

Figure 18. Differentially modulated phospho-proteins in p38α KO and p38α inhibitor treated cells. (A) Volcano plot of the log2FC of phosphosites in KO/WT. (B) Volcano plots of the log2FC of phosphosites in PH/WT. Green indicates the downregulated phosphosites with FC<-1.5, and the red the up-regulated proteins with FC>1.5. (C) Venn diagram showing the numbers of phosphosites (left) and the corresponding phosphoproteins (right) positively regulated by p38α (p-value<0.05 and FC>1.5). (D) Venn diagram showing the numbers of phosphosites (left) and the corresponding phosphoproteins (right) negatively regulated by p38α (p-value<0.05 and FC<-1.5). Intersections in (C) and (D) indicate phosphosites significantly (p-value<0.05 and FC>1.5 or FC<-1.5) down- or up- regulated in both KO/WT and PH/WT. Top 15 changed phosphosites are labeled.

To identify phosphorylation events that were most likely regulated by p38α under homeostatic conditions, we compared phosphosites that significantly changed upon both p38α deletion and inhibition. We identified 26 phosphosites (9.2%) on 21 proteins that were significantly downregulated (**Figure 18C** & **Supplementary Table 3**) and 88 phosphosites on 62 proteins that were upregulated in both p38α KO and PH treated cells versus WT cells (**Figure 18D** & **Supplementary Table 4**). These two groups are referred to as common down and common up.

p38α dependent phosphorylations: amino acid distribution and motifs

We analyzed the phospho-amino acid distribution for all the significantly down- or upregulated phosphosites. For KO/WT conditions, we observed no significant changes in Tyr, while Thr phosphorylation was slightly more down-regulated than up-regulated. For PH/WT condition, a small percentage of Tyr was observed, and opposite from KO/WT, Thr phosphorylation was

found less down-regulated than up-regulated (**Figure 19**). Regarding phosphosites that significantly changed in both KO/WT and PH/WT conditions, Ser represented around 90% and Thr 10% for either down- or up-regulated phosphosites.

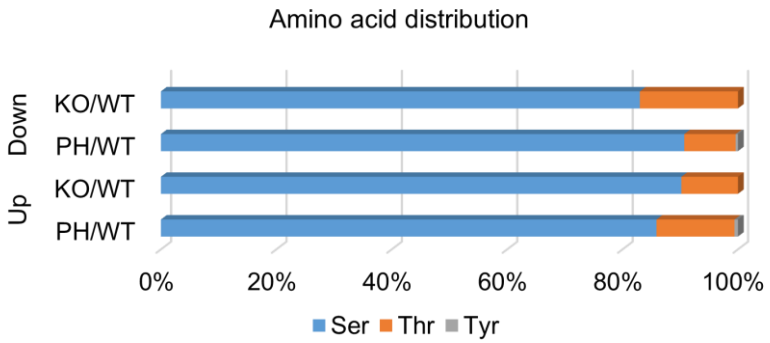

Figure 19. p38α regulated phosphorylation of specific amino acids. Bar chart showing the percentage of phosphorylated Ser, Thr and Tyr in the phosphosites that are significantly down- or up-regulated in KO/WT and PH/WT.

Kinase-substrate interactions are based on several mechanisms, one of which involves the recognition of phosphorylation residues as well the surrounding linear sequence motif. Detailed knowledge of these characteristics increases the confidence of linking identified phosphorylation sites to kinases, predicting phosphosites, and designing optimal peptide substrates. To further characterize the p38α regulated phosphoproteome, we analyzed sequence patterns in the regulated phosphopeptides using iceLogo (Colaert et al., 2009).

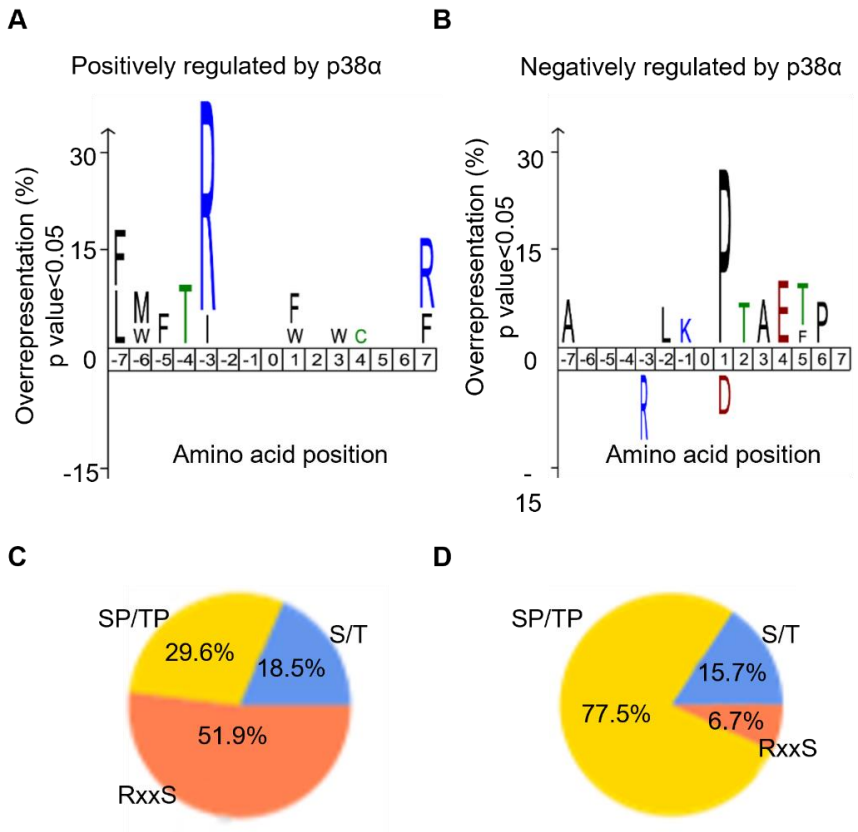

Figure 20. Motif signatures of p38α regulated phosphorylation sites in both KO/WT and PH/WT. (A and B) Sequence motif analysis using iceLogo of the phosphosites positively regulated by p38α (A) or negatively regulated by p38α (B). The frequency of seven amino acids flanking the phosphorylated residue is shown. The frequencies of amino acids surrounding the phosphorylated residue in phosphosites positively regulated by p38α, both in KO and in PH, were compared with the frequencies in all the quantified phosphosites. Green, blue, red and black colors represent polar, basic, acidic and hydrophobic amino acids, respectively. (C and D) Pie charts showing the percentage of S/T, SP/TP and RxxS motifs in phosphosites positively regulated by p38α (C) or negatively regulated p38α (D) in both KO/WT and PH/WT.

For p38α negatively regulated phosphopeptides (common up), we found a significant overrepresentation of motifs with Pro at +1 position, and to a lesser extent, Leu at -2, Thr at +2, Ala at +3 and Glu at +4, while Arg at -3 was clearly underrepresented (**Figure 20B**). In addition, 77.5% of the phosphosites were pSer/pThr-Pro sites, and only 6.7% were Arg-XX-pSer sites (**Figure 20D**). In addition to MAPKs, proline-directed sites are also known to be phosphorylated by other kinases, including CDKs and mTOR. However, the preference of Thr at +2 suggests the implication of other p38 MAPK family members, JNKs, ERK1/2, or CDK7 as the most likely kinases responsible for these phosphorylations. The Arg-x-x-Ser sites could be targeted by PKC or Akt family kinases.

To examine possible differences between p38α deletion and inhibition conditions, we generated sequence logos of all phosphopeptides that were significantly and independently down- or up-regulated in KO/WT (**Figure 21A** & **C**) and PH/WT (**Figure 21B** & **D**). The analysis revealed that the sequence logo of KO/WT regulated phosphopeptides was more similar to the common groups than to PH/WT. We also found a preference of Asn at +1 and Gly at +3 for downregulated peptides in KO/WT, which suggest a motif recognized by kinases involved in DNA damage, like ATM/ATR/DNA-PKcs (Kim et al., 1999; O'Neill et al., 2000), and is consistent with the observation that decreased p38α signaling results in impaired ATR activation (Cánovas et al., 2018).

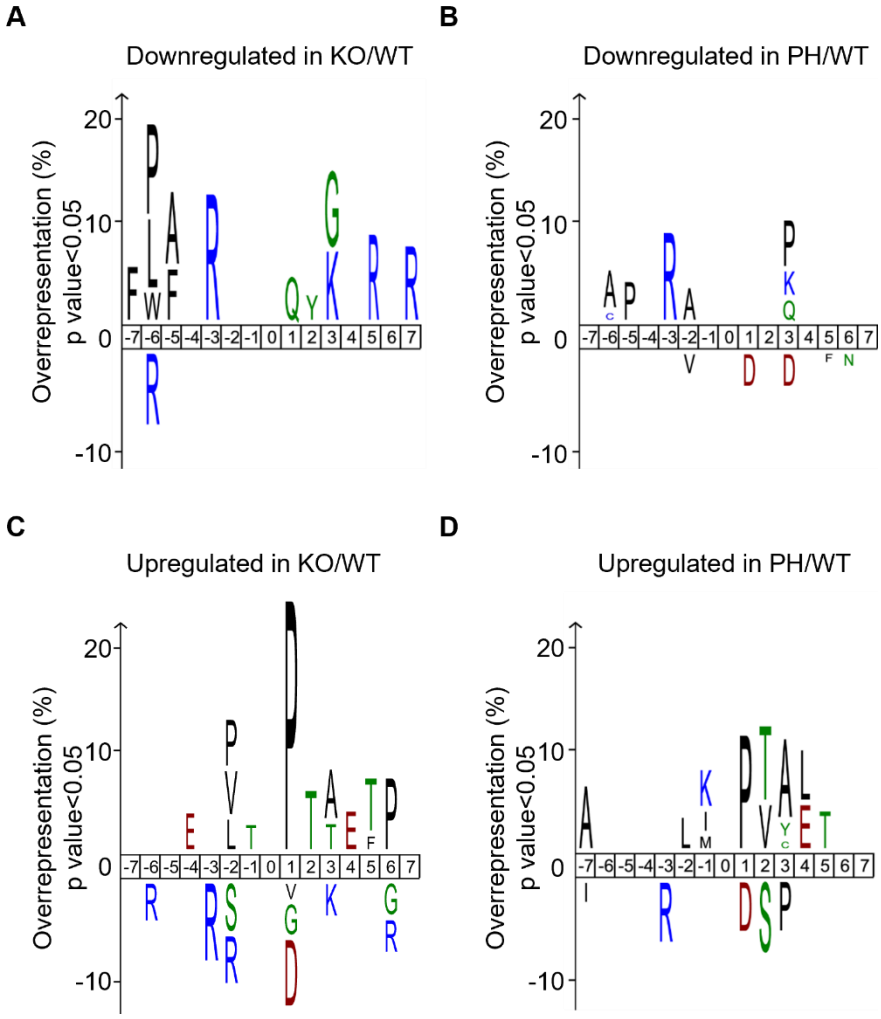

Figure 21. Motif signatures of p38α regulated phosphorylation sites in KO/WT or PH/WT. Sequence motif analysis of the phosphosites positively regulated by p38α in KO/WT (A), positively regulated by p38α in PH/WT (B), negatively regulated by p38α in KO/WT (C), and negatively regulated by p38α in PH/WT (D). The signature plots were analyzed using iceLogo and show the frequencies of seven amino acids flanking the phosphorylated residue. The frequencies of amino acids surrounding the phosphorylated residues negatively or positively regulated by p38α in KO/WT and PH/WT were compared with the frequencies in all the phosphosites quantified. Green, blue, red, and black colors represent polar, basic, acidic and hydrophobic amino acids, respectively.

3.4. Known substrates for p38α and MKs

To check the consistency of p38α substrates in different biological systems, we compared our phosphoproteomic dataset with p38 MAPK substrates either in the literature (Han et al., 2020; Trempolec et al., 2013) or in the PhospositePlus database. We found a total of 371 phosphosites on 199 proteins that have been reported to be phosphorylated by p38 MAPK family members. Among them, p38α has been reported to target 317 phosphosites (174 proteins). At the protein level, we found 40 p38α substrates in all our dataset, 29 of which have been verified in the literature (**Figure 22A**). At the phosphosite level, 27 phosphosites (on 18 proteins) were targeted by p38α, including Drosha (S354) and Ranbp2 (S2505) (Knight JD et al., 2012; Yang et al., 2015).

Since MK2 is an important mediator for many p38α signaling responses, endogenous MK2 and p38α form a complex in mammalian cells in homeostasis, and the level of MK2 protein is reduced in p38α-deficient cells (Gutierrez-Prat et al., 2021; Sudo et al., 2002; Weber et al., 2005), we analyzed MK2 substrates in our dataset. We found 15 MK2 substrates and 9 phosphosites (on 7 proteins), including *Hspbp1* (S15, S86) and the RNA-binding proteins *Nelfe* (S51) and *Rbm7* (S136) (**Figure 22B**).

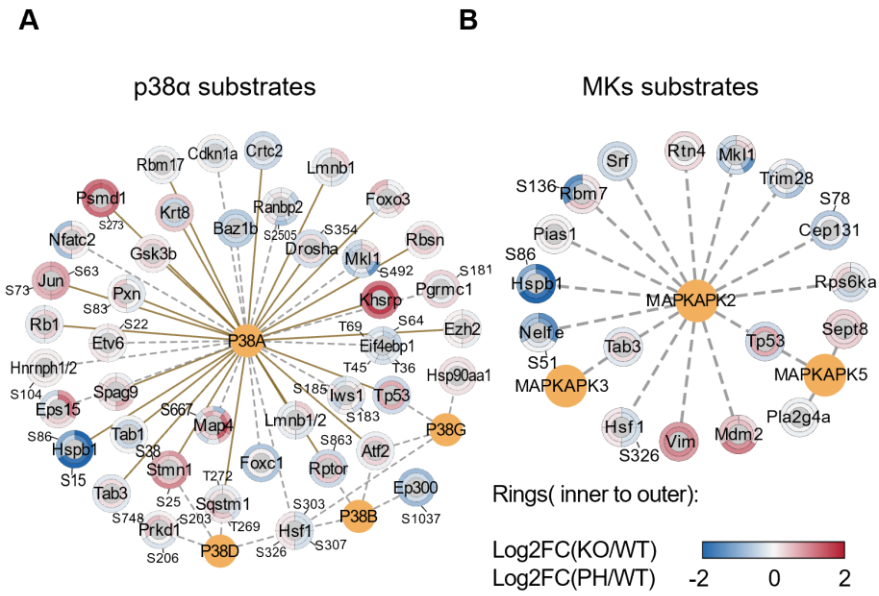

Figure 22. Known p38 and MK substrates. (A) Known substrates for p38 MAPKs described in the literature or in the PhosphositePlus database that were identified in the p38α regulated phosphoproteome. (B) Known substrates for MKs identified in the p38α regulated phosphoproteome and reported in the PhosphositePlus database. The ochre line indicates a kinase-substate relationship validated in the literature, and the dashed line when it was reported only in the database. Specific phosphosites for p38 or MK2/3/5 substrates are indicated. In rings with different colors, each color refers to a different phosphosite.

3.5. Potential p38α interactors

In addition to recognizing the linear sequence motif Ser/Thr-Pro, p38α may also interact with its activators or substrates via its common docking motif domain and the D domain of the substrate or activator (Biondi and Nebreda, 2003; Tanoue et al., 2000). To identify the most reliable p38α substrate candidates, we mapped potential p38α interactors in our phosphoproteomic dataset by taking advantage of unpublished data in our group, which predicted 150

physical interactors and 40 functional interactors for p38α based on the presence of a Ser/Thr-Pro site, consensus docking motif, and putative docking sequence curated in the set of experimentally identified p38 substrates. Physical interactors were reported in the literature based on protein binding assays such as pull-downs, immunoprecipitations and yeast two-hybrid (Y2H) screenings. Functional interactors were identified by kinase assays or other enzymatic studies.

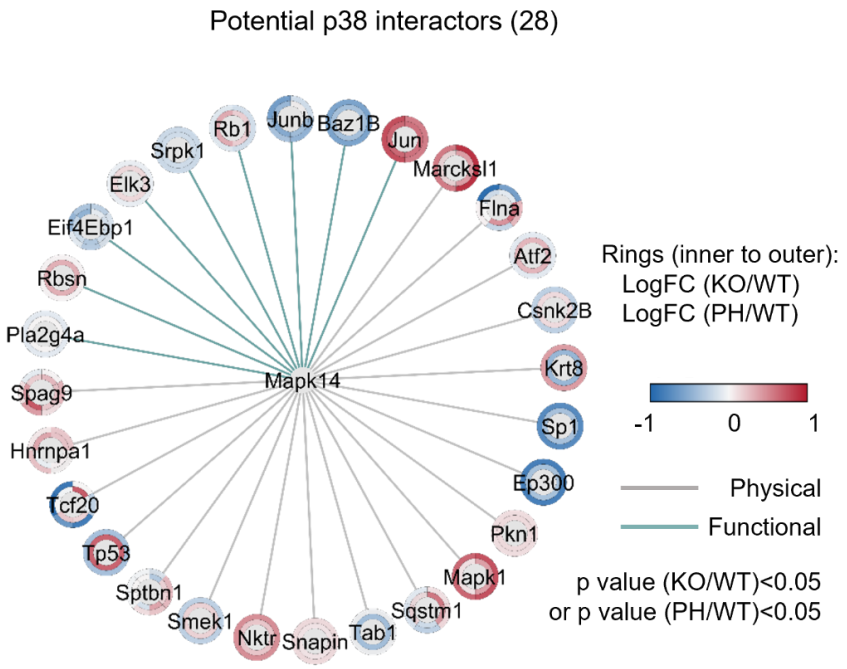

Figure 23. Potential p38α (Mapk14) interactors in our phosphoproteomic dataset. Physical refers to the interactor being identified by protein binding assays in the literature. Functional indicates that interactors were identified by kinase assays or other enzymatic studies. Fold change of interactors with phospho-sites p< 0.05 in KO/WT or PH/WT are indicated by the rings. In rings with different colors, each color refers to a different phosphorylation site.

A total of 28 phosphoproteins were identified as potential p38α interactors in our phosphoproteomic data, including 19 physical and 9 functional interactors (**Figure 23**). Some of them have been reported as p38α substrates, including functional interactors Elk3, Pla2g4a, Rb1 and Rbsn, and physical interactors Atf2, Ep300, Krt8, Sp1, Tp53, and Spag9. Although some phosphosites of these interactors were upregulated upon p38α inactivation, the changes in phosphorylation status for each site is highly context-dependent, and in some cases the reported phosphosites are different from our data, or the phosphosite information was not available in the literature. Other proteins, such as Flna, Hnrnpa1, Eif4ebp1, and JunB, were related to p38α but no kinase-substrate relationship has been reported yet, while Baz1b, Srpk1and Tcf20 have never been linked to p38α. These interactors could be candidates for new p38α substrates.

3.6. Upstream kinases

To identify kinases that are potentially regulated by p38α, we mapped the putative kinases for the p38α regulated phosphosites using the Kinase-Substrate Dataset from PhosphositePlus (Hornbeck et al., 2015). Out of the 26 p38α regulated phosphosites in the common down group, we found that 8 of them were mapped to 11 upstream kinases, including one p38α substrate, *Mkl1*(S492) (Zhang M et al., 2020), and three MK2 substrates, *Hspb1*(S15), *Nelfe*(S15) and *Rbm7*(S136). Other kinases that can target those phosphosites are CDK2, ERK1/2, mTOR, PKC and PLK1 as shown in **Figure 24A**.

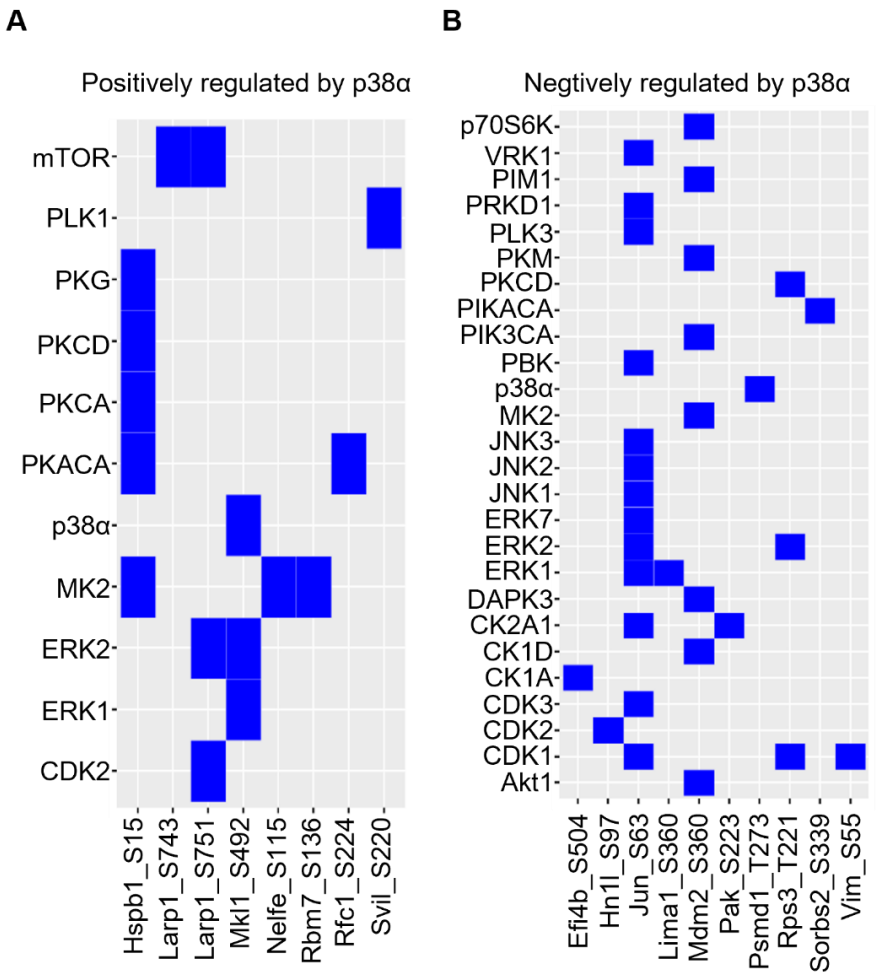

Figure 24. Kinases for the p38α regulated phosphorylation sites. Potential upstream kinases for the phosphosites positively regulated by p38α (A) or negatively regulated by p38α (B) in both KO/WT and PH/WT. The analysis was done using the Kinase-Substrate dataset in PhosphositePlus.

In the common up group, out of 85 phosphosites negatively modulated by p38α, 10 were mapped to 26 potential upstream kinases (**Figure 24B**), including ERK1/2, JNKs, CDKs and others like PKC, PKA and p70S6K. We found that several phosphosites can be

targeted by more than one upstream kinase, such as Jun, Rps13 and Mdm2. Many of the kinases predicted to target the phosphosites regulated by p38α are members of the CAMG and AGC families. In summary, the results suggest that there might be substantial cross-talk between p38α signaling and other kinase pathways.

3.7. Kinase signature associated with p38α inactivation pinpoints mTOR down-regulation

We next investigated kinase signature for phosphosites that change in p38α KO/WT or PH/WT conditions by the Kinase-Substrate Enrichment Analysis (KSEA) algorithm, which scores each kinase based on the relative hyper-phosphorylation or dephosphorylation of the majority of its substrates, indicated by kinase Z-score. The negative or positive value of the score implies a decrease or increase in the kinase's overall activity relative to the control (Casado et al., 2013; Horn et al., 2014; Hornbeck et al., 2015; Wiredja et al., 2017).

To perform this analysis, we used all quantified phosphosites, conserved in humans, with the corresponding FC and p-value for KO/WT or PH/WT as input. The results showed that the kinase activities of MK2 and mTOR, a central regulator of mammalian metabolism, were significantly downregulated in both KO/WT and PH/WT conditions (**Figure 25**). This result is consistent with MK2 being a key p38α downstream effector. On the other hand, the identification of mTOR was more unexpected, although it is known that mTOR can be controlled by p38α in response to specific stresses and growth factors in regulatory T cells and in heart ischemia

(Canovas B and Nebreda AR, 2021; Cully et al., 2010; Hernández et al., 2011; Li et al., 2019).

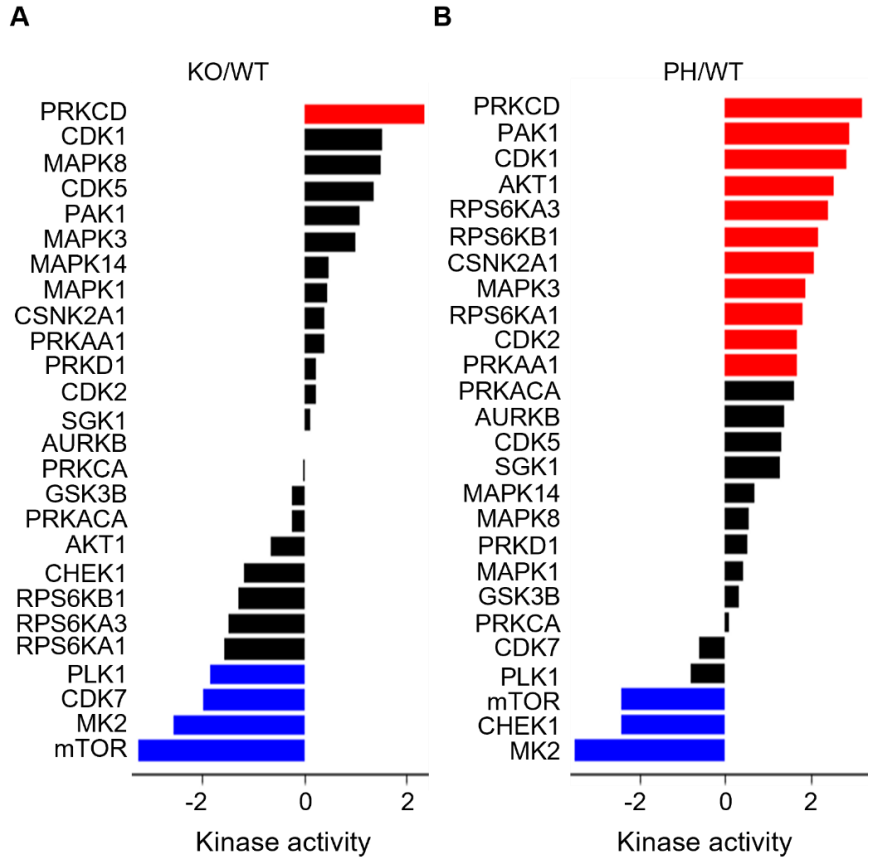

Figure 25. Kinase-substrate enrichment analysis (KSEA) for the p38α regulated phospho-proteome. (A and B) KSEA results of the p38α regulated phospho-proteome in KO/WT (A) and in PH/WT (B). Kinases with ≥5 potential substrates among the p38α regulated phosphoproteins were plotted. Blue and red bars have p value<0.05 and black bars p value>0.05. Negative values indicate that kinase activity is decreased (Blue) and positive value that kinase activity is increased (Red).

Besides MK2 and mTOR, we also found that PLK1 and CDK7 activities were downregulated in p38α KO and PH inhibited samples,

although to a lesser extent. PLK1 and CDK7 are both Ser/Thr-protein kinases that regulate the cell cycle.

3.8. Biological functions regulated by the p38α modulated phosphoproteome

As there is very little information for phosphosite annotation, elucidating the biological functions that might be controlled by the p38α-modulated phosphoproteome is challenging. Therefore, we decided to analyze gene ontology for the identified phosphoproteins in the DAVID database (Huang DW, Sherman BT et al. 2009;). Although phosphorylation does not necessarily mean the activation of the pathway or a particular function, in order to avoid ontology enrichment dominated by negatively regulated phosphorylations, we carried out a separate ontology analysis for phosphoproteins with positive or negative phosphorylation changes. Then we overlapped the enriched GO terms that passed cutoffs in both KO/WT and PH/WT conditions (FDR<0.05 & gene count >5).

We found that both p38α positively and negatively regulated phosphoproteins were enriched for cell adhesion and Poly(A) RNA binding (**Figure 26**). Interestingly, many of the p38α positively regulated phosphoproteins were associated with nuclear components, which correlate with the functions controlled by p38α positively regulated proteome, including DNA replication, DNA repair and cell cycle. In contrast, the negatively regulated phosphoproteins mainly highlight cytoplasmic components and participate in cytoskeletal regulation, which correlates with the functions predicted for the proteome negatively regulated by p38α.

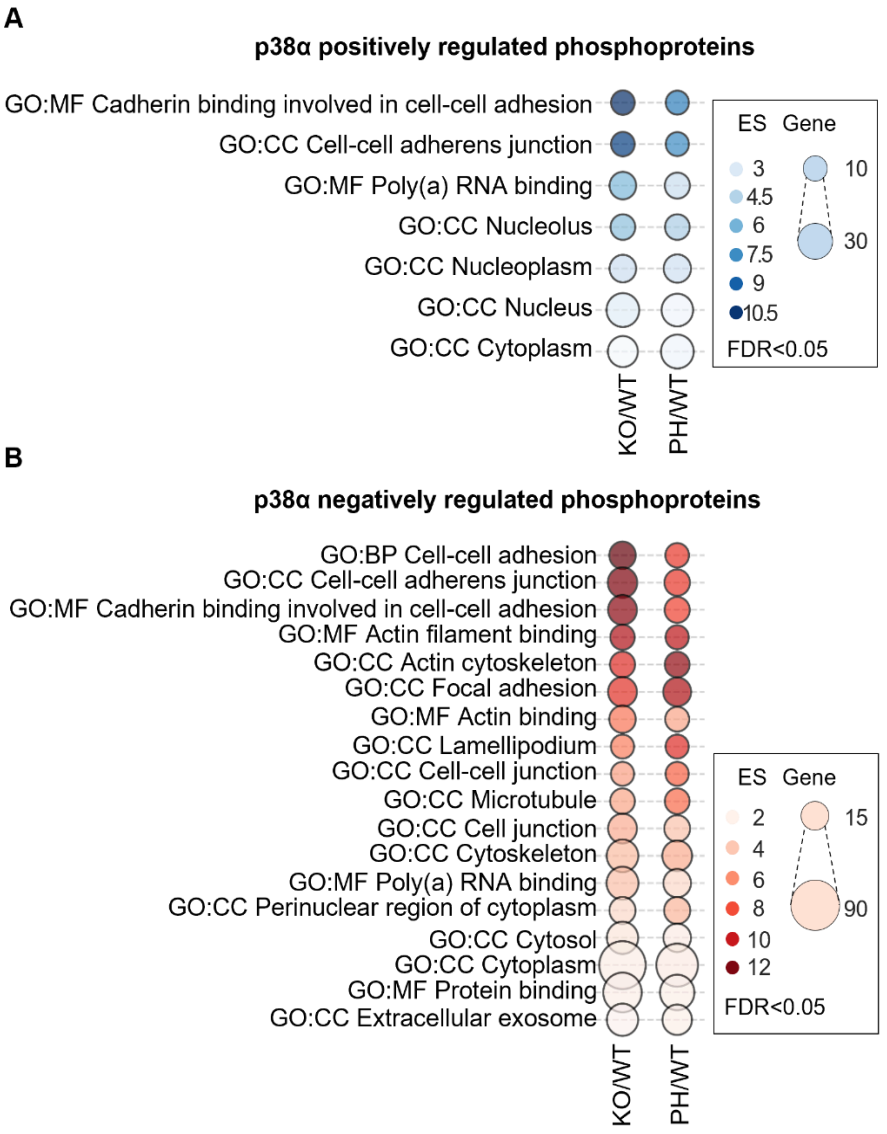

Figure 26. GO analysis of the phosphoproteins that include the p38α regulated phosphosites. Enriched biological funcions and processes in the phosphoproteins that include phosphosites positively regulated by p38α (A) or negatively regulated by p38α (B). GO analysis was done using the DAVID database. ES stands for enrichment score, and Gene indicates the number of genes involved in the corresponding biological process in the input datasets. FDR was estimated by the Benjamini–Hochberg procedure.

4. Functional network for the p38α dependent proteome and phospho-proteome

One role of phosphorylation is to modulate physical interactions between proteins, thereby integrating different signaling pathways. Therefore, mapping phosphoproteomic data onto networks of known interacting proteins can reveal tandem phosphorylations that regulate the biological activities of the shared proteins.

To this end, we constructed high confidence protein-protein interaction (PPI) networks (PPI score ≥0.7) of proteins and phosphoproteins that changed significantly (FC 1.5, $p<0.05$) using STRING and visualized in Cytoscape. Moreover, proteins were grouped together according to their functions (**Figure 27**). Although we did not observe many high confident interactions (40 nodes out of 113 had 43 edges), the functions of proteins in this network mostly pointed to the regulation of RNA processing, including some ribosomal proteins and RNA binding proteins, like *Rps3*, *Rps8*, *Rpl29* and R*bm22*, and proteolytic pathways, which involved both endosome-lysosome system and the ubiquitin-proteasome system. Other biological functions likely affected include cell cycle, DNA replication and DNA repair, as well as cytoskeleton organization and cell adhesion, which is the function including more of the upregulated proteins and phospho-proteins.

Overall, the combined results of the proteomic and phospho-proteomic analyses identify the regulation of mRNA translation, cell cycle progression and cytoskeleton organization as important functions of p38α signaling to balance cancer cell homeostasis.

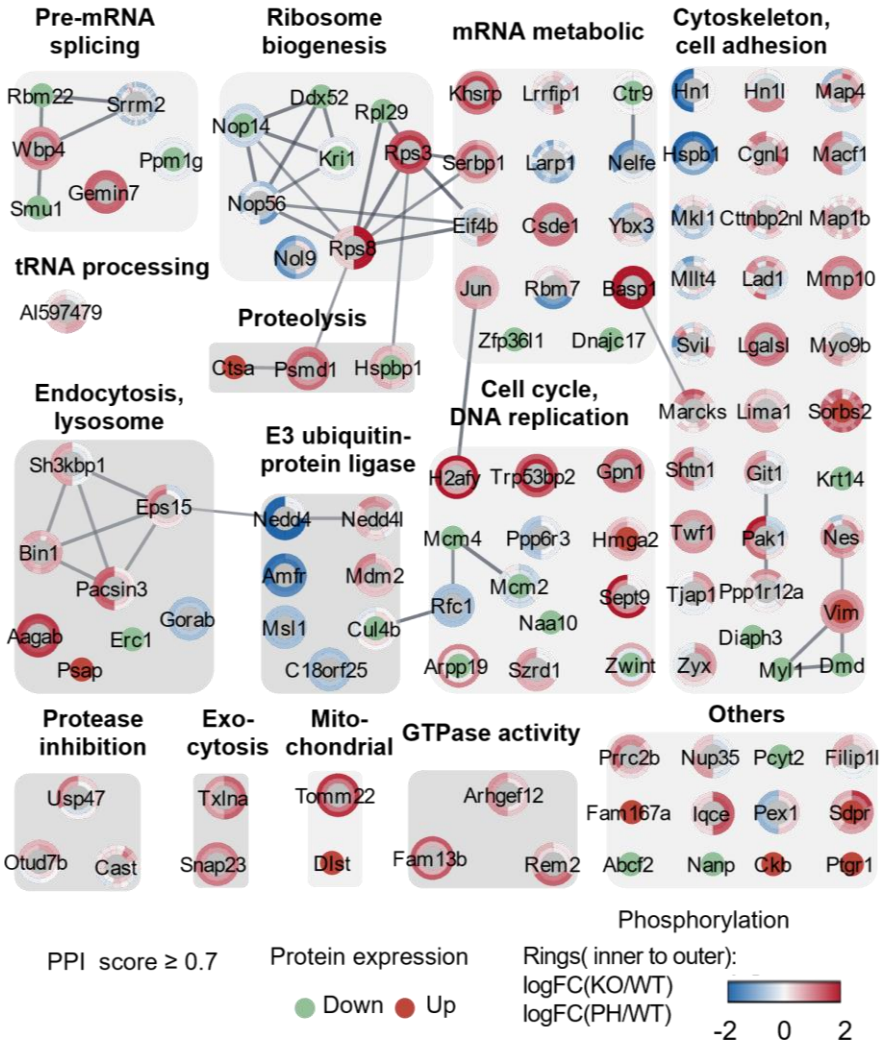

Figure 27. Functional signalling interaction networks modulated by p38α. p38α regulated protein and phosphoprotein networks were constructed using STRING and visualized in Cytoscape. Only interactions with high confidence score (≥0.7) are represented in the networks. Red and green inside indicates that protein expression was increased and decreased, respectively, upon p38α deletion. The inner ring indicates the log2FC (KO/WT) and the outer ring log2FC (PH/WT). In rings with different colors, each color refers to a different phosphosite.

5. Validation of proteomic and phosphoproteomic changes

The combined results of the proteomic and phospho-proteomic analyses pointed to the regulation of DNA replication, mRNA translation and cell adhesion as potentially important functions regulated by p38α. It is known that in the BBL358 cell line, p38α deletion causes impaired DNA replication and the accumulation of DNA damage through controlling ATR-CHK1 signaling (Cánovas et al., 2018).

Moreover, the p38α substrate MK2 is a key regulator of RNA-binding proteins and mRNA stability (Soni et al., 2019). A recent study has also reported that p38α signaling regulates ribosome-related gene expression, rRNA precursor processing, polysome formation and protein translation during primitive endoderm differentiation in the mouse blastocyst (Bora et al., 2021).

However, the role of p38α in cell adhesion is still poorly understood, and we decided to focus on this function.

5.1. Role of p38α in cell adhesion

Cell adhesion is a prominent and complex biological process, which is essential for cell communication and the development and maintenance of tissues. The adhesion network contains not only proteins involved in adhesion but also other protein groups, such as adaptors, cytoskeleton proteins, Ser/Thr kinases and phosphatases, Tyr kinases and phosphatases, small GTPases, GTPase-activation

proteins, guanine nucleotide exchange factors and transmembrane receptors (Zaidel-Bar et al., 2007).

Our phosphoproteomic analysis identified cell adhesion as one of the most enriched biological function. In addition, many (phospho-)proteins were involved in the adhesion network protein groups. Therefore, we hypothesized that p38α potentially regulates cell adhesion.

p38α regulates extracellular matrix adhesion

The interaction of a cell with the extracellular matrix (ECM), is mediated by multi-protein adhesion structures such as focal adhesions, fibrillar adhesions and podosomes. The ECM is a network of extracellular molecules that are secreted locally to ensure cell and tissue cohesion. The major classes of ECM molecules are proteoglycans, collagens and multi-adhesive matrix proteins, such as laminin and fibronectin.

To mimic the cell-ECM adhesion, we used collagen and fibronectin to coat the plates. We found that p38α KO cells showed decreased adhesion ability on ECM-coated plates compared to WT cells (**Figure 28A** & **B**), and similar results were observed when cells were treated with the p38α inhibitors PH and LY2228820 (LY) (**Figure 28A** & **C**).

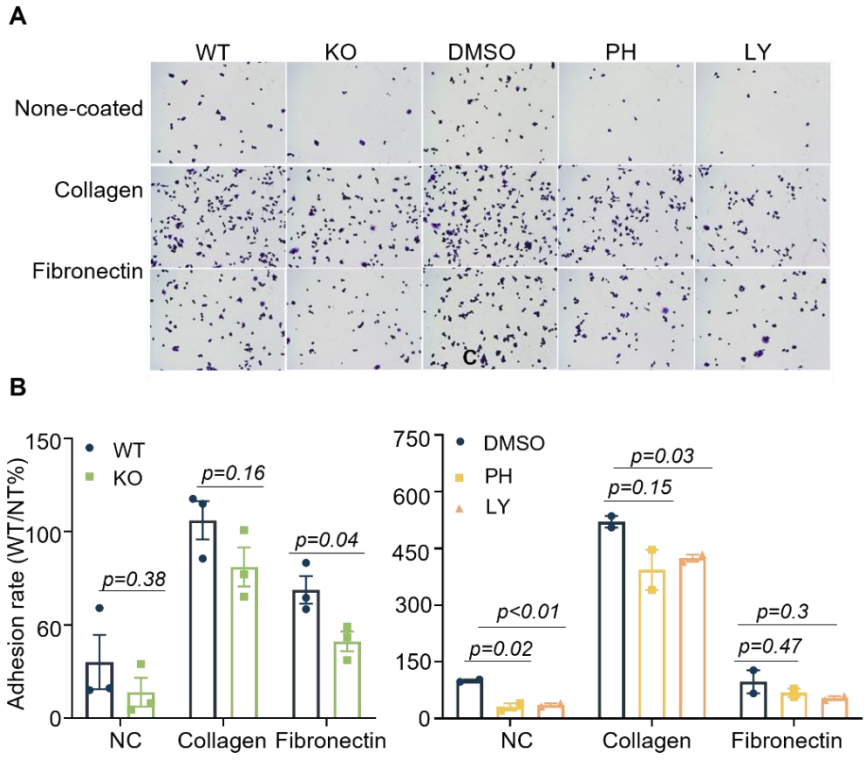

Figure 28. p38α regulates cancer adhesion to extracellular matrix components. (A) Same numbers of p38α WT cells, either untreated (WT) or treated with DMSO or the p38α inhibitors PH797804 (PH) or LY2228820 (LY), and p38α KO cells were seeded on plates pre-coated with collagen or fibronectin and after 1 h the unattached cells were removed. The remaining cells were fixed and stained for quantification. (B and C) Quantification of the attachment results in p38α WT and KO cells (B) and in cells treated with p38α inhibitors (C).

In addition, to mimic the microenvironment that cancer cells encounter in tumors, we generated ECM derived from fibroblasts. In brief, fibroblasts were plated and maintained in culture in a confluent state. After 10 days, an intact fibroblast-derived 3D matrix was obtained by removing the fibroblasts, and the attachment of WT and p38α KO cells on the matrices was quantified. Similar to the results

using plates coated with ECM components, we found that p38α KO cells tend to show poorer adhesion on the fibroblast-derived matrix than the WT cells (**Figure 29**).

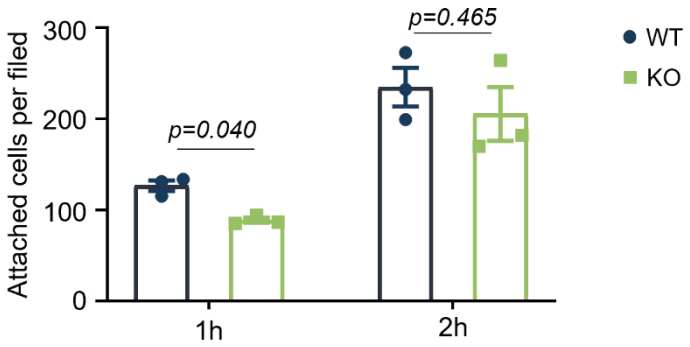

Figure 29. p38α influences cancer cell adhesion to a fibroblast-derived extracellular matrix. WT and p38α KO cells were seeded onto a fibroblast-derived ECM. After incubation for the indicated times, the unattached cells were removed, and the remaining cells were fixed and quantified.

Conversely, the cell adhesion capability of a cell probably depends on the balance between cell attachment and detachment, which represents the termination of adhesion interactions by physical, chemical or other means. To investigate if p38α controls cell detachment, we treated WT and p38α KO cell monolayers with trypsin for a short time and then quantified the undetached cells. We found that fewer p38α KO cells than WT cells remained on the plates (**Figure 30**), suggesting a weaker adhesion capability of p38α KO cells. In conclusion, we consistently found that inactivation of p38α impairs cancer cell adhesion to the ECM.

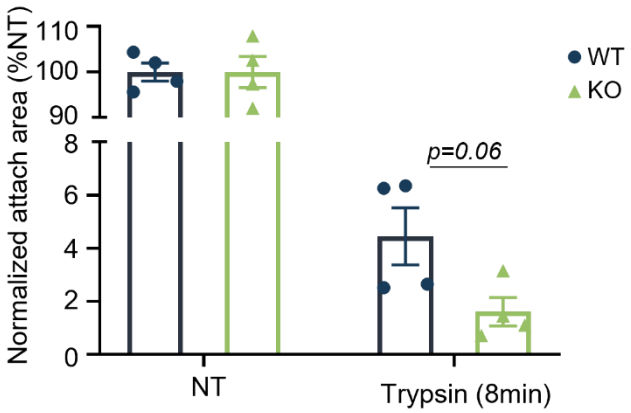

Figure 30. p38α influences cell detachment. The detachment ability of WT and p38α KO cells was examined by treating cell monolayers with trypsin for 8 min followed by quantification of the cells remaining in the plates and comparison with untreated plates (NT).

p38α regulates cell-cell adhesion

Besides cell-ECM adhesion, cell-cell adhesion is also essential for integrating cell-cell contacts with the changes in morphology. Epithelial cells adhere tightly to their neighbors, and several specialized adhesive structures, such as adherens junctions and tight junctions, ensure the appropriate integrity of epithelial sheets. However, epithelial cells are typically encased within a closely packed tissue mass in which cells establish intimate connections with many near-neighbors and with ECM components. 3D spheroids are regarded as a more faithful in vitro model to mimic the arrangements of the cells in vivo by tuning the relative strength of the cell-cell adhesion over cell-ECM adhesion.

To study the cell-cell adhesion, we used 3D spheroids in which cells directly interact with each other and with the ECM by hanging drop

method (Foty, 2011). We found that WT cells consistently formed bigger spheroids than p38α KO cells, and a similar phenotype was observed when we used the p38α inhibitor PH or an MK2 inhibitor (**Figure 31**).

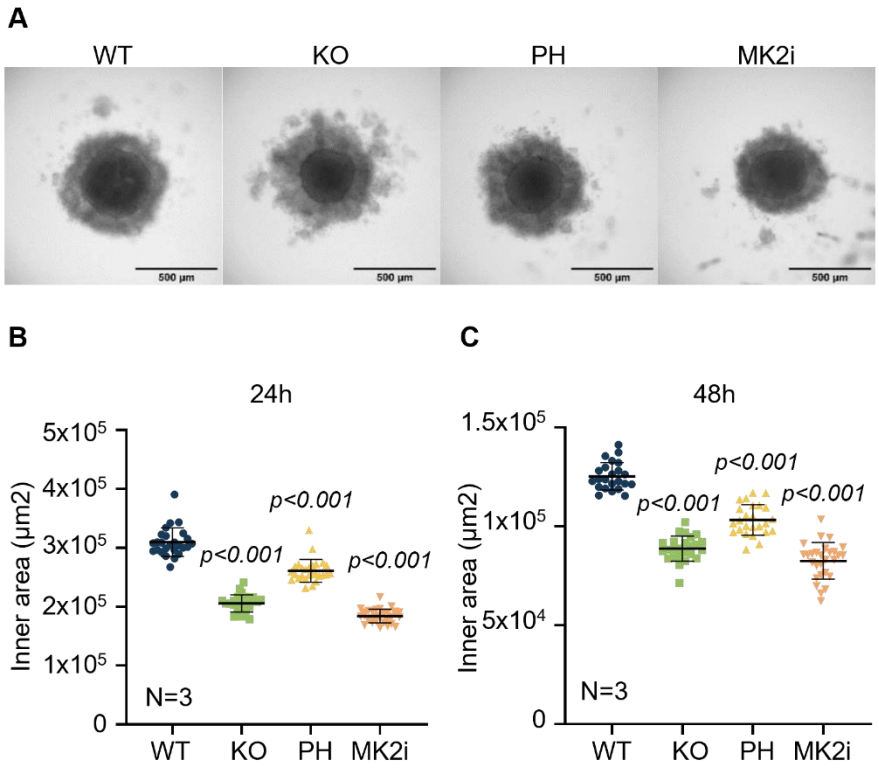

Figure 31. p38α controls cell-cell adhesion. (A) p38α WT cells either untreated (WT) or treated overnight with the p38α inhibitor PH or the MK-2 Inhibitor III (MK2i), and p38α KO cells were cultured by the hanging drop method for 48 h. (B and C) Quantification of spheroid sizes (inner part indicated with a red circle) after 24 h (B) and 48 h (C).

To know if the smaller spheroids formed upon p38α inactivation were due to the impaired adhesion, we tested the expression level of the tight junction protein ZO-1, using immunofluorescence staining in spheroids formed by WT, p38α KO, and PH-inhibited cells.

Consistent with their spheroid size, we observed that the ZO-1 intensity in spheroids formed by p38α KO cells and PH inhibited cells was clearly lower than in spheroids formed by WT cells (**Figure 32**). Interestingly, p38α has been described to control ZO-1 expression during both embryonic development and EMT (Bell and Watson, 2013; Strippoli et al., 2010), which further supports our results. In summary, we concluded that p38α is essential for cell-cell adhesion regulation in the 3D spheroids model.

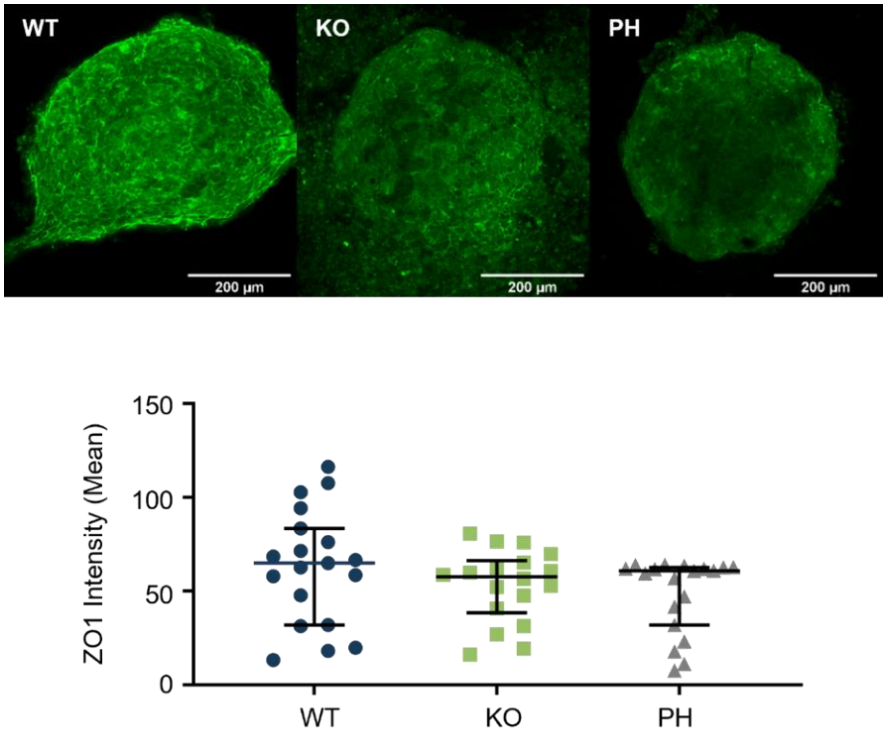

Figure 32. p38α regulates ZO1 expression in 3D spheroids. (A). Representative confocal images showing ZO1 expression levels as determined by immunofluorescence in spheroids formed by WT, p38α KO and PH treated cells. (B) Quantification of ZO-1 mean intensity of each z-stack image. Median and interquartile range are shown. Spheroids were cultured for 48 h.

5.2. Verification of p38α regulated proteome candidates

Based on the proteomic data, we verify the expression levels of several candidates by qPCR. For p38α positively regulated proteins, we selected *Ddx52*, *Hspbp1*, *Krt14*, *Zfp36l1* and *Zfp36l2*, but *Krt14* was the only candidate found slightly downregulated upon p38α inactivation (**Figure 33A**). For p38α negatively regulated proteins, we selected *Cyb5a*, *Sorbs2* and *Vim*, and the three had higher expression in p38α KO cells than WT cells. Nevertheless, treatment with the PH inhibitor only had some effect for *Sorbs2* (**Figure 33B**).

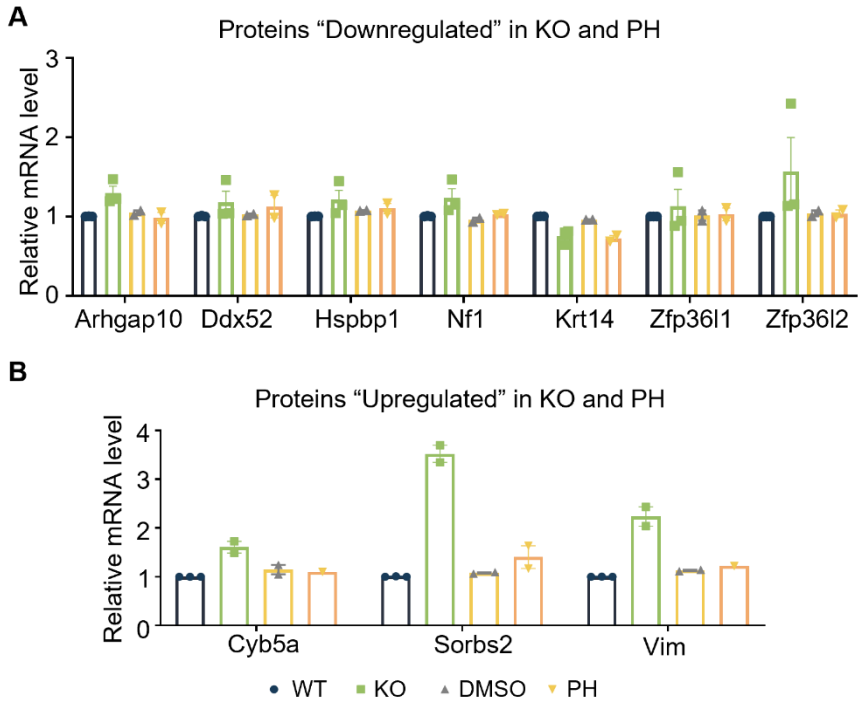

Figure 33. Validation of p38α regulated proteome candidates. (A) mRNA levels of the top down-regulated proteins (A) or up-regulated proteins (B) according to the p38α regulated proteomic data were tested by qRT-PCR.

In order to understand if the difference in *Sorbs2* mRNA level between p38α KO and PH treated cells was due to the period of treatment, we did a time-course incubation with PH and LY up to 48 h. We found that the *Sorbs2* mRNA induction began to increase after 8 h of p38α inhibition, and remained increased up to 48 h, indicating that the inhibitor had a relatively mild effect on *Sorbs2* expression compared with p38α KO (**Figure 34**). We further assessed whether the observed upregulation of *Sorbs2* mRNA levels in the absence of p38α, were also detected at the protein level. We found that the levels of ArgBP2 protein (encoded by *Sorbs2*) were notably increased in p38α KO cells, and to a lower extent in PH-treated cells, compared with WT cells, which was consistent with the mRNA level results (**Figure 34**).

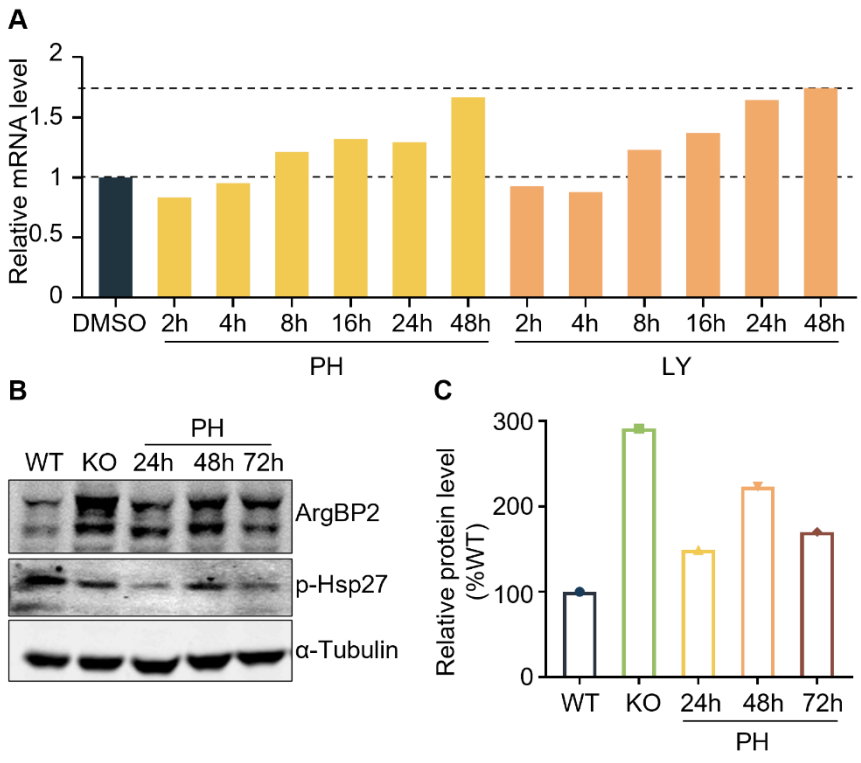

Figure 34. p38α negatively regulates *Sorbs2* expression in BBL358 cancer cells. (A) *Sorbs2* mRNA levels were determined by qRT-PCR in cells treated with the p38α inhibitors PH or LY for the indicated times. (B) The *Sorbs2*-encoded ArgBP2 protein levels were detected by Western blotting in WT and p38α KO cells and in cells treated with PH for the indicated times. (C) Quantification of ArgBP2 protein levels in p38α KO and PH inhibited cells normalized to WT cells.

p38α negatively regulates *Sorbs2* (ArgBP2) expression at the transcriptional level

Our results indicated that *Sorbs2* expression was upregulated at both mRNA and protein levels upon p38α inactivation in BBL358 cells. To characterize how p38α negatively controls *Sorbs2* expression, we used the transcription inhibitor Actinomycin D to test whether p38α affects *Sorbs2* mRNA stability. We found that p38α did not seem to affect the stability of *Sorbs2* mRNA (**Figure 35A**).

To determine the impact of p38α on *Sorbs2* transcriptional regulation, we designed primers for the *Sorbs2* pre-mRNA spanning intron-exon junction using the USCS database (Zeisel et al., 2013). This experiment showed a significant elevation of *Sorbs2* pre-mRNA levels in the absence of p38α, supporting that p38α negatively regulates *Sorbs2* transcription (**Figure 35B**).

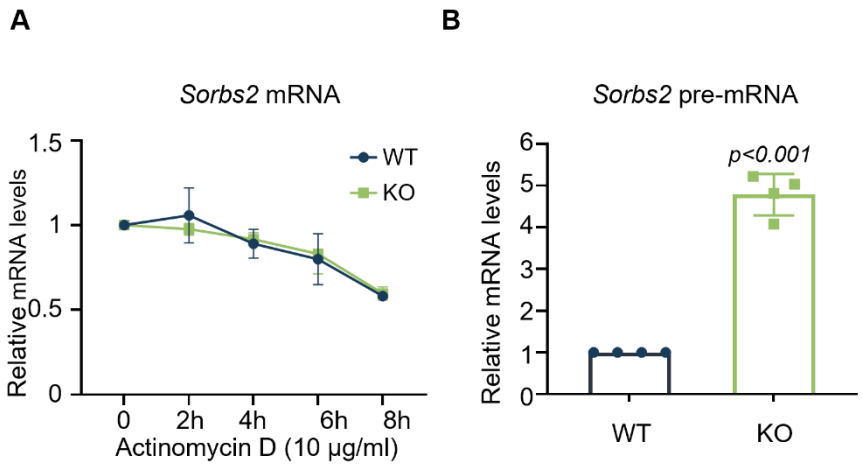

Figure 35. p38α regulates *Sorbs2* transcription. (A) WT and p38α KO cells were treated with actinomycin D and RNA samples were collected at the indicated times. *Sorbs2* mRNA levels were determined by qRT-PCR and were referred to the expression level in the untreated cells (time 0). No significant differences were found between samples. (B) *Sorbs2* pre-mRNA levels in WT and p38α KO cells determined by qRT-PCR using primers that span exon-intron junctions.

5.3. Role of ArgBP2 in p38α regulated cell-adhesion

The protein ArgBP2 encoded by *Sorbs2* is a member of the SoHo family of adapter proteins that contain a SoHo (Sorbin Homology) domain in their N-terminus and three SH3 (Src homology 3) domains in their C-terminus. ArgBP2 has been shown to interact with several proteins involved in the regulation of actin (Roignot and Soubeyran, 2009), and there is also evidence supporting a potential role of ArgBP2 in the regulation of cell adhesion (Taieb et al., 2008). Therefore, we postulated that ArgBP2 might be involved in p38α-mediated cell adhesion.

To evaluate this hypothesis, we firstly generated ArgBP2 knockout BBL358 cells using the CRISPR-Cas9 system. These cells were

treated with 4-OHT to induce p38α and ArgBP2 double knockout (DKO) cells. Then, cell adhesion was determined by the hanging drop assay, and we found that while the WT cells formed intact and compact spheroids, many of the p38α KO cells formed spheroids that were damaged. Importantly, this phenotype observed in p38α KO cells was largely rescued in the p38α and ArgBP2 DKO cells (**Figure 36**).

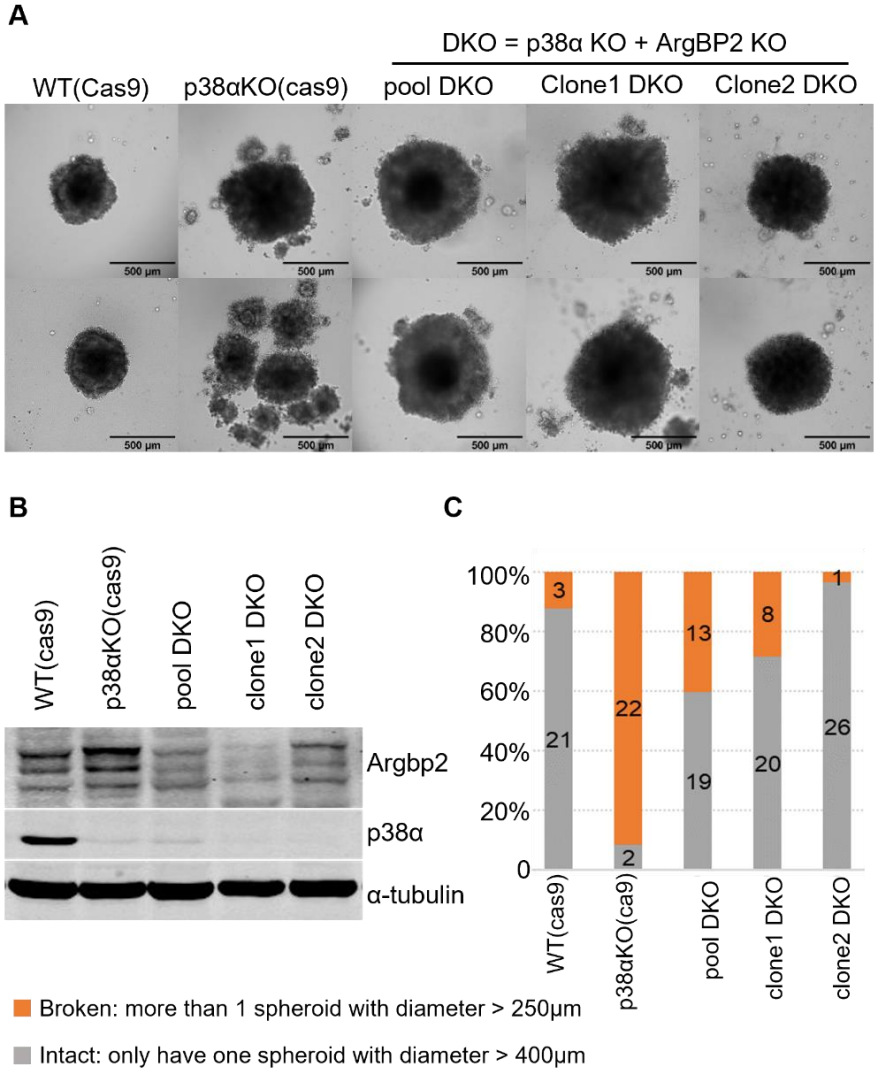

Figure 36. ArgBP2 is involved in the regulation of cell-cell adhesion by p38α. (A) Spheroid morphologies of WT and p38α KO cells, as well as p38α and ArgBP2 double KO cells (DKO). ArgBP2 KO was induced using the CRISPR/Cas9 system, and DKO cells were obtained by treating ArgBP2 KO cells with 4-OHT. (B) Expression of p38α and ArgBP2 in the indicated cell lines was tested by Western blotting. (C) Quantification of intact and broken spheroid numbers in each cell line.

Taken together, we conclude that ArgBP2 is involved in p38α-mediated cell-cell adhesion and that the elevated levels of ArgBP2 expression observed in p38α KO cancer cells were probably responsible for their impaired cell adhesion.

5.4. Correlation of *Sorbs2* expression with p38α activity in cancer cell lines

Overwhelming evidence suggests that p38α can control many cellular processes in a highly context-dependent manner. Therefore, we decided to investigate whether our observation that p38α negatively regulates *Sorbs2* expression was also conserved in other cancer cell lines. To this end, we examined *Sorbs2* mRNA levels in several human cancer cell lines upon p38α inhibition using PH for 48 h. However, we were surprised that out of 10 tested cell lines, only the osteosarcoma cell line SAOS2 showed substantially upregulated *Sorbs2* mRNA levels upon p38α inhibition (**Figure 37**).

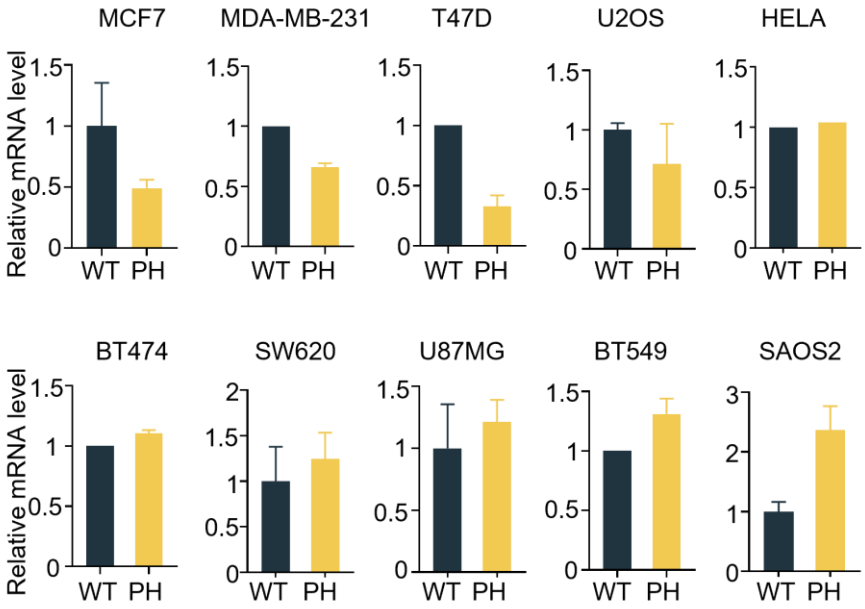

Figure 37. *Sorbs2* expression in human cancer cell lines. *Sorbs2* mRNA levels were determined by qRT-PCR in cells treated with the p38α inhibitor PH797804 for 48 h.

In recent years, extensive efforts have been made to identify genes that are essential for cancer cell fitness. For example, genetic dependencies that are specific to some cancer cells but are not present in normal cells. Alternatively, genetic dependencies, may exist and have some function in non-malignant cells, in which it can induce malignant transformation and is necessary for the continued tumor growth (Lin and Sheltzer, 2020). We speculated that the basal level of *Sorbs2* expression in cells may also play a role, and decided to check how the p38α gene dependency and *Sorbs2* expression levels compared in the selected cell lines.

We extracted the p38α gene effect dataset and *Sorbs2* expression dataset from the DepMap database (Dempster et al., 2019) and did a

bubble plot showing the relationship between p38α gene effect and *Sorbs2* mRNA expression. However, the results suggested that neither high nor low expression of *Sorbs2* at the basal level correlated with the observed response to p38α inhibition (**Figure 38**). Interestingly, we found that the most p38α-dependent cell line among the selected cell lines was SAOS2.

In summary, our results suggest that p38α dependent cancer cells could be more prone to involve p38α in the regulation of *Sorbs2* expression and maybe cell-cell adhesion.

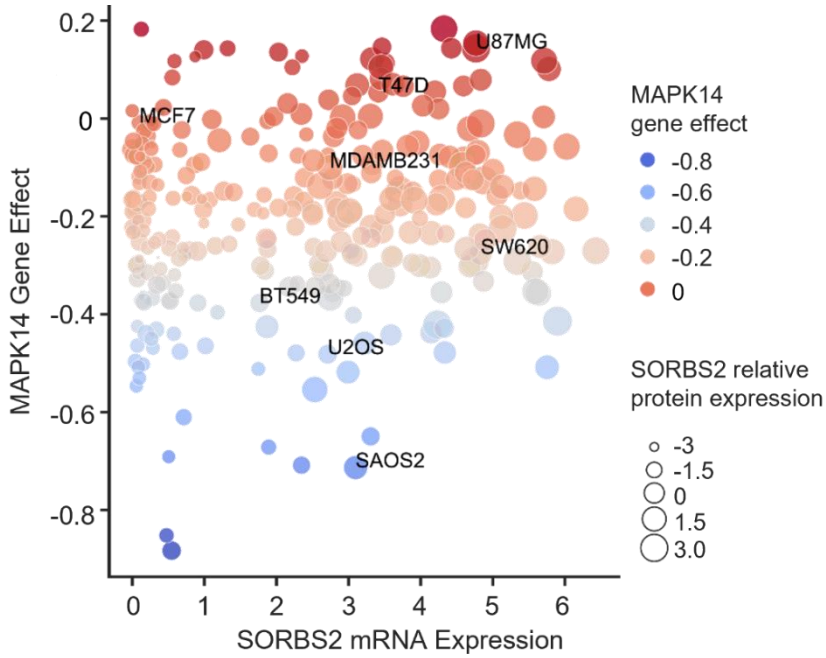

Figure 38. Correlation of *Sorbs2* mRNA expression with p38α dependency in human cancer cell lines. *Sorbs2* mRNA expression data and p38α gene effect data were downloaded from DepMap. Gene effect indicates the dependency level of a cell line on that particular gene. A negative gene effect score indicates depletion of the gene in the cell population, suggesting that it is an essential gene for cell proliferation/viability (Dempster, *et al., 2019*).

DISCUSSION

Protein phosphorylation is a regulatory mechanism that is central to a wide variety of physiological responses, and its misregulation has been linked to many human diseases (Lahiry et al., 2010; Torkamani et al., 2008). As key regulators of phosphorylation, protein kinases have gained increasing focus as potential therapeutic targets for pathologies like cancer and inflammatory diseases. In the past decade, developments in mass spectrometry (MS)-based proteomics have enabled large-scale unbiased profiling of changes in the phosphoproteome of a cell.

To date, 176 proteins, containing 317 phosphosites, have been identified the targets of p38α in PhosphositePlus. The ability of p38α to phosphorylate a plethora of substrates allows this pathway to interpret a wide range of external signals and respond appropriately by generating different biological effects. Despite the physiological importance of the p38a pathway and its pharmacological potential, a comprehensive picture of the substrate repertoire and biochemical mechanisms regulated by p38α signaling is still lacking. In this study, we performed a global quantitative (phospho-)proteomic analysis to explore novel substrates and functions that are regulated by p38α in cancer cell homeostasis. Our work identified several proteins whose phosphorylation or expression can be controlled by p38α, as well as the interplay between p38α and other kinase pathways. We also describe that transcriptional regulation of ArgBP2 expression by p38α regulates cell-cell adhesion.

1. p38α-regulated phosphoproteome

To our knowledge, there are not many studies on the p38 MAPK-regulated (phospho-)proteome. A recent study used the inhibitor SB203580 to investigate phosphoproteomic changes that are modulated by p38 MAPK signaling during the response to UV-induced DNA damage in U2OS cells (Borisova et al., 2018). The effects of the inhibitor SB202190 on the signaling networks detected in Hela cells treated with EGF have been also studied (Pan et al., 2009). Phosphoproteomic changes regulated by Hog1, the yeast homolog of the mammalian p38α, were investigated in response osmostress (Romanov et al., 2017). Recent research used the inhibitor SB220025 and label-free MS analysis to study the function of p38α in early mouse blastocyst development (Bora et al., 2021).

Most of the above studies rely on the use of pyridyl imidazole chemical inhibitors such as SB203580 and SB202190, which have been reported to have numerous off-target effects (Bain et al., 2007; Lali et al., 2000; Shanware et al., 2009). In addition, these compounds can inhibit both p38α and p38β with similar IC50 values, making it challenging to distinguish p38α specific effects. (Cuenda and Rousseau, 2007).

In our (phospho-)proteomic study, we employed both p38α genetic deletion, which has never been used in previous p38α phosphoproteomic studies, and the p38α inhibitor PH797804, which is thought to be more selective for the p38α family member. By overlapping both conditions, we expected to obtain more reliable results. In addition, we performed the analysis without any stimuli in

order to identify the p38α regulated (phospho-)proteome in cancer cell homeostasis, which has not been the focus of previous studies. In particular, our study identified with high confidence 25 proteins that are positively regulated by p38α and 10 proteins that are negatively regulated by p38α, most of which have not been previously linked to p38α. We also identified 26 phosphosites (on 21 proteins) positively regulated by p38α and 88 phosphosites (on 62 proteins) negatively regulated by p38α. Several of these proteins, such as Hspbp1, Nelfe and Rbm7, have been previoulsly reported as bona fide p38α and MK2 substrates validating our studies.

2. p38-MK2 signaling axis

We analyzed the sequence signatures in the p38α positively regulated phosphosites, which are potential p38α targets. We found that a sequence signature (Phe/Leu-Met-Phe-Thr-Arg-XX-Ser-Hydrophobic) that is close to the optimal phosphorylation motif of MK2 (Phe/Leu/Ile-XXX-Arg-Gln/Ser/Thr-Leu-Ser-Hydrophobic) was overrepresented in comparison with the optimal p38α phosphorylation motif (Gly-Pro-Gln-Ser/Thr-Pro-Ile) reported in the literature (Manke et al., 2005). Moreover, the KSEA analysis also supported that the activity of MK2 was significantly decreased in the absence of p38α.

As a key substrate and interactor of p38α, MK2 plays a substantial role in the p38α signaling pathway. For example, the p38-MK2 signaling axis controls the synthesis and release of inflammatory molecules in response to stress and inflammatory signals (Menon and Gaestel, 2018), and it can also modulate RNA metabolism by

phosphorylating the RNA-binding proteins, such as TPP, NELFE, RBM7 (Borisova et al., 2018; Tiedje et al., 2012, 2015). Moreover, p38α and MK2 can form a complex under homeostatic conditions and that the level of MK2 protein is reduced in p38α-deficient cells (Gutierrez-Prat et al., 2021). Our results support that under homeostatic conditions, MK2 plays an important role in the phosphorylation changes regulated by p38α signaling.

The extent to which MK2 is responsible for different signals or targets in the p38α-MK2 signaling axis is unclear. Nevertheless, we have noticed that out of the 26 phosphosites that are positively regulated by p38α, 13 and 8 have MK2 or p38a phosphorylation motifs, respectively. Further work should analyze how these phosphorylations contribute to the different functions regulated by p38α signaling in cancer cells.

3. p38α in DNA replication and cell cycle regulation

The functional enrichment analysis of the p38α positively regulated proteome detected a number of targets involved in DNA replication. Furthermore, several phosphoproteins regulated by p38α are involved in cell cycle regulation. Of note, previous work in our lab showed that p38α deletion in the BBL358 cell line used in this study causes DNA damage and impaired DNA replication, and evidence was obtained that p38α controls ATR-CHEK1 signaling (Cánovas et al., 2018). CHEK1 and p38α have been reported to synergistically prevent uncontrolled CDK1 activation, premature mitotic entry and associated DNA damage, thereby ensuring genome stability during the normal cell cycle (Cánovas et al., 2018; Lemmens et al., 2018).

In line with this, our KSEA analysis suggested that upon p38α deletion or inhibition, CHEK1 activity was downregulated, while CDK1 activity was upregulated, which might be the consequence of both p38α and CHEK1 reduced activity.

Our analysis also predicted that PLK1 activity was somewhat downregulated in the absence of p38α. PLK1 performs several vital functions throughout the M phase of the cell cycle, including regulating centrosome maturation and spindle assembly, removing cohesins from chromosome arms, inactivation of anaphase-promoting complex/cyclosome inhibitors and the regulation of mitotic exit and cytokinesis (Petronczki et al., 2008). It has been reported that the co-localization of phosphorylated p38α and MK2 with PLK1 to the spindle poles during prophase and metaphase is required for mitotic progression in the absence of stress. Furthermore, MK2 can phosphorylate Ser326 of PLK1, which is critical for the recruitment of γ-tubulin to the centrosome and subsequent establishment of a functional bipolar spindle (Tang et al., 2008).

In addition to PLK1, CDK7 kinase activity was also predicted to be decreased in our KESA analysis. CDK7 is the catalytic subunit of the CDK-activating kinase (CAK) complex, which is involved in cell cycle control and RNA polymerase II-mediated RNA transcription through the regulation of p53 activity (Kalan et al., 2017). CDK7 phosphorylates p53 upon DNA damage and is inactivated by a p53 feedback loop leading to cell cycle arrest or activation of transcription to help cell recovery or apoptosis (Schneider et al., 1998). CDK7 is also required for both formation and activation

of CDK2/cyclin complexes during G1/S transition (Larochelle et al., 2007). Moreover, CDK7 ablation or pharmacological inhibition impairs the transcriptional activity of MYC through downregulating p38α and sensitizes non-small cell lung cancer cells to p38α inhibition (Wang et al., 2020).

These results are consistent with the published observations showing that p38α deletion in BBL358 cell line results in a variety of mitotic aberrations, abnormal cytokinesis, increased aneuploidy and a CIN phenotype (Cánovas et al., 2018). However, it would be interesting to further validate whether PLK1 and/or CDK7 activities are decreased upon p38α deficiency and how exactly they could interplay with p38α in the regulation of these processes.

In the same line, we found that p38α positively regulated the expression of Mcm2 and Mcm4, two proteins involved in DNA replication, and unpublished results from our lab indicate that Mcm2 and Mcm4 mRNA and protein levels are indeed downregulated in p38α KO cells, further supporting the results that we have obtained.

Collectively, our observations suggest an important role for p38α in DNA replication and cell cycle control, perhaps not through the regulation of one or two proteins but by controlling a broad protein network that cooperatively regulates these processes. In addition, our results suggest that inhibition of other kinases such as CHEK1, PLK1 or CDK7 could synergize with p38α inhibition, providing combinations of potential clinical relevance.

4. p38α in protein synthesis regulation and the crosstalk with mTOR

The ribosome is essential for protein synthesis and cell survival, and its function must be tightly controlled with respect to activity, selectivity and fidelity. Many drugs, such as translation inhibitors (e.g., anisomycin and cycloheximide), ribotoxins (e.g., ricin, Shiga toxin and α-sarcin), chemotherapeutics (e.g., doxorubicin) and UV-radiation, are known to cause structural damage to rRNA and impair ribosome function, leading to strong activation of p38α and JNK through the upstream MAP3K ZAKα, also known as MAP3K20 or MLTK ((Laskin et al., 2002).

Our analysis indicated that rRNA processing and ribosome biogenesis, two processes related to the translation machinery, are associated with p38α positively regulated proteomic changes. In addition, several proteins involved in the translation machinery form high confident protein-protein interaction (PPI ≥ 0.7) networks in the combined phosphoproteomic and proteomic analysis. This network includes ribosomal proteins Rps3, Rps8 and Rpl29, RNA helicase Ddx52, nuclear protein Nop14 and Nop56, which participate in ribosomal subunit assembly, spliceosome proteins Rbm22, Smu1, Srrm2, Gemin7 and Wbp4, and some regulators of mRNA turnover. It has been reported that the p38 MAPK pathway plays a major role in ribosomal stress surveillance (Vind et al., 2020). The knockdown of Rps3 or Rps6 induces aberrant ribosome biogenesis, which triggers ASK1-mediated p38α activation, p53 induction and phosphorylation and G1 arrest, while depletion or pharmacological

inhibition of p38α abrogates G1 arrest caused by ribosomal stress (Kim et al., 2011). Interestingly, our dataset contains several phosphoproteins related to ribosome functions, and most of these phosphosites do not have a reported function yet.

The interactions between the translation machinery, especially ribosomal proteins, and p38α are not well understood. Recently, p38 MAPK inhibition has been implicated in the regulation of ribosome-related gene expression, rRNA precursor processing, polysome formation and protein translation during mouse blastocyst primitive endoderm differentiation, which can be partially reversed by concomitant mTOR activation (Bora et al., 2021). Curiously, our KSEA analysis predicted that mTOR activity is downregulated upon p38α deficiency. mTOR is a global regulator of translation and maintains cellular energy homeostasis in response to extracellular stimuli, such as growth factors and nutrient availability. In particular, the mTORC1 complex has been reported to specifically control transcription and translation of ribosomal genes/proteins, synthesis and processing of rRNA, and biogenesis and availability of ribosomes to ultimately dictate general translation of mRNA transcripts (Fonseca BD et al., 2014), while the mTORC2 complex has so far been associated with the actin cytoskeleton control and maintenance, co-translational protein degradation and lipolysis (Jacinto et al., 2004).

There is evidence that mTOR signaling can be controlled by p38α in response to specific stresses and growth factors in regulatory T cell function and heart ischemia (Canovas B and Nebreda AR, 2021; Cully et al., 2010), but the integration between p38α and mTOR

signaling in the regulation of ribosome function is understudied. Our data suggests that it may be worth characterizing the crosstalk between both pathway in the regulation of translation.

5. p38α regulates cell adhesion

Homeostasis in healthy tissues strongly relies on cell adhesion, which is required not only for physically anchoring of the cells but also for the integration of a diverse range of signaling between the cells and the extracellular microenvironment. The network of proteins involved in cell adhesion has been assigned into 20 different groups according to their biological activity. Adaptor proteins, adhesion receptors and actin regulators form the physical structure of the adhesome that connect the membrane with the actin cytoskeleton. In addition, there are protein kinases, Rho GTPases, lipids, and proteases that regulate the assembly and turnover of the adhesion as well as signaling from the adhesion into the cell (Zaidel-Bar et al., 2007).

The GO analysis of our data highlighted cell adhesion as the most enriched function among the p38α regulated phosphoproteome changes, especially considering the negatively regulated phosphoproteins. Moreover, adhesion-related functions, such as extracellular structures and plasma membrane organization, were also enriched in the p38α negatively regulated proteome, further supporting the potential role of p38α in cell adhesion regulation.

Experiments to investigate the role of p38α in ECM adhesion showed that the attachment ability of BBL358 cells on both purified ECM

components and fibroblast-derived cell-free matrixes was consistently decreased upon p38α deletion or inhibition. In addition, we investigated whether cell-cell adhesion is affected by p38α by using the 3D spheroid model, which may mimic cell-cell interactions that occur during three-dimensional arrangements of the cells in vivo. We found that the spheroids formed by p38α-deficient cells were markedly smaller in size and showed reduced expression of the tight junction protein ZO-1, compared with those formed by WT cells, suggesting that p38α is required for cell-cell adhesion.

The work reported in the literature suggest that the effect of p38α on cell adhesion might depend on the stress strength and the experimental conditions. Thus, inhibition of p38α may prevent the stress-induced junction disruption in 2D models. A study showed that a short treatment (8 h) of HaCaT cells with either p38 inhibitors or anisomycin (which activates p38α) induces a ZO-1 staining pattern that is characteristic of mature junctions but upon longer treatment (24 h), p38α inhibition has no effect on ZO-1 accumulation, suggesting that p38α is crucial in the early events (Minakami et al., 2015). Prolonged SB203580 treatment (72h) was also shown to have no effect on ZO-1 intracellular labeling in normal human keratinocytes (Siljamäki et al., 2014). Interestingly, different roles have been reported for p38α in 2D and 3D cultures. In 2D, anisomycin treatment for 12 h inhibited the formation of mature junctions, which was restored upon JNK inhibition but not by inhibiting p38α. However, in 3D, anisomycin treatment for two weeks activated only p38α and removed CLDN7 from ZO-1-positive spots on the surface of 3D cultures, disrupting tight junctions. Thus,

short-term anisomycin treatment inhibited maturation of cell-cell junctions by JNK activation, but p38 activation by long-term anisomycin treatment affected the morphology of stratified structures and paracellular permeability in 3D (Nikaido et al., 2019). However, how p38α might regulate cell adhesion in 3D cultures was not investigated.

On the other hand, our results are consistent with previous reports proposing a role for p38α in cell adhesion during embryonic development and epithelial-mesenchymal transition (EMT). It has been reported that p38α inhibition compromises tight junction integrity during blastocyst formation through increasing tight junction permeability and shifting of ZO-1 localization (Bell and Watson, 2013). In the same line, p38α blockade disrupts intercellular junctions through disorganization and downregulation of cytokeratin filaments and ZO-1 during EMT, accompanied by elevated vimentin expression, allowing cells to adapt to migratory and invasive phenotypes (Strippoli et al., 2010).

It is important to keep in mind that our set of experiments was performed using a 3D model similar to these two experiment settings and in homeostatic conditions. It is therefore not completely unexpected that the cell signaling events, and in particular how p38α contributes to a particular function like cell adhesion, differ when compared to the response to stress stimuli.

6. ArgBP2 in p38α regulated cell adhesion

Although many publications suggest a role of p38α in cell adhesion control through modulating different CAMs, such as ICAM-1, VCAM-1, E-selectin, paxillin, tight junction proteins and claudins, the contribution of all these changes to the process and how exactly they are regulated by p38α is not well understood. Interestingly, our results indicate that around 40 proteins and phospho-proteins that are significantly regulated p38α were involved in cytoskeleton or cell adhesion regulation. Moreover, a number of these phospho-proteins were negatively regulated by p38α, including Pak1, Git1, Nestin, Tjap1, Vim, Twf1, Svil, ArgBP2 and Zyxin.

Notably, the adaptor protein ArgBP2, which is encoded by Sorbs2, was one of the top hits negatively regulated by p38α. ArgBP2 has been described to associate with the Abl/Arg non-receptor tyrosine kinase pathway to negatively regulate cell adhesion and sarcomere architecture (Taieb et al., 2008). Therefore, we hypothesized that ArgBP2 might be involved in p38α regulated cell adhesion. Importantly, rescue experiments knocking down ArgBP2 expression supported that enhanced ArgBP2 levels might account, at least in part, for the impaired cell-cell adhesion observed upon p38α inhibition. However, how p38α regulates ArgBP2 and the role of ArgBP2 in cell-cell adhesion still needs to be clarified. For example, since ArgBP2 is a component of the apical junction complex of epithelial cells (Fredriksson-Lidman et al., 2017), it would be interesting to know whether p38α regulates the localization of ArgBP2. As a scaffold protein, ArgBP2 interacts with many

cytoskeletal components to control the balance between adhesion and motility. Whether ArgBP2 is related to the decreased expression of ZO-1 induced by p38α deficiency and whether the overexpression of ArgBP2 leads to the actin cytoskeleton disruption are questions worth exploring in the future.

We confirmed that p38α negatively regulates *Sorbs2* expression at the transcriptional level, but the mechanisms implicated are not yet fully understood. *Sorbs2* transcription has been described to be regulated by MEF2A and MEF2D (Wales et al., 2014; Yan et al., 2019), which are both p38α substrates and may function as transcription repressors when phosphorylated (Kang et al., 2006; Zhao et al., 1999). However, the phosphorylation of MEF2A an MEF2D that has been linked to their function as transcription repressors, is different from the sites that are known to be phosphorylated by p38α. On the other hand, our (phospho-)proteomic analysis suggested other potential regulators of *Sorbs2* that could be worth exploring further, such as *Larp1*, *Lima1* and *Mdm2*.

7. Difference between genetic KO and pharmacological inhibition

The analysis of our (phospho-)proteomic datasets, indicated a positive correlation between p38KO/WT and PH/WT comparisons, with Pearson coefficient correlation 0.707 for proteome and 0.758 for phosphoproteome. Intriguingly, when a more stringent filtering criteria was applied ($p<0.05$ and fold change > 1.5 or fold change <

-1.5), we found an unexpected difference in the number of significant hits retrieved between p38α deletion (KO/WT) and chemical inhibition (PH/WT). For example, we detected around three-fold more changes for total proteins either positively or negatively regulated p38α in PH/WT proteomic dataset compared to KO/WT. This difference was even higher for the phosphoproteomic dataset, with around five-fold more changes for p38α positively regulated phosphorylation events in PH/WT than in KO/WT.

Genetic compensation (genetic buffering) might explain why we observed fewer changes in p38α deletion than in pharmacological inhibition with PH. Genetic robustness may arise from redundant genes, whereby the loss of one gene may be compensated by another with overlapping functions and expression patterns (El-Brolosy and Stainier, 2017). Another form of robustness arises from tightly regulated cellular networks, including metabolic, signaling, and transcriptional networks (El-Brolosy et al., 2019). Perturbation of a particular gene's function in a network may alter the expression of other genes within the same network, thereby maintaining cellular homeostasis. Additionally, in response to a gene knockout, organisms such as yeast can accumulate mutations in one or more genes modulating the affected pathway, leading to partial or full rescue of the outcome (Teng et al., 2013).

In our experimental system, the most likely candidates responsible for functional compensation are other p38 family members, especially p38β, whose functions are mostly redundant in the presence of p38α that is usually expressed at much higher levels. This

functional redundancy has been reported in various cell types. For instance, p38α and p38β have overlapping functions during mouse development (Barrantes et al., 2011). Another study demonstrated that in response to TCR stimulation, p38α-deficient T cells showed no obvious cell-autonomous defects when increased the expression of p38β. (Jirmanova et al., 2011). Other MAPKs, like ERK1/2, could also be responsible for the compensation effect. For example, cardiomyocytes and fibroblasts lacking p38α are more resistant to apoptosis induced by different stimuli, and elevated ERK1/2 activity in these cells contributes to the reduced levels of apoptosis by the upregulation of the survival pathway (Porras et al., 2004).

The functions of p38 MAPKs are typically associated with the phosphorylation of substrates on Ser/Thr-Pro motifs, but p38 MAPKs have also reported to have some kinase-independent roles. These are thought to be mediated to the binding to other proteins in the absence of phosphorylation, possibly by structural modification of the targets, changes in their subcellular location or competition with their binding to other proteins (Cuadrado and Nebreda, 2010). For instance, protein O-GlcNAcylation catalyzed by the O-GlcNAc transferase (OGT) enzyme has been proposed to be regulated by p38α in a kinase-independent manner in the context of ischemia-induced stress in the brain. In this case, p38α does not seem to phosphorylate OGT, interacts with the OGT C terminus, regulating its activity by recruiting it to specific targets, such as neurofilament H, and stimulating its O-GlcNAcylation (Cheung and Hart, 2008). Since the changes observed only in the p38α KO condition, when both the mRNA and the protein are removed, are fewer compared to PH,

which only impairs protein activity, it seems like not many kinase-independent events of p38α are likely to occur in our experimental setting.

Another possibility is that PH could be also inhibiting p38β, PH can also inhibit p38β with a higher IC50 (Xing et al., 2009). In addition, since PH binds to the ATP-binding sites (Coulthard et al., 2009), we do not know whether this PH-bounded p38α form will have unexpected conformational changes and functions. Moreover, 4-OHT inducible Cre recombinase system may cause some side effects (Donocoff et al., 2020). Finally, we should also acknowledge that the isotopic dilution and scrambling between high-, medium- and light-isotopes cannot be completely eliminated, although use of this method can markedly improve the label specificity (Tong et al., 2008).

In summary, our results identify some common (phospho-)proteomic changes upon both p38α deletion and inhibition, but we do also find substantive differences, which at the moment are difficult to account for. Some of them might reflect the ability of PH to inhibit also p38β, or the synergistic modulation of other (unidentified) signaling pathways. However, non-catalytic functions of p38α should be also considered. Alternative approaches such as the use of PROTACs to induce p38α protein degradation (Donoghue et al., 2020), or the use of additional chemical inhibitors of p38α (Campbell et al., 2014) or downstream targets like MK2 (Shah et al., 2017) should be considered.

8. Future perspectives

Rapid advances in phosphoproteomics have revealed over 100,000 different phosphosites in human cells; while less than 5% of phosphosites have identified kinases, not to mention that the phosphosites function assignments are almost negligible (Needham et al., 2019). Despite the challenges in the interpretation of phosphoproteome data, recently developed methods to assign functional scores (Ochoa et al., 2019) allowed us to determine the potential importance of phosphosites in cell fitness. These scores could be helpful for further considering whether particular candidates are worth validation and analyzing.

Although our study was performed under tumor cell homeostatic condition, which differs from the response to stress stimuli, it is possible that some of the p38α targets or crosstalks identified could be relevant to the response to some stresses.

This work highlights the complexity of the p38α regulated signaling networks, provide valuable information on p38α-dependent phosphorylation events in cancer cells, and provide new insights into the mechanisms modulated by p38α in cell-cell adhesion.

CONCLUSIONS

1. We have identified several proteins whose expression or phosphorylation can be regulated by p38α in cancer cells.

2. p38α regulates cell-cell adhesion in cancer cells.

3. ArgBP2 is a likely candidate to mediate the role of p38α in cancer cell adhesion, and is transcriptionally controlled by p38α

4. p38α maintains cancer cell homeostasis mainly through regulation of DNA replication, protein synthesis and cell adhesion.

SUPPLEMENTARY

Supplementary Table 1. List of p38α positively regulated proteins. Proteins were filtered by p-value<0.05 and log2FC<-0.58 (FC<-1.5).

Gene name	Protein name	Log2FC (KO/WT)	Log2FC (PH/WT)	p-value (KO/WT)	p-value (PH/WT)
Abcf2	ATP-binding cassette sub-family F member 2	-0.72	-0.79	1.7E-02	9.9E-03
Arpp19	cAMP-regulated phosphoprotein 19	-0.93	-0.89	2.0E-02	2.5E-02
Ctr9	RNA polymerase-associated protein CTR9 homolog	-1.23	-0.99	1.9E-03	8.3E-03
Cul4b	Cullin-4B	-0.59	-0.67	3.9E-02	2.1E-02
Ddx52	Probable ATP-dependent RNA helicase DDX52	-1.92	-2.35	3.8E-03	8.3E-04
Diaph3	Protein diaphanous homolog 3	-0.91	-0.97	2.7E-02	2.0E-02
Dmd	Dystrophin	-0.63	-0.74	4.4E-02	2.1E-02
Dnajc17	DnaJ homolog subfamily C member 17	-0.96	-0.97	3.1E-03	3.0E-03
Erc1	ELKS/Rab6-interacting/CAST family member 1	-1.46	-1.15	8.0E-03	2.9E-02
Hspbp1	Hsp70-binding protein 1	-0.63	-0.82	2.8E-07	1.2E-08
Kri1	Protein KRI1 homolog	-0.72	-0.63	3.7E-04	1.2E-03
Krt14	Keratin, type I cytoskeletal 14	-0.68	-1.11	5.3E-08	1.0E-10
Mcm2	DNA replication licensing factor MCM2	-0.89	-0.84	1.4E-03	2.1E-03
Mcm4	DNA replication licensing factor MCM4	-0.71	-0.71	2.4E-02	2.4E-02
Myl1;Myl3	Myosin light chain 1/3	-1.17	-1.12	5.0E-04	7.5E-04
Naa10	N-alpha-acetyltransferase 10	-1.11	-1.04	1.3E-03	2.1E-03
Nanp	N-acylneuraminate-9-phosphatase	-1.00	-0.84	5.9E-04	2.4E-03
Nop14	Nucleolar protein 14	-0.87	-1.28	1.8E-02	1.6E-03
Pcyt2	Ethanolamine-phosphate cytidylyltransferase	-0.68	-0.61	3.5E-03	7.5E-03
Ppm1g	Protein phosphatase 1G	-0.60	-0.60	3.8E-04	3.6E-04
Rbm22	Pre-mRNA-splicing factor RBM22	-0.81	-0.62	4.8E-05	5.6E-04
Rpl29	60S ribosomal protein L29	-1.30	-1.12	1.8E-05	8.0E-05
Smu1	WD40 repeat-containing protein SMU1	-0.87	-0.85	5.6E-03	6.3E-03
Zfp36l1	Zinc finger protein 36, C3H1 type-like 1	-1.02	-0.64	2.4E-07	4.5E-05
Zwint	ZW10 interactor	-1.44	-1.37	4.7E-03	6.6E-03

Supplementary Table 2. List of p38α negatively regulated proteins. Proteins were filtered by p-value<0.05 and log2FC>0.58 (FC>1.5).

Gene name	Protein name	Log2FC (KO/WT)	Log2FC (PH/WT)	p-value (KO/WT)	p-value (PH/WT)
Ckb	Creatine kinase B-type	0.79	1.10	3.0E-03	2.0E-04
Ctsa	Lysosomal protective protein	0.64	1.14	2.8E-04	6.5E-07
Dlst	Dihydrolipoamide S-Succinyltransferase	0.76	1.07	7.8E-03	6.4E-04
Fam167a	Protein FAM167A	1.01	0.71	7.4E-04	8.8E-03
Hmga2	High mobility group protein HMGI-C	0.61	0.71	3.2E-08	4.6E-09
Psap	Prosaposin	0.60	1.10	1.9E-05	1.6E-08
Ptgr1	Prostaglandin reductase 1	0.62	0.65	1.5E-06	8.0E-07
Sdpr	Serum deprivation-response protein	0.99	1.32	1.1E-07	3.4E-09
Sorbs2	Sorbin and SH3 domain-containing protein 2	0.88	1.04	2.3E-09	2.4E-10
Vim	Vimentin	1.11	0.86	1.0E-09	2.6E-08

Supplementary Table 3. List of p38α positively regulated phosphosites. phosphosites were filtered by p-value<0.05 and log2FC<-0.58 (FC<-1.5).

Gene name	Protein name	Amino acid	Phospho sites	Log2FC (KO/WT)	Log2FC (PH/WT)	p value (KO/WT)	p value (PH/WT)
Amfr	E3 ubiquitin-protein ligase AMFR	LPSEGTSSDPVTLRR	S619	-1.76	-1.86	2.5E-03	1.6E-03
		RLLPSEGTSSDPVTL	T617	-1.74	-1.46	7.9E-03	2.1E-02
		LLPSEGTSSDPVTLR	S618	-1.59	-1.45	1.7E-02	2.7E-02
C18orf25	Uncharacterized protein C18orf25 homolog	LMELRRDSSESQLAS	S66	-0.60	-0.74	4.7E-02	1.8E-02
Eppk1	Epiplakin	PGLRRQVSASELCTS	S2705	-0.63	-0.71	6.2E-03	2.6E-03
Gorab	RAB6-interacting golgin	SQKPRSPSPVAPSPL	S82	-0.59	-0.75	4.2E-04	3.8E-05
Hn1	Jupiter microtubule associated	PGTQRSNSSEASSGD	S87	-1.60	-2.36	2.2E-10	6.6E-13
Hspb1	Heat shock protein beta-1	FSLLRSPSWEPFRDW	S15	-1.76	-2.46	7.8E-09	6.6E-11
		VPFSLLRSPSWEPFR	S13	-1.52	-2.02	1.6E-08	2.8E-10
Larp1	La-related protein 1	EGRKRCPSQSSSRPA	S1032	-0.74	-1.21	3.7E-05	8.2E-08
		EPSTIARSLPTTVPE	S743	-0.77	-0.86	5.6E-05	1.5E-05
		LPTTVPESPNYRNAR	S751	-0.60	-0.88	1.9E-03	5.8E-05
Mkl1	MKL/myocardin-like protein 1	TGSTPPVSPTPSERS	S492	-0.80	-1.38	1.4E-05	1.2E-08
Mllt4	Afadin	ELMTRTSSVVTLEVA	S1083	-0.88	-1.28	4.0E-03	1.7E-04
Msl1	Male-specific lethal 1 homolog	RWKSIRKSPLGGGGG	S207	-0.74	-0.73	8.6E-03	8.7E-03
Nedd4	E3 ubiquitin-protein ligase NEDD4	FTTRRQISEDVDGPD	S309	-2.06	-2.27	1.1E-08	2.7E-09
Nelfe	Negative elongation factor E	QPFQRSMSADEDLQE	S115	-1.16	-1.45	8.6E-07	4.8E-08
Nol9	Polynucleotide 5'-hydroxyl-kinase	RSRPAPRSPPTPSVP	S88	-0.89	-1.39	2.1E-02	1.1E-03
Nop56	Nucleolar protein 56	EEAASPTTPKKKRKF	T546	-0.62	-1.36	3.2E-02	9.8E-05
Pex1	Peroxisome biogenesis factor 1	HPVFRTPSQEGCQDL	S1182	-0.70	-0.90	1.7E-03	1.9E-04
Ppp6r3	Ser/thr-protein phosphatase 6	QDDIGNVSFDRVSDI	S550	-0.71	-0.59	7.9E-04	3.1E-03
Rbm7	RNA-binding protein 7	QMVQRSFSSPEDYQR	S136	-1.14	-1.46	4.3E-03	6.4E-04
Rfc1	Replication factor C subunit 1	IKKARKDSEEGEESF	S244	-0.73	-0.71	1.6E-05	2.0E-05
Srrm2	Serine/arginine repetitive matrix	RSSRRSSSELSPEVV	S1340	-0.67	-0.80	3.2E-03	7.4E-04
Svil	Supervillin	FFSERSISFPEVPRS	S220	-1.04	-1.49	5.0E-03	2.6E-04
Ybx3	Y-box-binding protein 3	PAALLAGSPGGDAAP	S52	-0.59	-0.76	3.6E-04	2.7E-05

Supplementary Table 4. List of p38α negatively regulated phosphosites. phosphosites were filtered by p-value<0.05 and log2FC>0.58 (FC>1.5).

Gene name	Protein name	Amino acid	Phospho sites	Log2FC (KO/WT)	Log2FC (PH/WT)	p value (KO/WT)	p value (PH/WT)
Aagab	Alpha- and gamma-adaptin-binding protein p34	HSEQQEPSPTAERTE	S211	1.52	1.72	2.7E-10	4.1E-11
AI597479	Ashwin	PVKSPPLSPVGTTPV	S193	0.70	0.70	2.4E-05	2.7E-05
Arhgef12	Rho guanine nucleotide exchange factor 12	LSVAGLQSPDRVLGL	S1176	0.75	0.88	2.1E-03	5.3E-04
Basp1	Brain acid soluble protein 1	AGTEEEGTPKESEPQ	T36	2.04	2.64	1.6E-04	1.0E-05
Bin1	Myc box-dependent-interacting protein 1	PSPPPDGSPAATPEI	S304	0.72	0.62	1.4E-06	9.0E-06
		APEKGNKSPSPPPDG	S296	0.63	0.72	1.7E-06	3.7E-07
		PGATIPKSPSQLRKG	S332	0.69	0.72	6.7E-04	4.9E-04
Cast	Calpastatin	QKPFTPASPVQSTPS	S219	1.19	0.83	1.0E-08	1.2E-06
		GSNQAPNSPSEGNSL	S602	1.53	1.53	9.4E-12	9.7E-12
Cgnl1	Cingulin-like protein 1	CFPKSYGSQPNSPTS	S199	1.19	1.09	5.3E-09	1.7E-08
		SYGSQPNSPTSEDLA	S203	1.14	1.09	2.7E-08	5.3E-08
		TLSPRRKSPTAPSPQ	S257	0.97	0.70	4.2E-08	3.2E-06
Csde1	Cold shock domain-containing protein E1	SPAAPGQSPTGSVCY	S123	1.15	1.14	2.6E-05	2.7E-05
Cttnbp2nl	CTTNBP2 N-terminal-like protein	QGPIKPVSPNSSPFG	S522	1.25	0.70	4.0E-08	4.8E-05
Eif4b	Eukaryotic translation initiation factor 4B	SSDTEQPSPTSGGGK	S504	1.06	0.83	1.2E-03	7.0E-03
Eps15	Epidermal growth factor receptor substrate 15	QKNITGSSPVADFSA	S324	1.23	0.81	1.4E-05	9.1E-04
Fam13b	Protein FAM13B	ESGEAQLSPQAARMT	S437	0.59	1.40	1.5E-04	3.9E-09
Filip1l	Filamin A-interacting protein 1-like	SLNGRRISDPQVFSK	S789	0.69	0.59	4.4E-03	1.1E-02
Gemin7	Gem-associated protein 7	_____MQSPLTIPVP	S3	1.27	1.31	7.6E-05	5.4E-05
Git1	ARF GTPase-activating protein GIT1	QQGKSLSSPTDNLEL	S371	1.00	0.71	4.7E-03	3.3E-02
Gpn1	GPN-loop GTPase 1	EAGKGNASPVLDPSD	S314	1.29	1.16	4.2E-09	1.7E-08
H2afy	Core histone macro-H2A.1	ADSTTEGTPTDGFTV	T178	0.73	2.31	2.5E-04	1.1E-10
Hn1l	Jupiter microtubule associated homolog 2	KTSDIFGSPVTATAP	S97	0.97	1.00	8.5E-07	6.5E-07
Iqce	IQ domain-containing protein E	KQPKGDQSPEDLPKV	S387	1.53	1.37	4.7E-07	1.9E-06
Jun	Transcription factor AP-1	KNSDLLTSPDVGLLK	S63	0.64	0.75	5.9E-03	1.8E-03
Khsrp	Far upstream element-binding protein 2	SGCKVQISPDSGGLP	S182	1.65	1.11	5.5E-11	1.7E-08
Kiaa1598	Shootin-1	TAEADSSSPTGILAT	S494	1.29	0.83	2.9E-04	8.8E-03
Lad1	Ladinin-1	DEDADTPSPTLLTYS	S367	0.94	1.03	5.0E-08	1.4E-08
		KTSVTEKSPVPEKTL	S240	1.10	0.59	4.1E-07	4.2E-04

Continued on next page

Gene name	Protein name	Amino acid	Phospho sites	Log2FC (KO/WT)	Log2FC (PH/WT)	p value (KO/WT)	p value (PH/WT)
Lgalsl	Galectin-related protein	HLNNSLGSPVQADVY	S25	1.19	1.05	3.4E-08	2.0E-07
Lima1	LIM domain and actin-binding protein 1	PMHPKPLSPDARTSS	S360	0.65	0.71	7.3E-04	3.3E-04
Lrrfip1	Leucine-rich repeat flightless-interacting protein	TDILDQNSPQCEDRE	S649	1.30	1.08	1.5E-09	2.0E-08
Macf1	Microtubule-actin cross-linking factor 1	AEEELAASGGQSPTG	S5547	1.01	1.13	3.4E-03	1.5E-03
Map1b	Microtubule-associated protein 1B	SPLTPRESSPLYSPG	S1788	0.62	0.66	6.5E-06	3.0E-06
		RESSPLYSPGFSDST	S1793	0.60	0.68	3.5E-04	1.0E-04
Map4	Microtubule-associated protein 4	LGMAKDMSPLPESEV	S475	1.72	0.94	4.4E-10	1.6E-06
		VPGNDTTSPKETETT	S345	1.17	0.67	1.4E-04	1.2E-02
		AEDGAAPSPSSETPK	S138	0.98	0.79	7.9E-08	1.3E-06
Marcks	Myristoylated alanine-rich C-kinase substrate	AEPAEPSSPAAEAEG	S113	1.25	1.48	3.3E-07	3.4E-08
		EAEPAEPSSPAAEAE	S112	0.86	1.40	4.2E-03	5.9E-05
Mdm2	E3 ubiquitin-protein ligase Mdm2	SSRRRSISETEENTD	S163	0.89	1.05	1.4E-05	1.9E-06
Mmp10	Stromelysin-2	LPRQSVDSAIEKALK	S132	1.01	1.06	9.0E-09	4.7E-09
Myo9b	Unconventional myosin-IXb	AGPDAGLSPGSQGDS	S1371	0.81	0.69	2.2E-03	6.8E-03
Nedd4l	E3 ubiquitin-protein ligase NEDD4-like	PASPVSRTSPQELSE	T331	0.89	0.74	2.1E-03	7.8E-03
		ASPVSRTSPQELSEE	S332	0.87	1.01	4.0E-03	1.3E-03
		ERQESLKSPEEEDQQ	S731	1.21	0.65	1.3E-08	3.1E-05
		EDQRFPRSPEEDQQA	S688	1.18	0.72	3.1E-08	1.8E-05
Nes	Nestin	LEKENVQSPRYLEED	S894	1.06	0.80	5.7E-06	1.3E-04
		ESQESLKSPEEEDQR	S819	0.93	0.61	3.5E-03	3.7E-02
		ERLVEKESQESLKSP	S813	0.72	0.66	1.6E-02	2.4E-02
Nup35	Nucleoporin NUP53	SDRGVLSSPSLAFTT	S258	0.75	0.81	4.3E-04	2.1E-04
Otud7b	OTU domain-containing protein 7B	GEDQPSDSPAEPKAM	S680	0.75	0.59	1.5E-03	7.8E-03
Pacsin3	PKC and casein kinase II substrate protein 3	RKEKGGRSPDEVTLT	S319	1.40	1.25	3.5E-05	1.2E-04
Pak1	Serine/threonine-protein kinase PAK 1	DVATSPISPTENNTT	S223	1.55	1.99	2.6E-08	8.1E-10
		ATSPISPTENNTTPP	T225	0.80	1.22	1.2E-02	4.9E-04
Ppp1r12a	Protein phosphatase 1 regulatory subunit 12A	SEKRDKKSPLIESTA	S299	0.60	0.91	1.9E-05	1.2E-07
Prrc2b	Protein PRRC2B	SAASLSASPTELGSR	S226	1.38	0.78	1.7E-09	3.5E-06
		AMGMHVRSPDEALPG	S793	0.97	0.83	6.4E-06	3.8E-05

Continued on next page

Gene name	Protein name	Amino acid	Phospho sites	Log2FC (KO/WT)	Log2FC (PH/WT)	p value (KO/WT)	p value (PH/WT)
Psmd1	26S proteasome non-ATPase regulatory subunit 1	ASAVAGKTPDASPEP	T311	1.36	1.16	1.7E-10	1.7E-09
		AGKTPDASPEPKDQT	S315	1.30	1.09	4.0E-10	4.8E-09
		QNLRTVGTPIASVPG	T273	0.84	1.22	3.1E-03	1.3E-04
Rem2	GTP-binding protein REM 2	GQRPEPSSPDGPAPP	S296	1.09	1.34	1.9E-09	1.0E-10
Rps3	40S ribosomal protein S3	KDEILPTTPISEQKG	T221	1.75	1.42	1.5E-05	1.3E-04
Rps8	40S ribosomal protein S8	RKKGAKLTPEEEEIL	T130	2.41	2.47	8.5E-10	5.9E-10
Sdpr	Serum deprivation-response protein	GNNSAVGSNADLTIE	S363	1.22	1.77	2.2E-09	9.5E-12
		KSSPFKVSPLSFGRK	S293	1.06	0.97	7.7E-08	2.5E-07
		KASSGKSSPFKVSPL	S288	0.87	0.73	7.0E-04	3.1E-03
Sept9	Septin-9	TGPALKRSFEVEEIE	S30	0.94	2.01	1.0E-05	4.3E-10
Serbp1	SERPINE1 mRNA-binding protein 1	VKDELTESPKYIQKQ	S234	1.41	0.89	8.6E-05	4.6E-03
Sh3kbp1	SH3 domain-containing kinase-binding protein 1	PIKLRPRSIEVENDF	S274	0.60	0.74	1.5E-03	2.6E-04
Snap23	Synaptosomal-associated protein 23	WGDGGDNSPSNVVSK	S110	0.80	1.10	8.8E-08	1.1E-09
Sorbs2	Sorbin and SH3 domain-containing protein 2	DFRKRRKSEPAVGPL	S339	1.08	1.27	2.0E-09	1.9E-10
		TSVKRVQSSPNLLAA	S27	1.46	1.33	9.8E-09	3.4E-08
		FTKSFISSSPSSPSR	S378	0.95	1.45	1.5E-05	7.4E-08
		SFISSSPSSPSRAQG	S381	0.97	1.53	2.0E-05	6.7E-08
		FISSSPSSPSRAQGG	S382	0.97	1.00	7.7E-05	5.3E-05
Svil	Supervillin	MVKKGLASPTSITPI	S1181	1.20	0.74	2.0E-09	1.4E-06
Szrd1	SUZ domain-containing protein 1	ARRRILGSASPEEEQ	S105	0.88	0.69	1.4E-03	8.2E-03
		RRILGSASPEEEQEK	S107	0.60	0.62	4.3E-02	3.7E-02
Tjap1	Tight junction-associated protein 1	PSPSSSLSPGAVVPT	S214	0.63	0.88	1.3E-03	5.7E-05
Tomm22	Mitochondrial Import Receptor Tom22	AGAGEPLSPEELLPK	S15	1.13	1.74	9.4E-04	1.3E-05
Tp53bp2	Apoptosis-stimulating of p53 protein 2	QKENLPVSPDGNLPQ	S328	1.87	1.34	1.2E-09	1.2E-07
Twf1	Twinfilin-1	KYLLSQSSPAPLTAA	S143	0.78	0.84	5.0E-03	2.8E-03
Txlna	Alpha-taxilin	SKEQGVESPGAQPAS	S515	1.04	1.34	3.6E-05	1.9E-06
Usp47	Ubiquitin carboxyl-terminal hydrolase 47	SDFENIESPLNERGS	S911	0.65	1.13	6.1E-05	6.9E-08
Vim	Vimentin	TSRSLYSSSPGGAYV	S55	0.98	0.79	5.4E-05	4.1E-04
Wbp4	WW domain-binding protein 4	DISEPTVSPVISTVQ	S97	1.21	0.86	5.6E-03	3.6E-02
Zyx	Zyxin	QNQNQVRSPGGPGPL	S336	0.99	0.75	6.2E-09	3.0E-07

MATERIALS AND METHODS

1. Materials

General buffers and solutions

PBS 10X
1.37 M NaCl
27 mM KCl
100 mM Na2HPO4
17.5 mM KH2PO4
pH 7.4

Protein Loading buffer 5X
250 mM Tris pH 6.8
50% glycerol
250 mM DTT
10% SDS
0.1% bromophenol blue

RIPA buffer
50 mM Tris-HCl (pH 7.5)
150 mM NaCl
5 mM EGTA
5 mM EDTA
1% NP-40
20 mM NaF
1 mM Na_3VO_4
1 mM PMSF
2.5 mM Benzamidine
10 μg/ml Pepstatin A
1 μM Mycrocystin
10 μg/ml Leupeptin
10 μg/ml Aprotinin

TBST 1X
20 mM Trizma base
150 mM NaCl
0.1% Tween 20

Running Buffer 10X
0.25 M Tris base
2 M glycine
1% SDS
pH 8.3

Transfer Buffer 10X
0.2 M Tris base
1.5 M glycine

Transfer Buffer 1X
10% Transfer Buffer 10X
20% 2-propanol
70% H2O

Ponceau Red
0.1% Ponceau Red powder
5% acetic acid
HBS buffer (2X)
50 mM HEPES
280 mM NaCl
1.5 mM Na2HPO4
pH 7.12

HBS buffer (2X)
50mM HEPES
280 mM NaCl
1.5mM Na2HPO4
pH 7.12

Commercial reagents

Reagent	Company	Reference
4-OH-Tamoxifen	Sigma	H6278
Acetic acid	Panreac	131008.1611
Acrylamide 40% 29:1	BioRad	161-0146
Ammonium bicarbonate	Sigma	9830
Aprotinin	Sigma	A6279
APS	Sigma	A3678
Benzamidine	Sigma	B6506
Bromophenol blue	Sigma	B8026
BSA	Sigma	A7906
Cresyl Violet	Sigma	10510-54-0
DAPI	LifeTechnologies	P36935
dNTPs	ThermoFisher	R0192
DMEM	Sigma	5796
DMSO	Sigma	D5796
DTT	GE Healthcare	17-1318-02
EDTA	Sigma	E4378
EGTA	Sigma	E46758
Ethanol absolute	Panreac	131086.1214
Fluorescence mounting	Dako	s3023
Fibronectin	Sigma	F2006
Glutamine	LabClinics	M11-004
Glycerol	Sigma	49782
HBSS	Gibco	14175-137
HEPES	Gibco	15630-049
Leupeptin	Sigma	L2884

Methanol	Panreac	131091.1214
MK-2 Inhibitor III	Calbiochem	CAS118664822
Nitrocellulose membrane	GE Healthcare	10600002
Non-treated multidishes	Nunc	150239
NP-40	AppliChem	A16960250
Paraformaldehyde 16%	Electron	15710
Penicillin/Streptomicin	LabClinics	P11-010
Pepstatin A	Sigma	P4265
PF-3644022	Sigma	PZ0188
PH-797804	Selleckchem	S2726
PMSF	Sigma	P7626
Polybrene	Sigma	H9268
Poly-D-lysine	Sigma	P7280
Polyethylenimine	Polysciences	23966-1
Ponceau S	Sigma	P3504
Protease inhibitor	Calbiochem	539134
Proteinase K	Roche	3115852001
Puromycin	Sigma	P9620
Random Primers	Invitrogen	48190-011
Rnase A	Roche	10109142001
RNAsin 2500U	Promega	N211
SDS	Sigma	71725
Sequencing grade	Promega	V5113
Sodium chloride	Sigma	433209
Sodium deoxycholate	Sigma	6504
Sodium Floride	Sigma	S7920
Sodium orthovanadate	Sigma	S6508
Sodium phosphate	Sigma	255793

Superfrost glass slides	VWR	J1800AMNZ
Superfrost Plus Adhesion	ThermoFisher	J7800AMNT
TC10 Automated cell	BioRad	S06BR2077
TEMED	Sigma	T9281
Triton X-100	Sigma	T9284
TRIZMA-base	Sigma	T6066
Trizol	ThermoFisher	15596026
Trypan Blue Solution	Gibco	Gibco
Trypsin-EDTA	Sigma	T3924
Tween-20	Sigma	P7949

Commercial Kits

Reagent	Company	Reference
FastDigest Esp3I	ThermoFisher	FD0454
GenElute™ Miniprep Kit	Sigma,	PNL350
MycoAlert	Lonza	LT07-318
PureLink on column DNAse	Invitrogen	121-85-010
QIAfilter plasmid maxi kit	Quiagen	12263
Quick Ligation™ Kit	NEB	M2200
QIAquick gel extraction Kit	Quiagen	28706X4
Random primers	Invitrogen	48190-011
RC DC protein assay kit II	BioRad	5000122
RNA PureLink Minikit	Ambion	12183018A
Superscript IV reverse	Invitrogen	18090010
SYBR Select master mix	ThermoFisher	4472942
T4 Ligation buffer	NEB	B0202S
T4 PNK	NEB	M0201

2. Methods

2.1. Cellular biology

Cell maintenance

BBL358, BBL350, BT-474, HELA, HEK293T, MCF-7, MDA-MB-231, T47D, SAOS2, SW620, U2OS, U-87MG cells were cultured in DMEM (high glucose) medium supplemented with 10% FBS, 1% penicillin/streptomycin and 1% L-glutamine. BT-549 cells were cultured in RPMI supplemented with 10% FBS, 1% penicillin/streptomycin and 1% L-glutamine. Cells were maintained at 37°C and 5% CO2.

For sub-culturing and passage, cells were washed with PBS and incubated with trypsin at 37°C until detached. Then, cells were suspended using complete media and diluted as desired depending on the confluence and re-plated in a new culture dish.

Cell collection

For harvesting, cell cultures were washed with PBS and trypsinized. Cells were suspended in complete fresh media and the suspension was transferred to a 15 ml conical tube and centrifuged at 1000 rpm for 5 min. Afterwards, media was aspirated, and the pellet was resuspended according to the following procedures.

Cell cryopreservation and thawing

For cryopreservation, cells were collected as described above and resuspended in freezing media consisting of 90% FBS and 10% DMSO and transferred to 1.5 ml cryo-tubes. Cryo-tubes were stored

in a Mr. Frosty container at -80°C for up to one week and then transferred to liquid nitrogen for long term storage.

For thawing, frozen cells were quickly placed in a 37°C water bath until completely thawed. Then, cells were diluted in pre-warmed media and transferred to a new plate. Next day, the media was replaced by fresh media to remove remaining DMSO in culture.

Mycoplasma detection

Cells were routinely tested for mycoplasma using Mycoplasma Detection Kit. 100 µl of cell media were taken, centrifuged, and transferred to a test tube. 100 µl of MycoAlert reagent (A) were added and lumines¬cence was measured after 5 min incubation. Then, 100 µl MycoAlert Substrate (B) was added, and luminescence was measured after 10 min. The ratio of B/A was used to determine the mycoplasma status according to the manufacturer´s protocol.

Cell treatments

p38α inhibitors and MK2 inhibitor were prepared in 100% DMSO and stored in aliquots at -20ºC. Inhibitors were used at the indicated concentrations and for the indicated times depending on each experiment.

Transfection of HEK293-T using calcium chloride

HEK293-T cells were plated in order to reach 60-70% confluence at the moment of transfection. DNA was dissolved in 450 µl of water to which 50 µl of CaCl2 was added. 500 µl of 2xHBS was added dropwise while bubbling the DNA mix and then incubated for 20 min at RT. The mix was added to the cells cultured in DMEM 10% FBS

and antibiotics and incubated O/N. The following day, medium was replaced.

Lentiviral infection

Viruses were produced in HEK293-T cells through calcium chloride transfection of packaging vector plasmids together with the desired or lentiviral vectors. 4.5 μg of δ89 plasmid (containing Gag, Pol, Rev, and Tat genes) and 0.5 μg of VSV-G plasmid (containing Env gene) were transfected together with vectors. The following day cell medium was refreshed. After 48 h, the supernatant containing the viruses was passed through a 0.45 μm PVDF filter and used for cell infection at a 1:1 ratio with fresh medium plus 8 mg/ml polybrene.

Generation of BBL358-Cas9 cells

BBL358 cells were transduced with lentivirus containing Cas9-Blast construct (Addgene, #52962). Lentivirus was generated in 293T cells using calcium chloride transfection and two rounds of infection (48h and 72h of virus generation) were performed in the presence of 8ug/ml Polybrene. Blasticidin selection (5ug/ml) was started 72h after the first infection. pXPR-011 reporter construct (Addgene, #59702) was used as described previously (Doench et al., 2014) to ensure that Cas9 is active in more than 70% of the cells.

Generation of BBL358-Cas9-sgSorbs2 cells

293T cells were transfected with the sgSorbs2 plasmid using calcium chloride method. Lentiviral infection of the target BBL358-Cas9 cells was performed in two rounds (48h and 72h of virus production), in the presence of 8 μg/mL polybrene. Transduced BBL358-Cas9-

Sorbs2 cells were harvested 72h post-infection and either single GFP positive cells (Clone1 and 2) or 250 GFP positive cells (Pool) were sorted per well into a 96 well plate (BD FACSAria Fusion Cell Sorter). Clones and bulk cell population were expanded and decrease of ArgBP2 was confirmed by western blotting.

Cell-ECM attachment assay

24-well plates either empty or coated with 500 µl fibronectin (DMEM, 15 mM HEPES, 0.1 mg/ml BSA, 10 µg/ml fibronectin), or collagen I (DMEM, 15 mM HEPES, 0.1 mg/ml BSA, 10 µg/ml Collagen I) overnight at 4°C. Plates were dried before use.

Cells were counted and diluted to 30,000 cells/ml and 1 ml cell suspensions were plated into each well of pre-coated plates. After 0.5h and 1h incubation, nonadherent cells were removed by washing three times with PBS. Adherent cells were fixed for 20 min with 4% paraformaldehyde in PBS and stained with crystal violet for 20min. After a wash step, plates were dried and images were took using TE200 NIKON (Olympus DP72).

Cell-Fibroblast derived ECM attachment assay

ECM production and harvesting protocols were adapted from Franco-Barraza et al., (2016). Briefly, fibroblasts derived from PyMT-induced tumors were seeded at confluence, and cultured for ten days while refresh the media every two days. After ten days of culture, cells were washed once with PBS, and then incubated at room temperature for 2 minutes in PBS with 50 mM ammonium hydroxide (NH_4OH) with 0.05% Triton X100. Cells were constantly observed with a light microscope at 10X to confirm proper removal

of all fibroblast debris. After decellularization, the matrices were washed 3 times with PBS and either stored at 4°C for up to one week, or used immediately.

For attachment assay, p38WT cells and p38KO cells were labeled with Cell Tracker Green and Cell Tracker Green Red, respectively, on the previous day according to manufacturer's protocol. After counting, cells were diluted to 5x104 and mixed together. The mixture were added to each well for 2 h. Thereafter, wells were washed with PBS for three times, and adhered cells were fixed in 4% paraformaldehyde in PBS. Different fields (10X magnification) of each well were photographed using LEICA DMi8 (Orca Flash LT). Green and red cells were counted using Fiji.

Cell detachment assay

Cell detachment assays were adapted from Löffek et al., 2014.Cells were plated at confluence in 6-well plates. After 24 hours, cells were washed with PBS and incubated with trypsin/EDTA (0.05/0.02%) for 8min. Then the wells were completely filled with full medium. Non-adherent cells were removed by washing with PBS. Adherent cells were fixed with 4% paraformaldehyde and stained with crystal violet. After a wash step, plates were dried and scanned. The cells areas were measured using Fiji. The adhesion of the cells was expressed as a percentage relative to untreated controls (0 minutes trypsin/EDTA).

3D spheroids formation assay

Spheroid formation assay was adapted from Ramsey Foty (2011). Cells were counted and diluted to 10^6 cells/ml. Lids of 10 cm culture plates were seeded with 20 µl cell suspension (20,000 cells).

To prevent dehydration of the drops, 10 ml PBS were added to the bottom of the plate. Cells were incubated at 37 °C and 5% CO2 for 24h and 48h to allow aggregation. At the indicated time, spheroids were visualized using LEICA DMi8 (Orca Flash LT). Spheroids area were measured using Fiji.

2.2. Molecular biology

Protein extraction

Cell plates were placed on ice and cells were washed twice with ice cold 1X PBS. Then, cells were lysed in RIPA buffer and collected using a scrapper. Lysates were transferred to pre-cooled microcentrifuge tubes and maintain constant agitation for 30 min on ice. Then centrifuged at 15000 rpm at 4°C for 15 min. Supernatants were collected and processed by western blot or frozen at -80°C.

Protein quantification

Protein concentration was estimated using the RC DC protein assay kit according to the manufacturer's instructions. Protein concentration was measured at 750 nm using a spectrophotometer (BioTek, #FLx800), and concentrations were calculated using a BSA standard curve as a reference.

Western Blottling

Total protein (20-40µg) was prepared using 5X loading buffer, with a final concentration of 1X, and boiled for 5 min at 95°C. Then, samples were loaded into the wells of SDS-PAGE gels along with a molecular weight marker. Gel composition is shown in **Table3**.

Table 3. Composition of SDS-polyacrylamide gels

Reagents	8% SDS-PAGE	10% SDS-PAGE	12% SDS-PADE	Stacking Gel
Distilled Water (µl)	4352	3952	3552	2476
40% (w/v) Acrylamide 29:1 (µl)	1600	2000	2400	500
1,5M Tris/HCl, pH8.8 & 0.4% SDS (µl)	2000	2000	2000	--
0.5 M Tris pH6.8 & 0.4% SDS (µl)	--	--	--	1000
APS 10% (µl)	40	40	40	20
TEMED (µl)	8	8	8	4

Proteins were resolved on 8-12% gradient SDS-PAGE gels depending on the protein molecular weight for under constant voltage using a wet-blotting transfer system. After electrophoresis, proteins were transferred from the polyacrylamide gel to a 0.22 um nitrocellulose membrane using a wet transfer system for 3h at 200 mA. Ponceau Red was used to check transfer quality and efficiency. After washing out Ponceau Red with TBST, the membrane was blocked with 5% non-fat milk in TBST at RT for 1h. The membrane was washed with TBST three times. Primary antibody (1:1000) was diluted in 5% BSA in TBST. Membrane was incubated with primary antibody at 4°C, rocking overnight. Then, membrane was washed three times in TBST and incubated with the secondary antibody (1: 5000) diluted in 5% non-fat milk in TBST for 1h at RT in the dark. Finally, membranes were extensively washed with TBST, and protein was detected using Odyssey Infrared Imaging System. Antibodies are indicated in the **Table 4**.

Table 4 Primary and secondary antibodies

Antibody	Company	Reference	Dilution
HSP27	Santa Cruz	sc-1049	1:1000
HSP27 phospho-S82	Cell Signaling	2401	1:1000
MK2 phospho-T334	Cell Signaling	3007	1:500
p38α	Cell Signaling	9218	1:1000
p38α	Santa Cruz	sc81621	1:1000
p38 phospho-T180/Y182	Cell Signaling	9211	1:1000
p38 phospho-T180/Y182	BD Biosciences	612288	1:1000
ArgBP2	Santa Cruz	sc-514671	1:1000
ZO-1	life technologies	40-2200	1:100
α-Tubulin	Sigma	T9026	1:10000
Alexa-Fluor anti-mouse 680	ThermoFisher	A21057	1:5000
Alexa-Fluor anti- rabbit 680	ThermoFisher	A21076	1:5000
Alexa-Fluor anti- rabbit 488	ThermoFisher	A11017	1:500

RNA isolation

Cells were washed twice with PBS, resuspended in 500 µl Trizol and placed in a 1.5 ml Eppendorf tube. 100 ml **Chloroform** were added, and tubes were centrifuged 15000g at RT for 10 min. Two liquid phases were generated and 200 µl of the fraction with less density was transferred into new tubes. 200 µl of 70% ethanol were added and mixed with samples. The RNA extraction was followed by using PureLink RNA mini kit. DNAse treatment was performed using on-column DNase treatment following manufacturer's instructions.

Reverse transcription

RNA samples were quantified using Nano Drop. 1 µg RNA was used for cDNA synthesis with SuperScript IV reverse transcriptase, RNAsin and random primers following Invitrogen's instructions. The synthesized cDNA was diluted with nuclease-free water to 2.5 ng/ul.

Quantitative real-time PCR

10 ng of cDNA, 5 ml SYBR green reagent and 0.25 µl of gene-specific forward and reverse primers were mixed with ddH20 up to a 10 µl final volume. The mix was processed using QuantStudio™ 6 Flex Real-Time PCR System with the following program: an initial step of 50°C for 2 min and 95°C for 10 min; 40 cycles of 95°C for 30 sec, 60°C for 40 sec and 72°C for 60 sec; and a final step of 95°C for 15 sec, 60°C for 2 min and 95°C for 15 sec. mRNA levels were analyzed in triplicates and normalized to the house keeping gene expression level. Primers are shown in **Table 5**.

For Sorbs2 pre-mRNA quantification, no template control (omitting any DNA or RNA template from a reaction) and no reverse transcriptase control (carrying out the reverse transcription step in the absence of reverse transcriptase) were used.

sgSorbs2 plasmid cloning

DNA corresponding to sgRNAs targeting Sorbs2 was cloned into Lenti_sgRNA_EFS_GFP (LRG, Addgene #65656) following the protocol from the Zhang Lab (MIT, USA). First sgRNA oligos were phosphorylated and annealed in a 10µl reaction containing 1µl of forward and reverse sgRNA oligos (100 µM stock, **Table 3**), 1µl of 10x T4 Ligation buffer and 1µl of T4 PNK using the following thermocycler program:

37ºC 30 min

95ºC 5 min

ramp down to 25ºC at 5ºC/min

For plasmid digestion, 5µg of LRG sgRNA expression plasmid was digested with FastDigest Esp3I and gel purified using QIAquick Gel Extraction Kit. The ligation mixture containing 50ng of digested LRG, 1ul of diluted (1:200) oligo duplex, 5ul of 2x Quick Ligase buffer and 1ul of Quick ligase in a final volume of 10ul was incubated for 10 min at room temperature and then used for transforming the DH5α competent cells. Ampicillin resistant clones were selected, expanded and DNA extracted with a Miniprep.

Table 5 Primers and small guide RNAs

Gene	Sequence from 5´ To 3´
Arhgap10_Fwd	ATGATTCCATTTGAGCACAG
Arhgap10_Rev	CTTCCTCTCTTCTTCTGAAAAC
Cyb5a_Fwd	GCCAAGCCTTCGGATACTCT
Cyb5a_Rev	GTTCTTCGGCTTCGGAGAGA
Ddx52_Fwd	CATTGGAGCAAGGAATTCTG
Ddx52_Rev	CAGAAGTTTTCCAGTCTCAG
Hspbp1_Fwd	CAAGGTCAAGTCAGCATTC
Hspbp1_Rev	GGGAAATCTGTCACAAGG
Krt14_Fwd	GAATGGTTCTTCAGCAAGAC
Krt14_Rev	TATTCTCCAGGGATGCTTTC
Nf1_Fwd	CTGTCATTTTCCTACTGGTTC
Nf1_Rev	CAGGCAGATCTTAAAGTGTTG
Sorbs2_Fwd	ACACCCTAAGCTCCAATAAG
Sorbs2_Rev	TTCTTGAAGTTCCCACAAAC
Sorbs2_2_Fwd	ATGTGGAACTCTCCCTGCG
Sorbs2_2_Rev	CTTGTCTGTTGGTTCCTGGG
Pre_Sorbs2_1_Fwd	TTTTCCCAATGCTCATTCCA
Pre_Sorbs2_1_Rev	CTTGTCTGTTGGTTCCTGGG
Pre_Sorbs2_2_Fwd	AGCAGCATTCTGTCCTATGTGTC
Pre_Sorbs2_2_Rev	CATTTTCACCTTGAAGGGTTTG
Vim_Fwd	GAACCTGAGAGAAACTAACC

Vim_Rev	GATGCTGAGAAGTCTCATTG
Zfp36l1_Fwd	ATGCAAGGGTAACAAGATGCTC
Zfp36l1_Rev	TGATGGAACTTGGAGCTGGG
Zfp36l2_Fwd	CAGGACCCAGAAAAATGTC
Zfp36l2_Rev	GATTTCTCCGTCTTGCAC
SORBS2_Fwd	CGATTCCACAGACACATATC
SORBS2_Rev	CTGTCGTTCTAATTGCTGTG
Gapdh_Fwd	CTTCACCACCATGGAGGAGGC
Gapdh_Rev	GGCATGGACTGTGGTCATGAG
GAPDH_Fwd	CTTTTGCGTCGCCAG
GAPDH_Rev	TTGATGGCAACAATATCCAC
sgRNA_Sorbs2_Fwd	CACCGAGACAAAAGATCACCGACCC
sgRNA_Sorbs2_Rev	AAACGGGTCGGTGATCTTTTGTCTC
sgRNA_Sorbs2_Fwd	CACCGGACACCAGGAAATTTCGAT
sgRNA_Sorbs2_Rev	AAACATCGAAATTTCCTGGTGTCC

Immunostaining and confocal imaging for spheroids

Samples were fixed with 4% paraformaldehyde for 45 min and quenched with 20 mM glycine for 20 min. Permeabilization was achieved with 0.5% Triton X-100 for 30 min at room temperature. Then a second blocking step with 1% BSA for 1 h at room temperature was performed. Samples were incubated with primary antibodies (1:100) overnight at 4°C in a dark chamber followed by incubation with the correspondent secondary antibody (1:500) for 1 h at room temperature in the dark (**Table 4**). Samples were incubated with DAPI for 15 min. Washes were performed between each step with PBS. Mounting media was applied on the slides and samples were visualized using Zeiss LSM 780 confocal microscope. The confocal images mean intensity was quantified using Fiji.

SILAC sample preparation and analysis

Samples were prepared by Begoña Cánovas. Cells were cultured in SILAC medium DMEM F-12 (Invitrogen, USA) supplemented with heavy, light or medium lysine and arginine. Following incorporation of labeled amino acids, cells were treated ETOH, 4-OHT (100 nM) and PH797804 (2µM), respectively. After 48h, Cells were washed and split normally. Heavy and light labeled cells were collected after culturing for 48h. Medium labeled cells were treated again 2µM PH797804 for 48h before collecting. Samples were lysed, digested and enriched for phosphopeptides at IRB Barcelona's Mass Spectrometry (MS) & Proteomics Facility.

Analysis was performed by IRB Barcelona's MS & Proteomics Facility. Peptides were analyzed using an Orbitrap Fusion Lumos™ Tribrid mass spectrometer (Thermo Scientific) equipped with a Thermo Scientific Dionex Ultimate 3000 ultrahigh pressure chromatographic system (Thermo Scientific) and an Advion TriVersa NanoMate (Advion Inc. Biosciences) as the nanospray interface.

MS/MS spectra were searched against the SwissProt (Mus musculus, release 2018_11) and contaminants database using MaxQuant v1.6.2.6 with andromeda search engine (Cox and Mann, 2008). Searches were run against targeted and decoy databases. Search parameters included trypsin enzyme specificity, allowing for two missed cleavage sites, carbamidomethyl in cysteine as static modification and oxidation in methionine, acetyl in protein N-terminal and phosphorylation in serine, threonine and tyrosine as

dynamic modifications. Peptide mass tolerance was 20 ppm and the MS/MS tolerance was 0.6 Da. The minimal peptide length was 7 amino acids, the minimum score for modified peptides was 40 and the minimum delta score was 8. Peptide, protein and site identifications were filtered at a false discovery rate (FDR) of 1 % based on the number of hits against the reversed sequence database.

Protein intensities were used for the statistical analysis. Within each SILAC experiment, protein quantitation was normalized by summing the abundance values for each channel over all proteins identified within an experiment. All abundance values were corrected in all channels by a constant factor (x 1E9) per channel, so that at the end the total abundance is the same for all channels.

2.3. Computational analysis of (phospho-)proteomic data

SILAC data processing

SILAC data were processed by IRB Barcelona's MS & Proteomics Facility. All abundance values was first transformed to log scale to apply a linear model. We filtered the data to retain only proteins with valid quantification values in at least 4 of the samples for the total protein dataset and in at least 3 of the samples for the p-sites dataset. Missing values were imputed with normally distributed random numbers (centered at -1.8 standard deviations units and spread 0.3 standard deviations units with respect non missing values). To adjust for batch effect a linear model was used with SILAC batch as fixed effect. Model fitting was accomplished with the lmFit function of the limma package (Ritchie et al., 2015) of R statistical software (R Core Team. (2014). R: A Language and Environment for Statistical

Computing. Available online at: http://www.Rproject.org). Comparison between groups was done (LH, MH, ML) to find out which species significantly changed. For each comparison, estimated fold changes and p values were calculated. Finally, p-values were adjusted using the Benjamini & Hochberg correction. Proteins with an adjusted p-value lower than 0.05 and fold change higher than 1.5 were considered statistically significant between groups. Clustering analysis was performed using the Perseus software vs 1.6.3 (Tyanova et al., 2016). Batch effect was remove form SILAC intensities. The resulting adjusted intensities were filtered with those proteins significant in at least one comparison, according to the fold change and p value, and z-score normalized.

Protein function analysis by Gene set enrichment analysis (GSEA)

GSEA software (v4.1.0) was used for pathway enrichment analysis (Subramanian et al., 2005). GSEA evaluates and determines whether a priori defined sets of genes show statistically significant, cumulative gene expression changes that correlate with a specific phenotype. Samples were ranked according to the log2FC were subjected to GSEA. Molecular Signatures Database (MSigDB) of Ontology gene sets (c5) was used for enrichment analysis. An FDR value of 0.05 or 0.25 was used as a cutoff. Enrichment score (ES) was calculated by first ranking the proteins from the most to least significant concerning the two phenotypes; the entire ranked list was then used to assess how the proteins of each gene set were distributed across the ranked list. Normalized enrichment score (NES) is based on the ES for all dataset permutations. A positive NES indicates gene

set enrichment at the top of the ranked list; a negative NES indicates gene set enrichment at the bottom of the ranked list. Overlapped GO terms in KO/WT and PH/WT were shown as bubble plots using the Python package.

Phosphoprotein function analysis by DAVID database

DAVID database (v6.8) was applied to analyze Oncology enrichment for phosphoproteins. Phosphoproteins of phosphosites with a p-value less than 0.05 and the fold change greater than 1.5 were selected to perform GO analysis. An FDR value of 0.05 was used as a cutoff. Overlapped GO terms in KO/WT and PH/WT were shown as bubble plots using the Python package.

Function score and kinase-substrates mapping

For function score analysis and kinase mapping, the mouse phosphosites were firstly aligned to their conserved human phosphosites. Then the analysis were implemented with the human phosphosites. SITE_GRP_ID from PhosphositePlus (update: 2021/04/19) was used to align the human phosphosite. The functional score obtained from Ochoa et al (2020) were assigned to the human phosphosites. Kinase_Substrates_Dataset from PhosphositePlus were used to map the upstream kinases for our phosphosites or p38 and MK2 substrates. The overlaping and kinases/substrates mapping were analyzed and visualized using Python package. p38 and MK2 substrates were visualized in Cytoscape (v3.8.2) and phosphosites fold changes were shown using Omics Visualizer plugin (Legeay et al., 2020).

Kinase-Substrate Enrichment Analysis (KSEA)

The KSEA app (v1) was used to analyze the kinase activity. KSEA estimates changes in a kinase's activity by measuring and averaging the amounts of its identified substrates instead of a single substrate, which enhances the signal-to-noise ratio from inherently noisy phosphoproteomics data (Casado et al., 2013; Wiredja et al., 2017). If multiple kinases shared the same phosphorylation motif, it was used to estimate all known kinases' activities. Using all curated substrate sequences of a particular kinase minimizes the overlapping effects from other kinases and thus improves the precise measurement of kinase activities. The information of kinase-substrate relationships was obtained from PhosphoSite (Hornbeck et al., 2015), Phospho.ELM (Dinkel et al., 2011), and PhosphoPOINT (Yang et al., 2008). The information of substrate motifs was obtained either from the literature (Schwartz and Gygi, 2005) or from an analysis of the KSEA dataset with Motif-X (Casado et al., 2013). All conserved human phosphosites with log2 fold changes in our data were used to perform this analysis.

Protein-protein interaction (PPI) network:

PPI networks were built in Cytoscape. PPI enrichment statistical analysis was done using the STRING database plugin with experimental and database sources set to the high confidence threshold (0.7). The interaction predictions were based on physical, genetic, and text mining evidence types. Phosphosites fold change was visualized using the Omics Visualizer plugin (Legeay et al., 2020). Function clusters were manually curated based on literature.

Code availability

No custom code was used. All software and code are available through the cited references.

Statistical analysis

Data are expressed as mean ± SEM if not mentioned within respective figures. Statistical analysis was performed by using a two-tailed Student's t-test for the comparison of two groups or ANOVA using Bonferroni posthoc correction for multiple groups using GraphPad Prism Software 8.02 (GraphPad Software, Inc., La Jolla CA).

BIBLIOGRAPHY

Adams, R.H., Porras, A., Alonso, G., Jones, M., Vintersten, K., Panelli, S., Valladares, A., Perez, L., Klein, R., and Nebreda, A.R. (2000). Essential role of p38α MAP kinase in placental but not embryonic cardiovascular development. Mol Cell *6*, 109–116.

Al-Ayoubi, A.M., Zheng, H., Liu, Y., Bai, T., and Eblen, S.T. (2012). Mitogen-activated protein kinase phosphorylation of splicing factor 45 (SPF45) regulates SPF45 alternative splicing site utilization, proliferation, and cell adhesion. Mol Cell Biol *32*, 2880–2893.

Alonso, G., Ambrosino, C., Jones, M., and Nebreda, A.R. (2000). Differential activation of p38 mitogen-activated protein kinase isoforms depending on signal strength. J Biol Chem *275*, 40641–40648.

Andersen, J.N., Mortensen, O.H., Peters, G.H., Drake, P.G., Iversen, L.F., Olsen, O.H., Jansen, P.G., Andersen, H.S., Tonks, N.K., and Møller, N.P.H. (2001). Structural and Evolutionary Relationships among Protein Tyrosine Phosphatase Domains. Mol Cell Biol *21*, 7117–7136.

Angers-Loustau, A., Côté, J.F., Charest, A., Dowbenko, D., Spencer, S., Lasky, L.A., and Tremblay, M.L. (1999). Protein tyrosine phosphatase-PEST regulates focal adhesion disassembly, migration, and cytokinesis in fibroblasts. J Cell Biol *144*, 1019–1031.

Ardito, F., Giuliani, M., Perrone, D., Troiano, G., and Muzio, L. lo (2017). The crucial role of protein phosphorylation in cell signalingand its use as targeted therapy (Review). Int J Mol Med *40*, 271–280.

Arthur, J.S.C. (2008). MSK activation and physiological roles. Front Biosci *13*, 5866–5879.

Bain, J., Plater, L., Elliott, M., Shpiro, N., Hastie, C.J., Mclauchlan, H., Klevernic, I., Arthur, J.S.C., Alessi, D.R., and Cohen, P. (2007). The selectivity of protein kinase inhibitors: a further update. Biochem J *408*, 297–315.

Barford, D., Das, A., and Marie-Pierre, E. (1998). The structure and mechanism of protein phosphatases: insights into catalysis and regulation. Annu Rev Biophys Biomol Struct *27*, 133–164.

Barrantes, I.D.B., Coya, J.M., Maina, F., Arthurd, J.S.C., and Nebreda, A.R. (2011). Genetic analysis of specific and redundant roles for p38α and p38β MAPKs during mouse development. PNAS *108*, 12764–12769.

Barsyte-Lovejoy, D., Galanis, A., and Sharrocks, A.D. (2002). Specificity determinants in MAPK signaling to transcription factors. J Biol Chem *277*, 9896–9903.

Beardmore, V.A., Hinton, H.J., Eftychi, C., Apostolaki, M., Armaka, M., Darragh, J., McIlrath, J., Carr, J.M., Armit, L.J., Clacher, C., et al. (2005). Generation and characterization of p38β (MAPK11) gene-targeted mice. Mol Cell Biol *25*, 10454–10464.

Bell, C.E., and Watson, A.J. (2013). p38 MAPK regulates cavitation and tight junction function in the mouse blastocyst. PLoS ONE *8*, e59528.

Bhattacharyya, R.P., Reményi, A., Yeh, B.J., and Lim, W.A. (2006). Domains, motifs, and scaffolds: the role of modular interactions in the evolution and wiring of cell signaling circuits. Annu Rev Biochem *75*, 655–680.

Bikkavilli, R.K., Feigin, M.E., and Malbon, C.C. (2008). p38 mitogen-activated protein kinase regulates canonical Wnt-beta-catenin signaling by inactivation of GSK3beta. J Cell Sci *121*, 3598–3607.

Biondi, R.M., and Nebreda, A.R. (2003). Signalling specificity of Ser/Thr protein kinases through docking-site-mediated interactions. Biochem. J *372*, 1–13.

Bora, P., Gahurova, L., Mašek, T., Hauserova, A., Potěšil, D., Jansova, D., Susor, A., Zdráhal, Z., Ajduk, A., Pospíšek, M., et al. (2021). p38-MAPK-mediated translation regulation during early blastocyst development is required for primitive endoderm differentiation in mice. Commun Biol *4*, 1–19.

Borisova, M.E., Voigt, A., Tollenaere, M.A.X., Sahu, S.K., Juretschke, T., Kreim, N., Mailand, N., Choudhary, C., Bekker-Jensen, S., Akutsu, M., et al. (2018). P38-MK2 signaling axis regulates RNA metabolism after UV-light-induced DNA damage. Nat Commun *9*, 1017.

Briata, P., Forcales, S.V., Ponassi, M., Corte, G., Chen, C.Y., Karin, M., Puri, P.L., and Gherzi, R. (2005). p38-dependent phosphorylation of the mRNA decay-promoting factor KSRP controls the stability of select myogenic transcripts. Mol Cell *20*, 891–903.

Burnett, G., and Kennedy, E.P. (1954). The enzymatic phosphorylation of proteins. J Biol Chem *211*, 969–980.

Caldwell, K.K., Sosa, M., and Buckley, C.T. (2006). Identification of mitogen-activated protein kinase docking sites in enzymes that metabolize phosphatidylinositols and inositol phosphates. Cell Commun Signal *4*, 1–18.

Campbell, R.M., Anderson, B.D., Brooks, N.A., Brooks, H.B., Chan, E.M., de Dios, A., Gilmour, R., Graff, J.R., Jambrina, E., Mader, M., et al. (2014). Characterization of LY2228820 dimesylate, a potent and selective inhibitor of p38 MAPK with antitumor activity. Mol Cancer Ther *13*, 364–374.

Cánovas, B., Igea, A., Sartori, A.A., Gomis, R.R., Paull, T.T., Isoda, M., Pérez-Montoyo, H., Serra, V., González-Suárez, E., Stracker, T.H., et al. (2018). Targeting p38α Increases DNA damage, chromosome instability, and the anti-tumoral response to taxanes in breast cancer cells. Cancer Cell *33*, 1094–1110.

Canovas, B., and Nebreda, A.R. (2021). Diversity and versatility of p38 kinase signalling in health and disease. Nat Rev Mol Cell Biol *22*, 346–366.

Carlucci, A., Gedressi, C., Lignitto, L., Nezi, L., Villa-Moruzzi, E., Avvedimento, E. v., Gottesman, M., Garbi, C., and Feliciello, A. (2008). Protein-tyrosine phosphatase PTPD1 regulates focal adhesion kinase autophosphorylation and cell migration. J Biol Chem *283*, 10919–10929.

Casado, P., Rodriguez-Prados, J.-C., Cosulich, S.C., Guichard, S., Vanhaesebroeck, B., Joel, S., and Cutillas, P.R. (2013). Kinase-substrate enrichment analysis provides insights into the heterogeneity of signaling pathway activation in leukemia cells. Sci Signal *6*, rs6.

Chen, M.J., Dixon, J.E., and Manning, G. (2017). Genomics and evolution of protein phosphatases. Sci Signal *10*, eaag1796.

Cheung, W.D., and Hart, G.W. (2008). AMP-activated protein kinase and p38 MAPK activate O-GlcNAcylation of neuronal proteins during glucose deprivation. J Biol Chem *283*, 13009–13020.

Cobb, M.H,, Boulton, T.G., and Robbins DJ (1991). Extracellular signal-regulated kinases: ERKs in progress. Cell Regulation *2*, 965–978.

Coghlan, V.M., Perrino, B.A., Howard, M., Langeberg, L.K., Hicks, J.B., Gallatin, W.M., and Scott, J.D. (1995). Association of protein kinase A and protein phosphatase 2B with a common anchoring protein. Science *267*, 108–111.

Cohen, P. (2002). The origins of protein phosphorylation. Nat Cell Biol *4*, E127–E130.

Colaert, N., Helsens, K., Martens, L., Vandekerckhove, J., and Gevaert, K. (2009). Improved visualization of protein consensus sequences by iceLogo. Nat Methods *6*, 786–787.

Coulthard, L.R., White, D.E., Jones, D.L., McDermott, M.F., and Burchill, S.A. (2009). p38MAPK: stress responses from molecular mechanisms to therapeutics. Trends Mol Med *15*, 369–379.

Cox, J., and Mann, M. (2008). MaxQuant enables high peptide identification rates, individualized p.p.b.-range mass accuracies and proteome-wide protein quantification. Nat Biotechnol *26*, 1367–1372.

Cuadrado, A., and Nebreda, A.R. (2010). Mechanisms and functions of p38 MAPK signalling. Biochem J *429*, 403–417.

Cuenda, A., and Rousseau, S. (2007). p38 MAP-Kinases pathway regulation, function and role in human diseases. Biochim Biophys Acta *1773*, 1358–1375.

Cully, M., Genevet, A., Warne, P., Treins, C., Liu, T., Bastien, J., Baum, B., Tapon, N., Leevers, S.J., and Downward, J. (2010). A role for p38 stress-activated protein kinase in regulation of cell growth via TORC1. Mol Cell Biol *30*, 481–495.

Deak, M., Clifton, A.D., Lucocq, J.M., and Alessi, D.R. (1998). Mitogen- and stress-activated protein kinase-1 (MSK1) is directly activated by MAPK and SAPK2/p38, and may mediate activation of CREB. EMBO J *17*, 4426–4441.

Dempster, J.M., Rossen, J., Kazachkova, M., Pan, J., Kugener, G., Root, D.E., and Tsherniak, A. (2019). Extracting Biological Insights from the Project Achilles Genome-Scale CRISPR Screens in Cancer Cell Lines. BioRxiv.

Dérijard, B., Hibi, M., Wu, I.-H., Barrett, T., Su, B., Deng, T., Karin, M., and Davis, R.J. (1994). JNK1: A protein kinase stimulated by UV light and Ha-Ras that binds and phosphorylates the c-Jun activation domain. Cell *76*, 1025–1037.

Dérijard, B., Raingeaud, J., Barrett, T., Wu, I.H., Han, J., Ulevitch, R.J., and Davis, R.J. (1995). Independent human MAP kinase signal

transduction pathways defined by MEK and MKK isoforms. Science *267*, 682–685.

Ding, L., Ellis, M.J., Li, S., Larson, D.E., Chen, K., Wallis, J.W., Harris, C.C., McLellan, M.D., Fulton, R.S., Fulton, L.L., et al. (2010). Genome remodelling in a basal-like breast cancer metastasis and xenograft. Nature *464*, 999–1005.

Dinkel, H., Chica, C., Via, A., Gould, C.M., Jensen, L.J., Gibson, T.J., and Diella, F. (2011). Phospho.ELM: a database of phosphorylation sites--update 2011. Nucleic Acids Res *39*, 261–267.

Dodge, K.L., Khouangsathiene, S., Kapiloff, M.S., Mouton, R., Hill, E. v, Houslay, M.D., Langeberg, L.K., and Scott, J.D. (2001). mAKAP assembles a protein kinase A/PDE4 phosphodiesterase cAMP signaling module. EMBO J *20*, 1921–1930.

Doench, J., Hartenian, E., Graham, D., Tothova, Z., Hegde, M., Smith, I., Sullender, M., Ebert, B., Xavier, R., and Root, D. (2014). Rational design of highly active sgRNAs for CRISPR-Cas9–mediated gene inactivation. Nat Biotechnol *32*, 1262–1267.

Donocoff, R., Teteloshvili, N., Chung, H., Shoulson, R., and Creusot, R. (2020). Optimization of tamoxifen-induced Cre activity and its effect on immune cell populations. Sci Rep *10*, 1–12.

Donoghue, C., Cubillos-Rojas, M., Gutierrez-Prat, N., Sanchez-Zarzalejo, C., Verdaguer, X., Riera, A., and Nebreda, A.R. (2020). Optimal linker length for small molecule PROTACs that selectively target p38α and p38β for degradation. Eur J Med Chem *201*, 112451.

van Drogen, F., Stucke, V.M., Jorritsma, G., and Peter, M. (2001). MAP kinase dynamics in response to pheromones in budding yeast. Nat Cell Biol *3*, 1051–1059.

El-Brolosy, M.A., and Stainier, D.Y.R. (2017). Genetic compensation: A phenomenon in search of mechanisms. PLoS Genetics *13*.

El-Brolosy, M.A., Kontarakis, Z., Rossi, A., Kuenne, C., Günther, S., Fukuda, N., Kikhi, K., Boezio, G.L.M., Takacs, C.M., Lai, S.L., et al. (2019). Genetic compensation triggered by mutant mRNA degradation. Nature *568*, 193–197.

Enslen, H., Raingeaud, J., and Davis, R.J. (1998). Selective activation of p38 mitogen-activated protein (MAP) kinase isoforms by the MAP kinase kinases MKK3 and MKK6. J Biol Chem *273*, 1741–1748.

Feldman, G., Kiely, B., Martin, N., Ryan, G., McMorrow, T., and Ryan, M.P. (2007). Role for TGF-β in cyclosporine-induced modulation of renal epithelial barrier function. Journal of the American Society of Nephrology *18*, 1662–1671.

Feng, G.S. (1999). Shp-2 Tyrosine phosphatase: signaling one cell or many. Exp Cell Res *253*, 47–54.

Fischer, E.H,, and Krebs, E.G. (1955). Conversion of phosphorylase b to phosphorylase a in muscle extracts. J Biol Chem *216*, 121–132.

Fonseca, B.D., Smith, E.M., Yelle, N., Alain, T., Bushell, M., and Pause, A. (2014). The ever-evolving role of mTOR in translation. Semin Cell Dev Biol *36*, 102–112.

Forcales, S.V., Albini, S., Giordani, L., Malecova, B., Cignolo, L., Chernov, A., Coutinho, P., Saccone, V., Consalvi, S., Williams, R., et al. (2012). Signal-dependent incorporation of MyoD-BAF60c into Brg1-based SWI/SNF chromatin-remodelling complex. EMBO J *31*, 301–316.

Foty, R. (2011). A simple hanging drop cell culture protocol for generation of 3D spheroids. Journal of Visualized Experiments.

Franco-Barraza, J., Beacham, D.A., Amatangelo, M.D., and Cukierman, E. (2016). Preparation of Extracellular Matrices Produced by Cultured and Primary Fibroblasts. Curr Protoc Cell Biol *71*, 10.9.1-10.9.34.

Fredriksson-Lidman, K., van Itallie, C.M., Tietgens, A.J., and Anderson, J.M. (2017). Sorbin and SH3 domain-containing protein 2 (SORBS2) is a component of the acto-myosin ring at the apical junctional complex in epithelial cells. PLoS ONE *12*.

Freshney, N.W., Rawlinson, L., Guesdon, F., Jones, E., Cowley, S., Hsuan, J., and Saklatvala, J. (1994). Interleukin-1 activates a novel protein kinase cascade that results in the phosphorylation of hsp27. Cell *78*, 1039–1049.

Garton, A.J., Burnham, M.R., Bouton, A.H., and Tonks, N.K. (1997). Association of PTP-PEST with the SH3 domain of p130 cas ; a novel mechanism of protein tyrosine phosphatase substrate recognition. Oncogene *15*, 877–885.

Ge, B., Gram, H., di Padova, F., Huang, B., New, L., Ulevitch, R.J., Luo, Y., and Han, J. (2002). MAPKK-independent activation of p38α mediated by TAB1-dependent autophosphorylation of p38α. Science *295*, 1291–1294.

Graves, J.D., and Krebs, E.G. (1999). Protein Phosphorylation and Signal Transduction. Pharmacol Ther *82*, 111–121.

Greenman, C., Stephens, P., Smith, R., Dalgliesh, G.L., Hunter, C., Bignell, G., Davies, H., Teague, J., Butler, A., Stevens, C., et al. (2007). Patterns of somatic mutation in human cancer genomes. Nature *446*, 153–158.

Guo, Y.L., and Yang, B. (2006). Altered cell adhesion and cell viability in a p38alpha mitogen-activated protein kinase-deficient mouse embryonic stem cell line. Stem Cells Dev *15*, 655–664.

Gupta, S., Campbell, D., Dérijard, B., and Davis, R.J. (1995). Transcription factor ATF2 regulation by the JNK signal transduction pathway. Science *267*, 389–393.

Gutierrez-Prat, N., Cubillos-Rojas, M., Cánovas, B., Kuzmanic, A., Gupta, J., Igea, A., Llonch, E., Gaestel, M., and Nebreda, A.R. (2021). MK2 degradation as a sensor of signal intensity that controls stress-induced cell fate. PNAS *118*, e2024562118.

Guy, C.T., Cardiff, R.D., and Muller, W.J. (1992). Induction of mammary tumors by expression of polyomavirus middle T oncogene: a transgenic mouse model for metastatic disease. Mol Cell Biol *12*, 954.

Han, J., Richter, B., Li, Z., Kravchenko, V. v., and Ulevitch, R.J. (1995). Molecular cloning of human p38 MAP kinase. Biochim Biophys Acta *1265*, 224–227.

Han, J., Wu, J., and Silke, J. (2020). An overview of mammalian p38 mitogen-activated protein kinases, central regulators of cell stress and receptor signaling. F1000Res *9*, 653.

Hayes, S.A., Huang, X., Kambhampati, S., Platanias, L.C., and Bergan, R.C. (2003). p38 MAP kinase modulates Smad-dependent changes in human prostate cell adhesion. Oncogene *22*, 4841–4850.

Hernández, G., Lal, H., Fidalgo, M., Guerrero, A., Zalvide, J., Force, T., and Pombo, C.M. (2011). A novel cardioprotective p38-MAPK/mTOR pathway. Exp Cell Res *317*, 2938–2949.

Ho, D.T., Bardwell, A.J., Abdollahi, M., and Bardwell, L. (2003). A docking site in MKK4 mediates high affinity binding to JNK MAPKs and competes with similar docking sites in JNK substrates. J Biol Chem *278*, 32662–32672.

Horn, H., Schoof, E.M., Kim, J., Robin, X., Miller, M.L., Diella, F., Palma, A., Cesareni, G., Jensen, L.J., and Linding, R. (2014). KinomeXplorer: an integrated platform for kinome biology studies. Nat Methods *11*, 603–604.

Hornbeck, P. v, Zhang, B., Murray, B., Kornhauser, J.M., Latham, V., and Skrzypek, E. (2015). PhosphoSitePlus, 2014: mutations, PTMs and recalibrations. Nucleic Acids Res *43*, D512–D520.

Huang, K.-Y., Lee, T.-Y., Kao, H.-J., Ma, C.-T., Lee, C.-C., Lin, T.-H., Chang, W.-C., and Huang, H.-D. (2019). dbPTM in 2019: exploring disease association and cross-talk of post-translational modifications. Nucleic Acids Res *47*, D298–D308.

Hubbard, S.R., and Till, J.H. (2000). Protein tyrosine kinase structure and function. Annu. Rev. Biochem. *69*, 373–398.

Hubbard, S.R. (1997). Crystal structure of the activated insulin receptortyrosine kinase in complex with peptide substrateand ATP analog. EMBO J *16*, 5572–5581.

Hunter, T. (2012). Why nature chose phosphate to modify proteins. Philos Trans R Soc Lond B Biol Sci *367*, 2513–2516.

Huttlin, E.L., Jedrychowski, M.P., Elias, J.E., Goswami, T., Rad, R., Beausoleil, S.A., Villén, J., Haas, W., Sowa, M.E., and Gygi, S.P. (2010). A tissue-specific atlas of mouse protein phosphorylation and expression. Cell *143*, 1174–1189.

Jacinto, E., Loewith, R., Schmidt, A., Lin, S., Rüegg, M.A., Hall, A., and Hall, M.N. (2004). Mammalian TOR complex 2 controls the actin cytoskeleton and is rapamycin insensitive. Nat Cell Biol *6*, 1122–1128.

Jacobs, D., Beitel, G.J., Clark, S.G., Robert Horvitz, H., Kornfeld, K., and Howard, † (1998). Gain-of-Function Mutations in the Caenorhabditis elegans lin-1 ETS Gene Identify a C-Terminal Regulatory Domain Phosphorylated by ERK MAP Kinase.

Jacobs, D., Glossip, D., Xing, H., Muslin, A.J., and Kornfeld, K. (1999). Multiple docking sites on substrate proteins form a modular system that mediates recognition by ERK MAP kinase. Genes Dev *13*, 163–175.

Janiszewska, M., Primi, M.C., and Izard, T. (2020). Beyond the migration of single cells. J Biol Chem *295*, 2495–2505.

Jirmanova, L., Torchia, M.L.G., Sarma, N.D., Mittelstadt, P.R., and Ashwell, J.D. (2011). Lack of the T cell-specific alternative p38 activation pathway reduces autoimmunity and inflammation. Blood *118*, 3280–3289.

Kalan, S., Amat, R., Schachter, M.M., Kwiatkowski, N., Abraham, B.J., Liang, Y., Zhang, T., Olson, C.M., Larochelle, S., Young, R.A., et al. (2017). Activation of the p53 Transcriptional Program Sensitizes Cancer Cells to Cdk7 Inhibitors. Cell Rep *21*, 467–481.

Kallunki, T., Su, B., Tsigelny, I., Sluss, H.K., D6rijard, B., Moore, G., Davis, R., and Karin, M. (1994). JNK2 contains a specificity-determining region responsible for efficient c-Jun binding and phosphorylation. Genes *8*, 2996–3007.

Kang, J., Gocke, C.B., and Yu, H. (2006). Phosphorylation-facilitated sumoylation of MEF2C negatively regulates its transcriptional activity. BMC Biochemistry *7*, 1–14.

Khoury, G.A., Baliban, R.C., and Floudas, C.A. (2011). Proteome-wide post-translational modification statistics: frequency analysis and curation of the swiss-prot database. Sci Rep *1*, 1–5.

Kim, H.D., Kim, T.S., and Kim, J. (2011). Aberrant ribosome biogenesis activates c-Myc and ASK1 pathways resulting in p53-dependent G1 arrest. Oncogene *30*, 3317–3327.

Kim, S.T., Lim, D.S., Canman, C.E., and Kastan, M.B. (1999). Substrate specificities and identification of putative substrates of ATM kinase family members. J Biol Chem *274*, 37538–37543.

Klaeger, S., Heinzlmeir, S., Wilhelm, M., Polzer, H., Vick, B., Koenig, P.-A., Reinecke, M., Ruprecht, B., Petzoldt, S., Meng, C., et al. (2017). The target landscape of clinical kinase drugs. Science *358*, eaan4368.

Klauck, T. M., Faux, M.C., Labudda, K., Langeberg, L.K., Jaken, S., and Scott, J.D. (1996). Coordination of three signaling enzymes by AKAP79, a mammalian scaffold protein. Science *271*, 1589–1592.

Knight, J.D., Tian, R., Lee, R.E., Wang, F., Beauvais, A., Zou, H., Megeney, L.A., Gingras, A.C., Pawson, T., Figeys, D., et al. (2012). A novel whole-cell lysate kinase assay identifies substrates of the p38 MAPK in differentiating myoblasts. Skelet Muscle *2*, 1–12.

Krishna, M., and Narang, H. (2008). The complexity of mitogen-activated protein kinases (MAPKs) made simple. Cell Mol Life Sci *65*, 3525–3544.

Kyriakis, J.M., and Avruch, J. (2012). Mammalian MAPK signal transduction pathways activated by stress and inflammation: a 10-year update. Physiol Rev *92*, 689–737.

Kyriakis, J.M., Banerjee, P., Nikolakaki, E., Dai, T., Rubie, E.A., Ahmad, M.F., Avruch, J., and Woodgett, J.R. (1994). The stress-activated protein kinase subfamily of c-Jun kinases. Nature *369*, 156–160.

Lahiry, P., Torkamani, A., Schork, N.J., and Hegele, R.A. (2010). Kinase mutations in human disease: interpreting genotype–phenotype relationships. Nat Rev Genet *11*, 60–74.

Lali, F.V., Hunt, A.E., Turner, S.J., and Foxwell, B.M.J. (2000). The pyridinyl imidazole inhibitor SB203580 blocks phosphoinositide-dependent protein kinase activity, protein kinase B phosphorylation, and retinoblastoma hyperphosphorylation in interleukin-2-stimulated T cells independently of p38 mitogen-activated protein kinase. J Biol Chem *275*, 7395–7402.

Larochelle, S., Merrick, K.A., Terret, M.E., Wohlbold, L., Barboza, N.M., Zhang, C., Shokat, K.M., Jallepalli, P. v., and Fisher, R.P. (2007). Requirements for Cdk7 in the assembly of Cdk1/cyclin B and activation of Cdk2 revealed by chemical genetics in human cells. Mol Cell *25*, 839–850.

Laskin, J.D., Heck, D.E., and Laskin, D.L. (2002). The ribotoxic stress response as a potential mechanism for MAP kinase activation in xenobiotic Toxicity. Toxicol Sci *69*, 289–291.

Lavoie, H., Gagnon, J., and Therrien, M. (2020). ERK signalling: a master regulator of cell behaviour, life and fate. Nat Rev Mol Cell Biol *21*, 607–632.

Lee, J.C., Laydon, J.T., McDonnell, P.C., Gallagher, T.F., Kumar, S., Green, D., McNulty, D., Blumenthal, M.J., Keys, J.R., Land vatter, S.W., et al. (1994). A protein kinase involved in the regulation of inflammatory cytokine biosynthesis. Nature *372*, 739–746.

Lee, J.D., Ulevitch, R.J., and Han, J. (1995). Primary structure of BMK1: A new mammalian MAP kinase. Biochem Biophys Res Commun *213*, 715–724.

Lee, T., Hoofnagle, A.N., Kabuyama, Y., Stroud, J., Min, X., Goldsmith, E.J., Chen, L., Resing, K.A., and Ahn, N.G. (2004). Docking motif interactions in MAP kinases revealed by hydrogen exchange mass spectrometry. Mol Cell *14*, 43–55.

Legeay, M., Doncheva, N.T., Morris, J.H., and Jensen, L.J. (2020). Visualize omics data on networks with Omics Visualizer, a Cytoscape App. F1000Res *9*, 157.

Lemmens, B., Hegarat, N., Akopyan, K., Sala-Gaston, J., Bartek, J., Hochegger, H., and Lindqvist, A. (2018). DNA replication determines timing of mitosis by restricting CDK1 and PLK1 activation. Mol Cell *71*, 117–128.

Levene, P.A., and Beatty, W.A. (1906). The cleavage products of vitellin. J Exp Med *8*, 463–466.

Ley, R., Hadfield, K., Howes, E., and Cook, S.J. (2005). Identification of a DEF-type docking domain for extracellular signal-regulated kinases 1/2 that directs phosphorylation and turnover of the BH3-only protein BimEL. J Biol Chem *280*, 17657–17663.

Li, L., Liu, X., Sanders, K.L., Edwards, J.L., Ye, J., Si, F., Gao, A., Huang, L., Hsueh, E.C., Ford, D.A., et al. (2019). TLR8-mediated metabolic control of human treg function: A mechanistic target for cancer immunotherapy. Cell Metab *29*, 103–123.

Lin, A., and Sheltzer, J.M. (2020). Discovering and validating cancer genetic dependencies: approaches and pitfalls. Nat Rev Genet *21*, 671–682.

Liu, Y., Shepherd, E.G., and Nelin, L.D. (2007). MAPK phosphatases — regulating the immune response. Nat Rev Immunol *7*, 202–212.

Lui, W.Y., Wong, C.H., Mruk, D.D., and Cheng, C.Y. (2003). TGF-β3 regulates the blood-testis barrier dynamics via the p38 mitogen activated protein (MAP) kinase pathway: An in vivo study. Endocrinology *144*, 1139–1142.

Maia, V., Ortiz-Rivero, S., Sanz, M., Gutierrez-Berzal, J., Álvarez-Fernández, I., Gutierrez-Herrero, S., de Pereda, J.M., Porras, A., and Guerrero, C. (2013). C3G forms complexes with Bcr-Abl and p38α MAPK at the focal adhesions in chronic myeloid leukemia cells: Implication in the regulation of leukemic cell adhesion. Cell Commun Signal *11*, 9.

Makrilia, N., Kollias, A., Manolopoulos, L., and Syrigos, K. (2009). Cell adhesion molecules: Role and clinical significance in cancer. Cancer Invest *27*, 1023–1037.

Manke, I.A., Nguyen, A., Lim, D., Stewart, M.Q., Elia, A.E.H., and Yaffe, M.B. (2005). MAPKAP kinase-2 Is a cell cycle checkpoint kinase that regulates the G2/M transition and S phase progression in response to UV irradiation. Mol Cell *17*, 37–48.

Manning, G., Whyte, D.B., Martinez, R., Hunter, T., and Sudarsanam, S. (2002). The Protein Kinase Complementof the Human Genome. Science *298*, 1912–1934.

Margolis, S.S., Perry, J.A., Forester, C.M., Nutt, L.K., Guo, Y., Jardim, M.J., Thomenius, M.J., Freel, C.D., Darbandi, R., Ahn, J.-H., et al. (2006). Role for the PP2A/B56delta phosphatase in regulating 14-3-3 release from Cdc25 to control mitosis. Cell *127*, 759–773.

Menon, M.B., and Gaestel, M. (2018). MK2–TNF–signaling comes full circle. Trends in Biochemical Sciences *43*, 170–179.

Miller, C.J., and Turk, B.E. (2018). Homing in: mechanisms of substrate targeting by protein kinases. Trends in Biochemical Sciences *43*, 380–394.

Minakami, M., Kitagawa, N., Iida, H., Anan, H., and Inai, T. (2015). p38 Mitogen-activated protein kinase and c-Jun NH2-terminal protein kinase regulate the accumulation of a tight junction protein, ZO-1, in cell-cell contacts in HaCaT cells. Tissue Cell *47*, 1–9.

Mitsushima, M., Suwa, A., Amachi, T., Ueda, K., and Kioka, N. (2004). Extracellular signal-regulated kinase activated by epidermal growth factor and cell adhesion interacts with and phosphorylates vinexin. J Biol Chem *279*, 34570–34577.

Mittelstadt, P.R., Yamaguchi, H., Appella, E., and Ashwell, J.D. (2009). T Cell receptor-mediated activation of p38α by mono-phosphorylation of the activation loop results in altered substrate specificity. J Biol Chem *284*, 15469–15474.

Modi, V., and Dunbrack, R.L. (2019). Defining a new nomenclature for the structures of active and inactive kinases. PNAS *116*, 6818–6827.

Moh, M.C., and Shen, S. (2009). The roles of cell adhesion molecules in tumor suppression and cell migration A new paradox. Cell Adh Migr *3*, 334–336.

Mudgett, J.S., Ding, J., Guh-Siesel, L., Chartrain, N.A., Yang, L., Gopal, S., and Shen, M.M. (2000). Essential role for p38α mitogen-activated protein kinase in placental angiogenesis. PNAS *97*, 10454–10459.

Mui, K.L., Chen, C.S., and Assoian, R.K. (2016). The mechanical regulation of integrin-cadherin crosstalk organizes cells, signaling and forces. J Cell Sci *129*, 1093–1100.

Murphy, L.O., Smith, S., Chen, R.H., Fingar, D.C., and Blenis, J. (2002). Molecular, interpretation of ERK signal duration by immediate early gene products. Nat Cell Biol *4*, 556–564.

Murphy, L.O., MacKeigan, J.P., and Blenis, J. (2004). A network of immediate early gene products propagates subtle differences in mitogen-activated protein kinase signal amplitude and duration. Mol Cell Biol *24*, 144–153.

Needham, E.J., Parker, B.L., Burykin, T., James, D.E., and Humphrey, S.J. (2019). Illuminating the dark phosphoproteome. Sci. Signal *12*, eaau8645.

Neel, B.G., Gu, H., and Pao, L. (2003). The 'Shp'ing news: SH2 domain-containing tyrosine phosphatases in cell signaling. Trends Biochem Sci *28*, 284–293.

Nguyen, A.N., Stebbins, E.G., Henson, M., O'Young, G., Choi, S.J., Quon, D., Damm, D., Reddy, M., Ma, J.Y., Haghnazari, E., et al. (2006). Normalizing the bone marrow microenvironment with p38 inhibitor reduces multiple myeloma cell proliferation and adhesion and suppresses osteoclast formation. Exp Cell Res *312*, 1909–1923.

De Nicola, G.F., Martin, E.D., Chaikuad, A., Bassi, R., Clark, J., Martino, L., Verma, S., Sicard, P., Tata, R., Atkinson, R.A., et al. (2013). Mechanism and consequence of the autoactivation of p38α mitogen-activated protein kinase promoted by TAB1. Nat Struct Mol Biol *20*, 1182–1190.

Nikaido, M., Otani, T., Kitagawa, N., Ogata, K., Iida, H., Anan, H., and Inai, T. (2019). Anisomycin, a JNK and p38 activator, suppresses cell–cell junction formation in 2D cultures of K38 mouse keratinocyte cells and reduces claudin-7 expression, with an increase of paracellular permeability in 3D cultures. Histochemistry and Cell Biology *151*, 369–384.

Ochoa, D., Jarnuczak, A.F., Viéitez, C., Gehre, M., Soucheray, M., Mateus, A., Kleefeldt, A.A., Hill, A., Garcia-Alonso, L., Stein, F., et al. (2019). The functional landscape of the human phosphoproteome. Nat Biotechnol *38*, 365–373.

Olsen, J.V., Blagoev, B., Gnad, F., Macek, B., Kumar, C., Mortensen, P., and Mann, M. (2006). Global, in vivo, and site-specific phosphorylation dynamics in signaling networks. Cell *127*, 635–648.

O'Neill, T., Dwyer, A.J., Ziv, Y., Chan, D.W., Lees-Miller, S.P., Abraham, R.H., Lai, J.H., Hill, D., Shiloh, Y., Cantley, L.C., et al. (2000). Utilization of oriented peptide libraries to identify substrate motifs selected by ATM. J Biol Chem *275*, 22719–22727.

Ong, S.E., Blagoev, B., Kratchmarova, I., Kristensen, D.B., Steen, H., Pandey, A., and Mann, M. (2002). Stable isotope labeling by amino acids in cell culture, SILAC, as a simple and accurate approach to expression proteomics. Mol Cell Proteomics *1*, 376–386.

Ono, K., and Han, J. (2000). The p38 signal transduction pathway Activation and function. Cell Signal *12*, 1–13.

Östman, A., Hellberg, C., and Böhmer, F.D. (2006). Protein-Tyrosine phosphatases and cancer. Nat Rev Cancer *6*, 307–320.

Owens, D., and Keyse, S. (2007). Differential regulation of MAP kinase signalling by dual-specificity protein phosphatases. Oncogene *26*, 3203–3213.

Pan, C., Olsen, J. v, Daub, H., and Mann, M. (2009). Global effects of kinase inhibitors on signaling networks revealed by quantitative phosphoproteomics. Mol Cell Proteomics *8*, 2796–2808.

Pearson, R.B., and Kemp, B.E. (1991). Protein kinase phosphorylation site sequences and consensus specificity motifs: Tabulations. Methods Enzymol *200*, 62–81.

Pearson, G., Robinson, F., Beers Gibson, T., Xu, B., Karandikar, M., Berman, K., and Cobb, M.H. (2001). Mitogen-activated protein (MAP) kinase Pathways: regulation and physiological functions. Endocr Rev *22*, 153–183.

Perrino, B.A., Ng, L.Y., and Soderling, T.R. (1995). Calcium regulation of calcineurin phosphatase activity by its B subunit and calmodulin: Role of the autoinhibitory domain. J Biol Chem *270*, 340–346.

Petronczki, M., Lénárt, P., and Peters, J.M. (2008). Polo on the rise—from mitotic entry to cytokinesis with Plk1. Dev Cell *14*, 646–659.

Pimienta, G., and Pascual, J. (2007). Canonical and alternative MAPK signaling. Cell Cycle *6*, 2628–2632.

Pinna, L.A., and Ruzzene, M. (1996). How do protein kinases recognize their substrates? Biochim Biophys Acta *1314*, 191–225.

Porras, A., Zuluaga, S., Black, E., Valladares, A., Alvarez, A.M., Ambrosino, C., Benito, M., and Nebreda, A.R. (2004). p38 Mitogen-activated Protein Kinase Sensitizes Cells to Apoptosis Induced by Different Stimuli. Mol Cell Biol *15*, 922–933.

Pulido, R., Zúñiga, A., and Ullrich, A. (1998). PTP-SL and STEP protein tyrosine phosphatases regulate the activation of the extracellular signal-regulated kinases ERK1 and ERK2 by association through a kinase interaction motif. EMBO J *17*, 7337–7350.

Ramazi, S., and Zahiri, J. (2021). Post-translational modifications in proteins: resources, tools and prediction methods. Database (Oxford) *04*, baab012.

Ramazi, S., Allahverdi, A., and Zahiri, J. (2020). Evaluation of post-translational modifications in histone proteins: A review on histone modification defects in developmental and neurological disorders. J Biosci *45*, 1–29.

Ritchie, M.E., Phipson, B., Wu, D., Hu, Y., Law, C.W., Shi, W., and Smyth, G.K. (2015). Limma powers differential expression analyses for RNA-sequencing and microarray studies. Nucleic Acids Res *43*, e47.

Roignot, J., and Soubeyran, P. (2009). ArgBP2 and the SoHo family of adapter proteins in oncogenic diseases. Cell Adh Migr *3*, 167–170.

Romanov, N., Hollenstein, D.M., Janschitz, M., Ammerer, G., Anrather, D., and Reiter, W. (2017). Identifying protein kinase–specific effectors of the osmostress response in yeast. Sci Signal *10*, eaag2435.

Rouse, J., Cohen, P., Trigon, S., Morange, M., Alonso-Llamazares, A., Zamanillo, D., Hunt, T., and Nebreda, A.R. (1994). A novel kinase cascade triggered by stress and heat shock that stimulates MAPKAP kinase-2 and phosphorylation of the small heat shock proteins. Cell *78*, 1027–1037.

Roux, P.P., and Blenis, J. (2004). ERK and p38 MAPK-activated protein kinases: a family of protein kinases with diverse biological functions. Microbiol Mol Biol Rev *68*, 320–344.

Sabio, G., Arthur, J.S.C., Kuma, Y., Peggie, M., Carr, J., Murray-Tait, V., Centeno, F., Goedert, M., Morrice, N.A., and Cuenda, A. (2005). p38γ regulates the localisation of SAP97 in the cytoskeleton by modulating its interaction with GKAP. EMBO J *24*, 1134–1145.

Sacco, F., Tinti, M., Palma, A., Ferrari, E., Nardozza, A.P., van Huijsduijnen, R.H., Takahashi, T., Castagnoli, L., and Cesareni, G. (2009). Tumor suppressor density-enhanced phosphatase-1 (DEP-1) inhibits the RAS pathway by direct dephosphorylation of ERK1/2 kinases. J Biol Chem *284*, 22048–22058.

Sacco, F., Perfetto, L., Castagnoli, L., and Cesareni, G. (2012). The human phosphatase interactome: An intricate family portrait. FEBS Lett *586*, 2732–2739.

Sanz, V., Arozarena, I., and Crespo, P. (2000). Distinct carboxy-termini confer divergent characteristics to the mitogen-activated protein kinase p38α and its splice isoform Mxi2. FEBS Lett *474*, 169–174.

Schneider, E., Montenarh, M., and Wagner, P. (1998). Regulation of CAK kinase activity by p53. Oncogene *17*, 2733–2741.

Schwartz, D., and Gygi, S.P. (2005). An iterative statistical approach to the identification of protein phosphorylation motifs from large-scale data sets. Nat Biotechnol *23*, 1391–1398.

Selness, S.R., Devraj, R. v., Devadas, B., Walker, J.K., Boehm, T.L., Durley, R.C., Shieh, H., Xing, L., Rucker, P. v., Jerome, K.D., et al. (2011). Discovery of PH-797804, a highly selective and potent inhibitor of p38 MAP kinase. Bioorg Med Chem Lett *21*, 4066–4071.

Shah, N.G., Tulapurkar, M.E., Ramarathnam, A., Brophy, A., Martinez, R., Hom, K., Hodges, T., Samadani, R., Singh, I.S., MacKerell, A.D., et al. (2017). Novel noncatalytic substrate-selective p38α-specific MAPK inhibitors with endothelial-stabilizing and anti-inflammatory activity. J Immunol *198*, 3296–3306.

Shanware, N.P., Williams, L.M., Bowler, M.J., and Tibbetts, R.S. (2009). Non-specific in vivo inhibition of CK1 by the pyridinyl imidazole p38 inhibitors SB 203580 and SB 202190. BMB Reports *42*, 142–147.

Shen, C.H., Lin, J.Y., Lu, C.Y., Yang, S. sen, Peng, C.K., and Huang, K.L. (2021). SPAK-p38 MAPK signal pathway modulates claudin-18 and barrier function of alveolar epithelium after hyperoxic exposure. BMC Pulm Med *21*, 58.

Sheridan, D.L., Kong, Y., Parker, S.A., Dalby, K.N., and Turk, B.E. (2008). Substrate discrimination among mitogen-activated protein kinases through distinct docking sequence motifs. J Biol Chem *283*, 19511–19520.

Shi, Y. (2009). Serine/Threonine Phosphatases: Mechanism through Structure. Cell *139*, 468–484.

Siljamäki, E., Raiko, L., Toriseva, M., Nissinen, L., Näreoja, T., Peltonen, J., Kähäri, V.M., and Peltonen, S. (2014). P38δ mitogen-activated protein kinase regulates the expression of tight junction protein ZO-1 in differentiating human epidermal keratinocytes. Arch Dermatol Res *306*, 131–141.

Soloaga, A., Thomson, S., Wiggin, G.R., Rampersaud, N., Dyson, M.H., Hazzalin, C.A., Mahadevan, L.C., and Arthur, J.S.C. (2003). MSK2 and MSK1 mediate the mitogen- and stress-induced phosphorylation of histone H3 and HMG-14. EMBO J *22*, 2788–2797.

Songyang, Z., Blechnert, S., Hoagland, N., Hoekstra, M.F., Piwnica-Worms, H., and Cantley, L.C. (1994). Use of an oriented peptide library to determine the optimal substrates of protein kinases. Curr Biol *4*, 973–982.

Soni, S., Saroch, M.K., Chander, B., Tirpude, N.V., and Padwad, Y.S. (2019). MAPKAPK2 plays a crucial role in the progression of head and neck squamous cell carcinoma by regulating transcript stability. J Exp Clin Cancer Res *38*, 1–13.

Stein, B., Brady, H., Yang, M.X., Young, D.B., and Barbosa, M.S. (1996). Cloning and characterization of MEK6, a novel member of the mitogen-activated protein kinase kinase cascade. J Biol Chem *271*, 11427–11433.

Strippoli, R., Benedicto, I., Foronda, M., Perez-Lozano, M.L., Sánchez-Perales, S., López-Cabrera, M., and del Pozo, M.Á. (2010). p38 maintains E-cadherin expression by modulating TAK1–NF-κB during epithelial-to-mesenchymal transition. J Cell Sci *123*, 4321–4331.

Sudo, T., Yagasaki, Y., Hama, H., Watanabe, N., and Osada, H. (2002). Exip, a new alternative splicing variant of p38α, can induce an earlier onset of apoptosis in HeLa cells. Biochem Biophys Res Commun *291*, 838–843.

Suelves, M., Lluís, F., Ruiz, V., Nebreda, A.R., and Muñoz-Cánoves, P. (2004). Phosphorylation of MRF4 transactivation domain by p38 mediates repression of specific myogenic genes. EMBO J *23*, 365–375.

Suzuki, T., Sakata, K., Mizuno, N., Palikhe, S., Yamashita, S., Hattori, K., Matsuda, N., and Hattori, Y. (2018). Different involvement of the MAPK family in inflammatory regulation in human pulmonary microvascular endothelial cells stimulated with LPS and IFN-γ. Immunobiology *223*, 777–785.

Taieb, D., Roignot, J., André, F., Garcia, S., Masson, B., Pierres, A., Iovanna, J.-L., and Soubeyran, P. (2008). ArgBP2-dependent signaling regulates Pancreatic cell migration, adhesion, and tumorigenicity. Cancer Res *68*, 4588–4596.

Takekawa, M., Maeda, T., and Saito, H. (1998). Protein phosphatase 2Cα inhibits the human stress-responsive p38 and JNK MAPK pathways. EMBO J *17*, 4744–4752.

Tang, J., Yang, X., and Liu, X. (2008). Phosphorylation of Plk1 at Ser326 regulates its functions during mitotic progression. Oncogene *27*, 6635–6645.

Tanoue, T., and Nishida, E. (2003). Molecular recognitions in the MAP kinase cascades. Cell Signal *15*, 455–462.

Tanoue, T., Adachi, M., Moriguchi, T., and Nishida, E. (2000). A conserved docking motif in MAP kinases common to substrates, activators and regulators. Nat Cell Biol *2*, 110–116.

Taylor, S.S., Kim, C., Vigil, D., Haste, N.M., Yang, J., Wu, J., and Anand, G.S. (2005). Dynamics of signaling by PKA. Biochim Biophys Acta *1754*, 25–37.

Tcherkezian, J., Danek, E.I., Jenna, S., Triki, I., and Lamarche-Vane, N. (2005). Extracellular signal-regulated kinase 1 interacts with and phosphorylates CdGAP at an important regulatory site. Mol Cell Biol *25*, 6314–6329.

Teng, X., Dayhoff-Brannigan, M., Cheng, W.C., Gilbert, C.E., Sing, C.N., Diny, N.L., Wheelan, S.J., Dunham, M.J., Boeke, J.D., Pineda, F.J., et al. (2013). Genome-wide consequences of deleting any single gene. Molecular Cell *52*, 485–494.

Tiedje, C., Ronkina, N., Tehrani, M., Dhamija, S., Laass, K., Holtmann, H., Kotlyarov, A., and Gaestel, M. (2012). The p38/MK2-driven exchange between Tristetraprolin and HuR regulates AU–Rich element–dependent translation. PLoS Genet *8*, e1002977.

Tiedje, C., Lubas, M., Tehrani, M., Menon, M.B., Ronkina, N., Rousseau, S., Cohen, P., Kotlyarov, A., and Gaestel, M. (2015). p38MAPK/MK2-mediated phosphorylation of RBM7 regulates the human nuclear exosome targeting complex. RNA *21*, 262–278.

Tomás-Loba, A., Manieri, E., González-Terán, B., Mora, A., Leiva-Vega, L., Santamans, A.M., Romero-Becerra, R., Rodríguez, E., Pintor-Chocano, A., Feixas, F., et al. (2019). p38γ is essential for cell cycle progression and liver tumorigenesis. Nature *568*, 557–560.

Tong, K.I., Yamamoto, M., and Tanaka, T. (2008). A simple method for amino acid selective isotope labeling of recombinant proteins in E. coli. J Biomol NMR *42*, 59–67.

Tonks, N.K. (2006). Protein tyrosine phosphatases: from genes, to function, to disease. Nat Rev Mol Cell Biol *7*, 833–846.

Topolska-Woś, A.M., Rosińska, S., and Filipek, A. (2017). MAP kinase p38 is a novel target of CacyBP/SIP phosphatase. Amino Acids *49*, 1069–1076.

Torkamani, A., Kannan, N., Taylor, S.S., and Schork, N.J. (2008). Congenital disease SNPs target lineage specific structural elements in protein kinases. PNAS *105*, 9011–9016.

Trempolec, N., Dave-Coll, N., and Nebreda, A.R. (2013). SnapShot: p38 MAPK Substrates. Cell *152*, 924-924.e1.

Tyanova, S., Temu, T., Sinitcyn, P., Carlson, A., Hein, M.Y., Geiger, T., Mann, M., and Cox, J. (2016). The Perseus computational platform for comprehensive analysis of (prote)omics data. Nat Methods *13*, 731–740.

Ubersax, J.A., and Ferrell, J.E. (2007). Mechanisms of specificity in protein phosphorylation. Nat Rev Mol Cell Biol *8*, 530–541.

Vinciguerra, M., Vivacqua, A., Fasanella, G., Gallo, A., Cuozzo, C., Morano, A., Maggiolini, M., and Musti, A.M. (2004). Differential phosphorylation of c-Jun and JunD in response to the epidermal growth factor is determined by the structure of MAPK targeting sequences. J Biol Chem *279*, 9634–9641.

Vind, A.C., Genzor, A.V., and Bekker-Jensen, S. (2020). Ribosomal stress-surveillance: three pathways is a magic number. Nucleic Acids Res *48*, 10648–10661.

Wales, S., Hashemi, S., Blais, A., and McDermott, J.C. (2014). Global MEF2 target gene analysis in cardiac and skeletal muscle reveals novel regulation of DUSP6 by p38MAPK-MEF2 signaling. Nucleic Acids Res *42*, 11349–11362.

Wang, J., Zhang, R., Lin, Z., Zhang, S., Chen, Y., Tang, J., Hong, J., Zhou, X., Zong, Y., Xu, Y., et al. (2020). CDK7 inhibitor THZ1 enhances antiPD-1 therapy efficacy via the p38α/MYC/PD-L1 signaling in non-small cell lung cancer. J Hematol Oncol *13*, 1–16.

Weber, H.O., Ludwig, R.L., Morrison, D., Kotlyarov, A., Gaestel, M., and Vousden, K.H. (2005). HDM2 phosphorylation by MAPKAP kinase 2. Oncogene *24*, 1965–1972.

Whitmarsh, A.J., Cavanagh, J., Tournier, C., Yasuda, J., and Davis, R.J. (1998). A mammalian scaffold complex that selectively mediates MAP kinase activation. Science *281*, 1671–1674.

Willoughby, E.A., Perkins, G.R., Collins, M.K., and Whitmarsh, A.J. (2003). The JNK-interacting protein-1 scaffold protein targets MAPK phosphatase-7 to dephosphorylate JNK. J Biol Chem *278*, 10731–10736.

Wiredja, D.D., Koyutürk, M., and Chance, M.R. (2017). The KSEA App: a web-based tool for kinase activity inference from quantitative phosphoproteomics. Bioinformatics *33*, 3489–3491.

Wong, W., and Scott, J.D. (2004). AKAP signalling complexes: Focal points in space and time. Nat Rev Mol Cell Biol *5*, 959–970.

Wu, H., Ming, W., Tan, J., Lu, Q., Shrestha, S.M., Li, N., Wu, G., Zhang, Z., and Shi, R. (2020). Role of MKP-5-p38/MAPK pathway in Clopidogrel-induced gastric mucosal epithelial cells apoptosis and tight junction dysfunction. Am J Transl Res *12*, 1741–1753.

Xing, L., Shieh, H.S., Selness, S.R., Devraj, R. v, Walker, J.K., Devadas, B., Hope, H.R., Compton, R.P., Schindler, J.F., Hirsch, J.L., et al. (2009). Structural bioinformatics-based prediction of exceptional selectivity of p38 MAP kinase inhibitor PH-797804. Biochemistry *48*, 6402–6411.

Xiu, M., Kim, J., Sampson, E., Huang, C.-Y., Davis, R.J., Paulson, K.E., and Yee, A.S. (2003). The Transcriptional Repressor HBP1 Is a Target of the p38 Mitogen-Activated Protein Kinase Pathway in Cell Cycle Regulation. Mol Cell Biol *23*, 8890–8901.

Xu, Z., Cetin, B., Anger, M., Cho, U.S., Helmhart, W., Nasmyth, K., and Xu, W. (2009). Structure and function of the PP2A-shugoshin interaction. Mol Cell *35*, 426–441.

Yamamoto, T., Kojima, T., Murata, M., Takano, K.I., Go, M., Hatakeyama, N., Chiba, H., and Sawada, N. (2005). p38 MAP-kinase regulates function of gap and tight junctions during regeneration of rat hepatocytes. J Hepatol *42*, 707–718.

Yan, B., Peng, Z., and Xing, C. (2019). SORBS2, mediated by MEF2D, suppresses the metastasis of human hepatocellular carcinoma by inhibitiing the c-Abl-ERK signaling pathway. Am J Cancer Res *9*, 2706–2718.

Yang, C.Y., Chang, C.H., Yu, Y.L., Lin, T.C.E., Lee, S.A., Yen, C.C., Yang, J.M., Lai, J.M., Hong, Y.R., Tseng, T.L., et al. (2008). PhosphoPOINT: a comprehensive human kinase interactome and phospho-protein database. Bioinformatics *24*, i14-20.

Yang, Q., Li, W., She, H., Dou, J., Duong, D.M., Du, Y., Yang, S.H., Seyfried, N.T., Fu, H., Gao, G., et al. (2015). Stress induces p38 MAPK-mediated phosphorylation and inhibition of Drosha-dependent cell survival. Mol Cell *57*, 721–734.

Yang, S.H., Yates, P.R., Whitmarsh, A.J., Davis, R.J., and Sharrocks, A.D. (1998). The Elk-1 ETS-domain transcription factor contains a mitogen-activated protein kinase targeting motif. Mol Cell Biochem *18*, 710–720.

Yang, S.H., Galanis, A., and Sharrocks, A.D. (1999). Targeting of p38 mitogen-activated protein kinases to MEF2 transcription factors. Mol Cell Biol *19*, 4028–4038.

Yang, T.T.C., Xiong, Q., Enslen, H., Davis, R.J., and Chow, C.-W. (2002). Phosphorylation of NFATc4 by p38 Mitogen-Activated Protein Kinases. Mol Cell Biol *22*, 3892–3904.

Yu, E., Ahn, Y.S., Jang, S.J., Kim, M.-J., Yoon, H.S., Gong, G., and Choi, J. (2006). Overexpression of the wip1 gene abrogates the p38 MAPK/p53/Wip1 pathway and silences p16 expression in human breast cancers. Breast Cancer Res Treat *101*, 269–278.

Zaidel-Bar, R., Itzkovitz, S., Ma'ayan, A., Iyengar, R., and Geiger, B. (2007). Functional atlas of the integrin adhesome. Nat Cell Biol *9*, 858–867.

Zeisel, A., Yitzhaky, A., Bossel Ben-Moshe, N., and Domany, E. (2013). An accessible database for mouse and human whole transcriptome qPCR primers. Bioinformatics *29*, 1355–1356.

Zhang, Y., and Dong, C. (2007). Regulatory mechanisms of mitogen-activated kinase signaling. Cell. Mol. Life Sci *64*, 2771–2789.

Zhang, Y.Y., Mei, Z.Q., Wu, J.W., and Wang, Z.-X. (2008). Enzymatic activity and substrate specificity of mitogen-activated protein kinase p38alpha in different phosphorylation states. J Biol Chem *283*, 26591–26601.

Zhang, J., Yang, P.L., and Gray, N.S. (2009). Targeting cancer with small molecule kinase inhibitors. Nat Rev Cancer *9*, 28–39.

Zhao, M., New, L., Kravchenko, V. v., Kato, Y., Gram, H., di Padova, F., Olson, E.N., Ulevitch, R.J., and Han, J. (1999). Regulation of the MEF2 Family of Transcription Factors by p38. Mol Cell Biol *19*, 21–30.

Zheng, J., Trafny, E.A., Knighton, D.R., Xuong, N.-H., Taylor, S.S., ten Eyck, L.F., and Sowadski, J.M. (1993). 2.2 A refined crystal structure of the catalytic subunit of cAMP-dependent protein kinase complexed with MnATP and a peptide inhibitor. Acta Crystallogr D Biol Crystallogr *49*, 362–365.

Zhong, L., Huot, J., and Simard, M.J. (2018). p38 activation induces production of miR-146a and miR-31 to repress E-selectin expression and inhibit transendothelial migration of colon cancer cells. Sci Rep *8*, 1–13.

Zhou, G., Bao, Z.Q., and Dixon, J.E. (1995). Components of a new human protein kinase signal transduction pathway. J Biol Chem *270*, 12665–12669.

Zvalova, D., Cordier, J., Mesnil, M., Junier, M.-P., and Chneiweiss, H. (2004). p38/SAPK2 controls gap junction closure in astrocytes. Glia *46*, 323–333.